PART I: HOW DID WE GET HERE? COLLEGE STUDENTS' PREINSTRUCTIONAL IDEAS ON THE TOPIC OF PLANET FORMATION, AND THE DEVELOPMENT OF THE PLANET FORMATION CONCEPT INVENTORY; **PART II**: EVIDENCE FOR MAGNETICALLY DRIVEN PROTOPLANETARY DISK WINDS

by

Molly Nora Simon

A Dissertation Submitted to the Faculty of the

DEPARTMENT OF PLANETARY SCIENCES

In Partial Fulfillment of the Requirements
For the Degree of

DOCTOR OF PHILOSOPHY

In the Graduate College

THE UNIVERSITY OF ARIZONA
2019

THE UNIVERSITY OF ARIZONA
GRADUATE COLLEGE

As members of the Dissertation Committee, we certify that we have read the dissertation prepared by Molly Nora Simon, titled ***Part I**: How did we get here? College Students' Preinstructional Ideas on the Topic of Planet Formation, and the Development of the Planet Formation Concept Inventory; **Part II**: Evidence for Magnetically Driven Protoplanetary Disk Winds*, and recommend that it be accepted as fulfilling the dissertation requirement for the Degree of Doctor of Philosophy.

Chris Impey — Date: May 7, 2019

Sanlyn Buxner — Date: May 7, 2019

Ilaria Pascucci — Date: May 7, 2019

Tim Swindle — Date: May 7, 2019

Steve Kortenkamp — Date: May 7, 2019

Final approval and acceptance of this dissertation is contingent upon the candidate's submission of the final copies of the dissertation to the Graduate College.

We hereby certify that we have read this dissertation prepared under our direction and recommend that it be accepted as fulfilling the dissertation requirement.

Chris Impey — Date: May 7, 2019
Dissertation Committee Co-Chair

Sanlyn Buxner — Date: May 7, 2019
Dissertation Committee Co-Chair

ACKNOWLEDGEMENTS

This dissertation could not have been completed without the support and guidance of so many amazing people!

To my advisor, Chris Impey, thank you for taking a chance on a third-year graduate student looking to shift her focus from astrophysics research to astronomy education research. Your constant support, encouragement, levelheadedness, and humor has kept me grounded and motivated throughout this process. It has been a pleasure to learn from one of the greats!

To Ilaria Pascucci, thank you for serving as my mentor for the first half of my studies. It was a true privilege to learn from you. Thank you for your continual support of my research interests throughout my entire time at LPL.

To Sanlyn Buxner, it is safe to say I could not have done this without you. Thank you for being the calming voice of wisdom that I have grown so reliant upon. You are a jack of all trades: statistics, science, education, you do it all! Thank you for molding me into the researcher I am today - I appreciate you more than I could ever express in this 1-2 page limit.

To Ed Prather, thank you for your wisdom and directness over the past few years. Your encouragement is what ultimately led me to pursue my passion for astronomy education research. Thank you for believing in me.

To the rest of the Impey Research Group - Matthew, Martin, and Zander. You have been such wonderful colleagues throughout this process. Thank you for your invaluable feedback on papers, presentations, and most importantly - for your friendship.

To the faculty members of LPL and Steward Observatory who allowed me to administer my surveys in your classes - thank you! This work could not have been completed without your willingness to let me pick your students' brains.

To the friends I have made during my time in Tucson that have really become more

like family: James Keane, Rachel Fernandes, Ali Bramson, Michelle Thompson, Kyle Pearson, John Noonan, Laci Brock, Shane Stone, Jon Bapst, and Margaret Landis. This process has been astronomically more pleasant because of your friendship. Thank you for your Matlab assistance, the dinner dates, and the late night problem set sessions.

To Sarah Peacock, how can I even begin to thank you in a few short sentences? You have been my best friend and partner in crime throughout this entire experience. Thank you for being my comfort blanket, a constant source of laughter, and my adventure buddy. I will miss you so very much!

To my parents, Pam and Scooter Simon, I could fill an entire book with reasons why I am so grateful for you both. There is zero exaggeration when I say that I truly have the best, most generous, and most loving parents. You have allowed me to pursue this passion for the planets ever since I could speak. Thank you for visiting planetariums with me around the world, for sneaking into my conference talks, and for claiming me as your own even when I carried a picture of the Solar System around with me everywhere I went. This is only possible because you made it so. I love you both so much!

To my family and friends near and far who have nurtured and supported my passion. I appreciate your willingness to (begrudgingly) sit through Journey to Infinity more times that you'd like to admit. The love I have for all of you is to infinity and beyond!

To Ari - thank you for your unconditional love when I needed it most. This is the just the beginning of our adventure - onward to Chicago! And to our "Perfect Pooch" Tyrion - thank you for the kisses and snuggles. I love you both the mostest!

Last but certainly not least, I'd like to thank my grandfather, Sheldon Simon and my great-uncle Norman Simon for instilling in me a love of education. I miss you both everyday, and I hope you would be proud.

It takes a village - and mine happens to be the best.

DEDICATION

To everyone who has taken an unconventional path towards pursuing their dream...
"Two roads diverged in a wood and I - I took the one less traveled by, and that has made all the difference" - Robert Frost

To Marilyn Simon, my greatest inspiration

Contents

Contents – *Continued*

Contents – *Continued*

List of Figures

List of Figures – *Continued*

List of Tables

List of Tables – *Continued*

List of Tables – *Continued*

ABSTRACT

This dissertation includes two independent research projects, one in astronomy education research and the other in planetary science/astrophysics research. In the first research effort, we investigate college students' conceptual and reasoning difficulties on the topic of planet formation pre-instruction. Through an analysis of over 1,000 responses to open-ended questions, we find that these students lack an understanding of fundamental topics in astronomy (e.g. gravity, basic definitions of a planet or solar system, mass versus density). The results from this analysis laid the foundation for the development of the Planet Formation Concept Inventory (PFCI), an educational research tool that can be used like a diagnostic test to assess students' pre- and post-instructional knowledge. Using iterative design and statistical processes consistent with Classical Test Theory (CTT), we are able to confirm that the PFCI is a reliable and valid instrument that can be utilized to measure college students' learning on the topic of planet formation over time.

In the second research effort, we analyze forbidden lines (predominantly the [O I] line at 6300 Å) from a sample of 33 T-Tauri stars with disks spanning a range of evolutionary stages. After removing a high-velocity component (HVC) associated with microjets, we focus our efforts on studying the low-velocity component (LVC) to better elucidate its origin. The LVC can be attributed to slow disk winds that are either thermally or magnetically driven. We find that the LVC itself can be resolved into two distinct components: a broad component (FWHM $>$ 40 km/s) and a narrow component (FWHM $<$ 40 km/s). Additionally, we find that the FWHM

of both components correlates with the disk inclination, consistent with Keplerian broadening from radii of 0.05 to 0.5 AU for the BC and 0.5 to 5 AU for the NC. Since the BC emission arises inward of 0.5 AU where the gravity of the star/disk system is strong, we eliminate the possibility that the BC traces a thermally-driven wind, and instead suggest that it traces the base of a magnetohydrodynamic (MHD) wind. For the NC, half of the features we observe have centroid velocities consistent with the stellar velocity, and the other half have blueshifts between -2 and -5 km/s. For this component of the LVC, the origin remains more elusive, and we cannot exclude the possibility that the NC arises in a photoevaporative wind.

1.0 INTRODUCTION

This dissertation includes two distinct research projects. Part I (Chapters 2 and 3) presents a thorough analysis of college students' preinstructional ideas on the topic of planet formation, and the multiple-choice instrument (concept inventory) that was developed as a result. Part II (Chapter 4) consists of an investigation into the type of winds that dominate the dispersal of material (primarily gas) in protoplanetary disks. The distinct nature of the two research projects presented reflects the author's desire to pursue a hybrid dissertation project, gaining experience in both quantitative and qualitative research practices.

Although the data acquisition and analysis processes between the two projects are vastly different, both projects contribute worthwhile results to their respective scientific communities. The educational instrument developed and validated in Part I will serve as a tool future college instructors can use to evaluate their students' understanding of planet formation and the relevant subtopics therein (gravity, condensation temperature, planetary motion and migration, etc...). If administered in a pre/post-test fashion, the Planet Formation Concept Inventory (PFCI) can also serve as a tool to track students' learning before and after relevant instruction.

Part II is an exploration into how protoplanetary disks (the birthplace of planets) disperse, and the role of winds in this dispersal process. We aim to investigate the empirical properties of observed disk-wind tracers in order to determine whether the winds we observe are thermally or magnetically driven. Disk dispersal via winds has direct and significant implications for planet formation, and Parts I and aspects of Part II are, therefore, topically related.

1.1 Part I: Background and Motivation

The constructivist teaching theory, simply stated, is that students enter the classroom with knowledge they have gained through their own personal experiences, and their understanding of new topics is based on personal pre-existing conceptions or conceptions reconstructed from memory (Bransford et al. 1999; National Academies of Sciences, Engineering, and Medicine 2018). If instructors neglect to address students' initial ideas and beliefs, student understanding can be much different than what the instructor intends (Bransford et al., 1999). The constructivist theoretical framework has guided the field of research into students' conceptual and reasoning difficulties. Investigations into these naive ideas is foundational to science education research in that students' preconceptions with respect to a variety of scientific topics are often incomplete or grounded in inaccuracies (McDermott, 1991). That students may convert scientific information into conceptual models, which are scientifically inaccurate, holds true for a variety of topics under the umbrella of astronomy education research (AER) as well (Bailey and Slater 2003; Slater and Adams 2003). The video, *A Private Universe*, famously illuminates the scientific inaccuracies that emerge as faculty members, alumni, and graduating seniors from Harvard University attempt to explain the cause of seasons or the phases of the Moon (Schneps, 1989). Since the debut of *A Private Universe*, hundreds of studies have attempted to ascertain individual's conceptual and reasoning difficulties related to a variety of topics relevant to astronomy such as gravity, the shape of Earth, lunar phases, and diurnal motion to highlight a select few (Williamson and Willoughby 2012; Albanese et al. 1997; Lindell and Olsen 2002; Vosniadou and Brewer 1994).

The study presented in Chapter 2 addresses students' preinstructional ideas and reasoning difficulties on the topic of planet formation (and the related subtopics therein). The project was motivated by a need to evaluate students' understanding of topics in astronomy that are actively being studied, and are at the forefront of current astronomical research (Pasachoff, 2002). Planet formation has become an exceedingly relevant area of astrophysics research in light of the discovery of

more than 3,700 extrasolar planets (planets orbiting stars other than our Sun). The discovery of an abundance of stellar systems with a diverse range of planetary properties raises the question of whether or not our Solar System is typical. Introducing the topic of planet formation into general education astronomy courses at the college level (hereafter, ASTRO 101) will allow students to develop a more scientific understanding of the physical and chemical processes that govern the creation of our own Solar System. This will then enable students to more adequately draw parallels between the characteristics of the planets in our own Solar System, and those that are constantly being discovered around other stars.

Despite its aforementioned relevance to the ASTRO 101 course curriculum, almost no studies exist in the astronomy education research (AER) literature that address students' reasoning difficulties on the topic of planet formation, especially with a large population of young adults (see Chapter 2, Section 2.2 for a more in-depth review of the relevant AER literature). As a result, we provided over 1,000 students enrolled in 13 different ASTRO 101 sections at The University of Arizona with one of six student-supplied-response (SSR) open-ended survey questions on the topic of planet formation *before* relevant instruction. Following the method outlined in Bailey et al. (2009), in Chapter 2 we present our analysis of the SSR surveys administered during the Fall 2016 and Spring 2017 semesters. We explore in depth the most common themes, ideas, and misconceptions that appear in student responses to the six SSR survey questions. This work provides significant new insight into what ASTRO 101 students know about the topic of planet formation before instruction - and what topics instructors should emphasize when teaching planet formation to address apparent gaps in student understanding.

Chapter 3 directly builds on the work conducted in Chapter 2 in that all of the test items on the PFCI originated from our research into students' understanding of planet formation before instruction. A concept inventory is a multiple-choice style instrument that covers a single topic or closely related set of topics. Concept inventories are distinguishable from traditional multiple-choice tests because the former uses research-based preinstructional ideas and reasoning difficulties as the

basis for their 'distractors' (incorrect answer choices) (Bailey et al., 2009). They are also particularly useful for assessing students' pre- and post-instructional conceptual knowledge, as well as the efficacy of newly implemented pieces of pedagogy designed to teach a specific topic more effectively (e.g. Lopresto and Murrell 2009; Prather et al. 2004).

In Chapter 3, we discuss the iterative process utilized to develop the final version of the PFCI. We then perform a in-depth statistical analysis of the PFCI's reliability and validity using methods consistent with classical test theory (CTT) (Crocker and Algina 1986; Bardar et al. 2006). Finally, we confirm from this work that the PFCI is a reliable and valid instrument that is successfully able to measure learning on the topic of planet formation over time. The PFCI is, as a result, ready to be utilized by the community of ASTRO 101 instructors as a means to evaluate students' understanding of planet formation over the course of the semester, as well provide insight into the efficacy of current methods of instruction.

1.2 Part II: Background and Motivation

Protoplanetary disks are a natural result of star formation, and they provide the material from which planets form. Observations of protoplanetary disks indicate that they evolve and eventually disperse over a timescale of a few million years (Myr). Although only approximately 1% of disk mass can be attributed to circumstellar dust, nearly our entire understanding of disk dispersal comes from dust observations (Ercolano and Pascucci, 2017).

Circumstellar dust in protoplanetary disks absorbs radiation from the central star, and re-emits it at longer wavelengths. Warmer dust (in the inner few AU of the disk) emits in the near-infrared (IR) wavelength range, while millimeter (mm) emission traces colder dust farther out in the disk (Alexander et al., 2014). As a result, young stars with excess emission at infrared wavelengths are surmised to be stars with disks (Class II objects), whereas stars that have gotten rid of their disks have very little excess emission at corresponding infrared wavelengths (Class

III objects). A small percentage (≈10%) of Class II objects are observed to have an optically thin inner disk (very little infrared emission at shorter wavelengths), and an excess of infrared emission at longer wavelengths, indicative of dust clearing from the inside-out (Skrutskie et al., 1990). These disks are classified as "transition disks" - and the mere fact that we observe so few of them indicates that the transition from full disk to no disk is rapid, on the order of 10^5 years (Alexander et al. 2014; Ercolano and Pascucci 2017). Although it is currently more difficult to directly image gas cavities when compared to dust cavities, accretion indicators (such as the Hα line) indicate that the rate at which gas is accreted onto the central star also declines as the disk evolves, with the fraction of accreting stars as a function of cluster age nearing zero at ≈ 10 Myr (Ercolano and Pascucci, 2017).

The most widely accepted models for disk dispersal include viscous accretion and photoevaporation, in particular. Accretion drives material onto the central star, while winds launch material (predominantly gas) out of the star-disk system. Although young disks accrete material efficiently onto the central star, the accretion rate slows to values below the disk wind rate after a few Myr (Ercolano and Pascucci, 2017). As the disk evolves, radiation from the central star penetrates the upper layers of the disk and heats the gas to temperatures significantly greater than the disk's midplane temperature (Alexander et al., 2014). Once the thermal velocity of the gas exceeds the orbital velocity at a given location, the material becomes unbound and flows away from the disk as a thermally driven (photoevaporative) wind. Depending on the type of radiation incident on the disk (EUV, X-Ray, or FUV), photoevaporative winds can lend to disk mass-loss rates on the order of 10^{-8} $M_{\odot}/year$ for a disk around a solar-type star (Owen et al. 2010; Owen et al. 2011; Owen et al. 2012). A gap forms in the disk as the wind becomes more efficient at removing protoplanetary material, and once this wind-driven dispersal process begins to dominate, the disk is readily depleted of protoplanetary material from the inside-out (Ercolano and Pascucci, 2017).

The vast majority of disk dispersal models include photoevaporative winds, but there are other potential disk winds that require consideration. Extended,

magnetically-launched jets and disk winds have the ability to remove both mass and angular momentum from the disk, and therefore may power accretion (Königl and Salmeron 2011; Alexander et al. 2014; Ercolano and Pascucci 2017). Only recently have models began to implement the conditions required to generate these MHD winds, and some suggest that even just a weak vertical magnetic field in the disk can produce a wind (Bai and Stone 2013; Ercolano and Pascucci 2017). These magnetically driven winds may be able to compete with viscous accretion as a means to efficiently deplete the disk of protoplanetary material closer to the central star. There is also evidence that these MHD disk winds evolve in conjunction with the disk and eventually disappear as the disk matures (Ercolano and Pascucci 2017; Banzatti et al. 2019). A visual schematic that summarizes the main stages of disk evolution and dispersal can be found in Figure 1.1.

High resolution optical spectroscopy of low mass, pre-main sequence stars known as T-Tauri stars (hereafter, TTS) has played an invaluable role in identifying tracers of both accretion and disk winds (Rigliaco et al., 2013). The blueshifted emission profiles of forbidden lines (e.g. the [O I] line at both 6300 Å and 5577 Å), for example, can be utilized as evidence in favor of material flowing out of the disk/star system (Ercolano and Pascucci, 2017). Previous work analyzing large samples of TTS have shown that these forbidden lines can be separated into two distinct components: a high-velocity component (HVC) and a low velocity component (LVC) (Hamann 1994; Hartigan et al. 1995; Hirth et al. 1997). HVC emission, typically blueshifted by 30-150 km/s, has been attributed to tracing material formed in microjets, while the origin of the LVC (with blueshifts on the order of $\approx$ 5 km/s) remains more elusive.

Previous studies suggest that the LVC forbidden line emission may trace material removed from the disk/star system via a thermally driven (photoevaporative) wind (e.g. Hartigan et al. 1995; Kwan and Tademaru 1995; Font et al. 2004). Attempts to better constrain the empirical properties of forbidden lines demonstrated that the LVC may itself have two distinct kinematic components, and that the LVC emission we observe is likely arising in a slow wind that is dense, warm, and mostly neutral

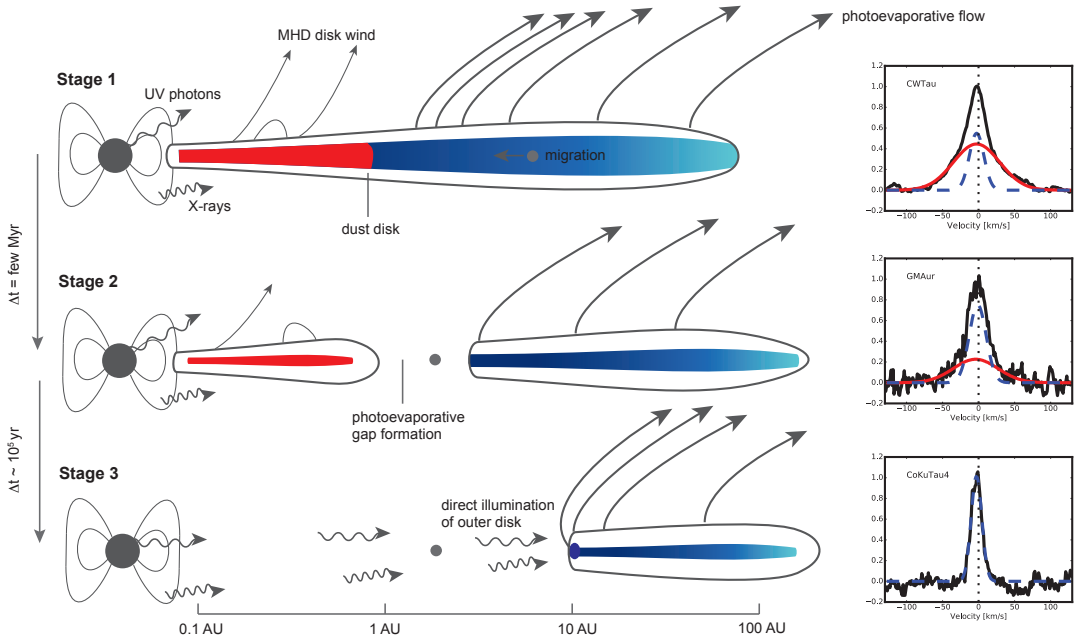

Figure 1.1 Accretion and disk winds (both thermally and magnetically driven) work in tandem throughout the disk's lifetime to deplete the disk of protoplanetary material (predominantly gas). Once the central star is no longer accreting, a majority of the disk's dust and gas has also been dispersed (Ercolano and Pascucci, 2017). There is new evidence that winds may evolve throughout the disk lifetime as well, as shown by the potential disappearance of MHD winds (represented by the red gaussian on the right-hand panels). The panels on the right side of the figure show sample [O I] 6300 Å low velocity emission from disks covering a range of evolutionary stages. The broad component (red gaussian) likely traces material at the base of an MHD wind, while the origin of the narrow component remains more elusive (Image Credit: Ercolano and Pascucci 2017, Figure 5).

(Rigliaco et al. 2013; Natta et al. 2014).

The work conducted in Chapter 4 continues the investigation into the empirical properties of the LVC forbidden lines in TTS to better determine their origin. Our study can be distinguished previous work in that we analyze optical high-resolution spectra from a sample of 33 TTS with disks spanning a larger range of evolutionary stages when compared to Hartigan et al. (1995). Furthermore, our spectral resolution of $\approx$ 7 km/s enables us to better define the kinematic structure of the LVC, to the point that we are able to detect two distinct kinematic components (a broad component and a narrow component) in about half of our sources (see Chapter 4, Section 4.4). We find that a majority of the broad component emission arises close to the central star (within 0.5 AU) with blueshifts frequently greater than 5 km/s. Furthermore, for the broad component of the LVC, we observe the trend between disk inclination and centroid velocity expected of a wind (see Chapter 4, Section 4.6.1). Since the emission likely arises within the gravitational well of the star, it is unlikely to trace a photoevaporative flow, but instead the base of an MHD wind. Although the narrow component is less prevalent amongst our sources, we deduce that it likely traces material slightly farther out in the disk (0.5-5 AU from the central star). We do not observe the expected relation between disk inclination and centroid velocity for the narrow component of LVC, but we are unable to rule out the possibility that this component may be associated with a photoevaporative wind. Our result is surprising in that we find evidence for MHD winds when we previously expected to observe only photoevaporative flows.

2.0 A SURVEY AND ANALYSIS OF COLLEGE STUDENTS' UNDERSTANDING OF PLANET FORMATION BEFORE INSTRUCTION

The contents of this chapter were published in Simon et al. (2018).

2.1 Introduction

From as early on as Kindergarten, students are taught about their "cosmic address" on planet Earth, and "our place in space." Learning about the physical properties of our Solar System (and the planets therein) transcends the K-12 curriculum, and is one of the most common topics taught in undergraduate introductory astronomy courses for non-majors, commonly referred to as "ASTRO 101" (Slater et al., 2001). However, instruction often stops after a brief overview of each planet, and students are left to ponder how our Solar System originated.

Since it is often taken as a General Education requirement, the ASTRO 101 course plays an important role in the science literacy of the these students who will represent our society's future politicians and teachers (Prather et al., 2009; Lawrenz et al., 2005). For these students, ASTRO 101 may the only (and final) science course they take at the college level, so it is critically important that they understand our place in the Universe before potentially beginning careers in government and education.

In the Earth Science section of the *National Science Education Standards* (National Research Council, 1996), the formation of our Solar System was recommended for study in grades 9-12. Furthermore, the evolution of planetary systems was named a content goal for ASTRO 101 after a meeting between astronomy department chairs and education leaders hosted by the American Astronomical Society (Partridge and Greenstein, 2003).

Considering that the topic of planet formation is recommended for study at the high school level, it is reasonable to infer that some ASTRO 101 students have had exposure to the topic before they begin their college astronomy course. To effectively teach planet formation at the college level, it is beneficial to diagnose any pre-instructional ideas or misconceptions students may have on this topic to help them develop a scientifically accurate understanding of how planets form and how solar systems come to exist.

Our current understanding of the Solar System's formation is consistent with the nebular theory, where our Solar System formed from the gravitational collapse of a rotating interstellar cloud (or nebula) composed of gas and dust. Once the interstellar cloud collapsed, it heated up, rotated faster (due to the conservation of angular momentum), and flattened into a disk-pushing material outward. A protostar formed at the center of the disk (eventually becoming our Sun), and the dust grains orbiting the protostar began to collide, accrete material, and grow into planets.

In the outer Solar System, the planets were able grow large enough to gravitationally attract surrounding Hydrogen and Helium gas, resulting in planets with solid cores surrounded by large gaseous envelopes. These massive gaseous envelopes are one of the defining physical features that distinguish the gas (Jupiter and Saturn) and ice giant (Uranus and Neptune) planets in the outer Solar System from the inner terrestrial planets (Mercury, Venus, Earth, and Mars). A more detailed explanation of the planet formation process can be found in Mordasini et al. (2010) and Lissauer (1993).

A general understanding of planet formation has become highly relevant to AS-

TRO 101 courses in light of the discovery of over 3,700 extrasolar planets, or exoplanets (planets outside of our Solar System). The discovery of so many exoplanets with diverse properties raises the issue of whether or not our Solar System is typical. Also significant is the recent discovery of the TRAPPIST-1 system, with seven Earth-sized planets orbiting around a slightly larger than Jupiter-sized host-star (Gillon et al., 2017). Three of these planets are located in their host-star's habitable zone, the region where liquid water could potentially exist on the planets' surface. Instruction on the formation of our Solar System (and the process of planet formation more generally) can lead to a better understanding of the architecture and habitability of exoplanetary systems.

Furthermore, teaching planet formation in ASTRO 101 courses allows students to be exposed to an array of critically important physics and astronomy concepts such as: planetary motion, gravity, angular momentum, accretion, condensation temperature, the physical and chemical properties of rocky and gas giant planets, and the configurations of planetary systems.

The characterization and discovery of thousands of exoplanets has excited public interest and led to enormous media attention. It has also created an intense research focus on the detection of worlds potentially suitable for extraterrestrial life. Astrobiology, the study of life in the universe, has recently become an independent course at colleges and universities that students are able to take in addition to ASTRO 101. After a preliminary analysis of 27 astrobiology course syllabi and lecture slides (see Section 2.3.2), we found that planet formation is rarely covered adequately in these courses before delving into the properties of exoplanetary systems.

Astrobiology is a rapidly developing field, and in terms of content coverage and pedagogy, the mode of instruction has not kept up with the subject. To effectively teach astrobiology courses, and to give suitable attention to planets in a general astronomy course, students must have an understanding of planet formation before they are able to understand the inherent differences between the thousands of solar systems we are continuing to discover, and our own.

Despite its relevance to both the astrobiology and ASTRO 101 course curricu-

lums, the topic of planet formation (from both teaching and assessment perspectives) is poorly represented in the Astronomy Education Research literature, especially at the college level. When developing the Test of Astronomy Standards (TOAST), Slater (2014) noted two topics (the formation of the Solar System, and cosmology) where "high quality test items that reflect our current understanding of students' conceptions were not available [in the literature]" (Slater 2014, p. 8). In this paper, we provide the astronomy education community with the first analysis of a large sample (n=1050) of ASTRO 101 students to show what they understand about the topic of planet formation before any relevant material is taught.

2.2 Review of the Literature

Educational research suggests that, "learning is enhanced when teachers pay attention to the knowledge and beliefs that learners bring to a learning task," and when instructors [use that] "knowledge as a starting point for new instruction" (Bransford et al. 1999, p. 11). According to this way of understanding how people learn, students enter the classroom with a range of prior knowledge that can significantly affect their ability to incorporate new concepts. Constructivist teaching theory argues that, "if students' initial ideas and beliefs are ignored, the understanding that they develop can be very different from what the teacher intends" (Bransford et al. 1999, p. 10).

The inclusion of planets, and by extension, their formation, into the K-12 curriculum, paired with students' religious or cultural viewpoints, indicates that introductory astronomy and planetary science (hereafter, ASTRO 101) students may have a diverse range of viewpoints about this topic. Unlike other topics in astronomy and Earth Science such as the greenhouse effect, stellar evolution, and lunar phases, almost no research has been conducted on students' pre-instructional ideas about planet formation, especially with a large sample of post-secondary learners.

A limited number of published articles address planet formation as part of a larger study on topics within Earth Science and astronomy. A literature review

conducted by Philips (1991) found that students (children, teens, and adults) commonly believed the Sun and planets in our Solar System formed directly from the Big Bang. Adults, in particular, commonly believed that the Universe contains only the planets in our Solar System, and that the Universe is static and unchanging.

Another survey conducted by DeLaughter et al. (1998b) investigated college non-science majors' pre-instructional beliefs about Earth Science and related topics. Of the 18 short-answer questions in the survey, two related to planetary systems. Question 1 asked students to sketch the relationship between the Sun, Earth, and Moon, and asked them to explain their relative motions. More than half (60%) of students drew a sketch of the Earth around the Sun, and the Moon near or around the Earth. Eighteen students (13%) drew the Sun and Moon orbiting around the Earth. A smaller percentage (10%) of students drew the Earth and Moon in different orbits around the Sun.

Question 11 asked students to identify the major differences between the Earth and Jupiter, and to explain what causes these differences. The vast majority of students chose size as the biggest difference between Earth and Jupiter, but students also mentioned temperature, compositional differences, Earth's ability to nurture life, and the planets' difference in location (distance from the Sun). Although students were generally able to correctly identify Jupiter as lifeless, larger, and further from the Sun than planet Earth, more than a quarter of those (28%) who mentioned size in their responses responded incorrectly (DeLaughter et al., 1998b).

An unpublished survey conducted at The University of Arizona in 2015 asked 44 undergraduate preceptors (teaching assistants) the question, "When do you think the Solar System formed in relation to the formation of the Universe?" We note that preceptors are non-science majors who have typically performed well in a previous introductory astronomy class. Although 30 of the 44 preceptors were able to correctly indicate that the Solar System formed after the Big Bang, many did not understand how long after, and answers ranged from "a few minutes after" to "many trillions of years after." Of these 30 preceptors, only eight (18%) were able to correctly explain that the Solar System formed billions of years after the Big Bang.

More than one quarter (27%) of preceptors believed that the Earth formed at the same time as the Universe. One student even stated that, "the Earth has always existed in some form because the Earth is star." The idea that the Earth has always existed, or that the Solar System is formed from the Big Bang, are misconceptions that students carry with them throughout their time in college and beyond if these topics are not addressed early on.

Sharp (1996) found that a significant percentage of students in their 6th year of elementary school in England commonly believed that the Solar System has always existed, and that it formed during the Big Bang. This misconception that the Solar System formed at the same time as the Universe is prevalent at every educational level.

Until recently, surveys published in the astronomy education research literature on the topic of planets focused predominantly on how well college students are able to explain planetary orbits. Yu et al. (2010) found that the most common misconception about Kepler's Laws among the 112 introductory astronomy students in their sample was the belief that planetary orbits were highly eccentric. They attributed this misconception to popular portrayals of planets in orbit around the Sun. These images commonly accentuate the elliptical nature of planetary orbits to emphasize Kepler's first law, or the actual small ellipticity is exaggerated because it is shown at a small inclination angle. More than half (60%) of the students interviewed were unable to provide any information about whether a planet's speed changes at different positions along its orbit (Yu et al., 2010).

A few years ago, however, Plummer et al. (2015) developed a Learning Progression for the Formation of the Solar System, which covered planetary motion as part of a broader range of topics related to how planets form. Example topics included: the physical properties of the planets, the role of gravity, planetary orbits, and accretion (Plummer et al., 2015).

After conducting student interviews, Plummer et al. (2015) developed linear construct maps aimed to describe "the typical levels that students' understanding might be expected to go through given instructional exposure [to the aforementioned

topics]" for K-12 students (Plummer et al. 2015, p. 1395). The college students' answers were originally intended to serve as the upper echelon of understanding for each of the construct maps, but the authors noted that they had interviewed too few students at the upper tier (6 college students in total). This motivated our more robust analysis of college students' understanding of planet formation.

Previous studies in Astronomy Education Research (hereafter, AER) have addressed the topic of planet formation, but there has yet to be a study that addresses this concept at the college level with a large sample size. This study is unique in terms of its sample size, due to the specific and detailed nature of the questions asked to the students, and its ability to characterize their understanding of this topic. This work uses student-supplied response (SSR), open-ended surveys to investigate the range and prevalence of students' ideas, prior to instruction, on the topic of planet formation. This study aims to answer the following research questions:

1. Before instruction, what do ASTRO 101 students know about the topic of planet formation?

2. What are the most common themes, misconceptions, and ideas that appear in student responses?

3. What are the most important topics to emphasize when teaching planet formation in order to address gaps in student understanding?

2.3 Methods

2.3.1 Setting and Participants

This survey was conducted at The University of Arizona, a public university located in Tucson, Arizona. In 2016, undergraduate enrollment exceeded 34,000 students. Approximately 52% of the undergraduate population identifies as female, and 48%

is male. Slightly more than half (51%) of the undergraduate students are Caucasian, 26% are Hispanic, 5% are Asian, and other ethnicities make up 17% of the population. Less than 1% of students reported that their ethnicity was unknown. At this university, 71% of students are in the age range of 18 to 22 (University of Arizona, 2016).

All of the participants in this study were undergraduate students enrolled in introductory astronomy or planetary science courses. Students enrolled in these courses are typically non-science majors taking the courses to fulfill their General Education requirements (Prather et al., 2009). At The University of Arizona, undergraduate students are required to take two 100-level (Tier 1) science courses, and one sophomore-level (Tier 2) science course. Introductory astronomy and planetary science courses are popular and so often fulfill these students' Natural Sciences requirement. Astrobiology is available as a Tier 2 option. We surveyed students in both Tier 1 and Tier 2 courses, but due to the introductory nature of the material taught at both levels, we categorize them both as "ASTRO 101" for the remainder of this work.

Due to the required nature of these courses, students enrolled in ASTRO 101 are typically in the first three years of their undergraduate tenure. The demographics of the students enrolled in these courses are consistent with The University of Arizona's undergraduate population as a whole. In order to conduct educational research with human subjects, The University of Arizona requires approval from the Institutional Review Board (IRB). This study has been approved and classified as "exempt," meaning the project does not pose any harm to the students participating in the study and is not subject to further review.[1]

ASTRO 101 courses at The University of Arizona typically enroll anywhere from 50-150 students (the Tier 1 courses generally have higher enrollments). These courses aim to provide students with an appreciation for the size, scale, and structure of the universe, in addition to providing instruction on a variety of basic topics such

[1]The Development and Validation of the Planet Formation Concept Inventory (PFCI), IRB Approval #1608796697 (see Appendix A)

as Moon phases, the Solar System, the nature of light, and stellar evolution (Slater et al., 2001). Typically, these courses are taught using a traditional, lecture-based format.

2.3.2 Instrument Development

To determine the topics for the SSR questions, we conducted a preliminary analysis of 27 syllabi and lecture slides (when available) from undergraduate introductory astrobiology courses taught predominantly in the United States. At first, we surveyed only astrobiology courses because planet formation is commonly taught in these courses as a precursor to exoplanetary systems. To expand the dataset, we then requested syllabi and lecture slides from instructors with any experience teaching planet formation in an introductory course regardless of the course title. After this request, we analyzed the content of seven additional courses, leading to a total of n = 34 courses surveyed. An analysis of the syllabi, lecture slides, and written notes showed that the following sub-topics were most commonly addressed when teaching planet formation:

1. The nebular theory (gravity and angular momentum)

2. Physical characteristics of the planets and the role condensation temperature plays in determining these characteristics

3. An understanding of accretion (from planetesimals into planets)

4. A conceptual understanding of planetary motion

Based on these findings, we developed six different SSR questions that incorporated elements from these topics. The final list of SSR Questions is presented in Table 2.1.

SSR Question 1 was the most general of the short answer questions, and was

Table 2.1 The Six Student-Supplied Response Survey Questions Administered During the Fall 2016 and Spring 2017 Semesters

Semester	SSR Questions
Fall 2016	1. Describe how our Solar System (planets) formed to the best of your ability. Include drawings when appropriate to help with your explanation.
Fall 2016	2. Describe the characteristics of the planets in our Solar System. What are they made of? Does their composition change with location (distance from the Sun)? Why or why not?
Fall 2016	3. Describe how objects (planets and moons) move in our Solar System. Do planets orbit in the same direction or different directions? Did all of the planets likely form in the same locations they are in now? Explain.
Spring 2017	4. What is the definition of a planet? What makes a planet different than other objects in the Solar System (like the Sun, asteroids, comets, etc.)?
Spring 2017	5a. What is a solar system? What kinds of objects would you expect to find in a solar system? 5b. What is an exoplanet? Would you expect to find exoplanets in our Solar System?
Spring 2017	6. Our Solar System has a very specific layout (architecture). The rocky planets are close to the Sun and the gas giant planets are further away. What does the layout of our Solar System tell us about how it formed? Do you think all solar systems have to follow the same layout?

SSR = student-supplied response

developed so we could explore common themes and misconceptions that appeared when asking students to explain the overall process of planet formation. SSR Questions 2 and 6 probed students' ability to describe and explain the architecture of planetary systems. We developed these questions because it is important for students to understand their solar neighborhood and the layout of our planetary system before they can comprehend the compositional and structural differences between our Solar System and other planetary systems.

SSR Questions 3 and 4 covered the topics of planetary motion and the definition of a planet, respectively. We expected college students would have previous exposure to these topics from high school or middle school, and thus we wanted to evaluate how well they understood these more basic concepts. According to the physical science content standards from the National Science Education Standards (National Research Council, 1996), position and motion of objects is recommended for study as early as the K-4 level. The concept of motion is to be emphasized with the inclusion of forces at the 5th-8th grade levels, and reiterated again at the high school level

(grades 9-12).

College-aged students were typically between the ages of 7-10 years old when the International Astronomical Union (IAU) modified the definition of a planet to the one that is currently upheld: a planet must be in orbit around a Sun, it must be massive enough for its self-gravity to lend to a [nearly] spherical shape, and a planet must clear its orbit of any debris (International Astronomical Union, 2006). The third and final criterion led to the demotion of Pluto to dwarf planet status. Although students are aware that Pluto is no longer a planet, the intent of SSR Question 4 was to probe whether or not students have an understanding of the current definition of a planet, and whether or not they are able to differentiate planets from other celestial objects (e.g. stars, comets, asteroids, moons).

SSR Question 5a was developed because when developing the Test of Astronomy Standards (TOAST), Slater (2014) reviewed the content of three expert position statements that discussed the most critical topics in astronomy. The National Science Education Standards (NSES), developed by the National Research Council (1996); Project 2061: Benchmarks for Science Literacy, developed by the American Association for the Advancement of Science (1993); and the American Astronomical Society's Goals for ASTRO 101 (Partridge and Greenstein, 2003), all converged on the idea that the evolution and structure of the Solar System was one of the most important topics to discuss in introductory astronomy courses. SSR Question 5a evaluated students' understanding of the basic definition of a solar system. After coding SSR Questions 2, it was clear that many students were unable to correctly explain the structure of our Solar System, and many were unable to differentiate between the Solar System and the Universe more generally. As a result, 5a asked students to provide a definition of a solar system in addition to what objects they would expect to find there.

SSR Question 5b asked students to provide the definition of an exoplanet. In the last twenty two years, we have discovered over 3,700 planets that orbit stars other than our Sun (NASA Exoplanet Science Institute, 2018). These exoplanetary systems are often at different evolutionary stages than our own Solar System, and can

thus shed light on the planet formation process. We can use exoplanetary systems with Jupiter-sized planets orbiting on very short orbital periods, for example, as evidence for planetary migration during solar system formation (Armitage, 2010). Articles in the popular media commonly discuss the discovery of new exoplanets, particularly those with characteristics similar to Earth orbiting in the habitable zone around their host star[s]. Due to the relatively recent introduction of exoplanets into the ASTRO 101 curriculum, as well as their extensive coverage in the popular media, we developed SSR Question 5b to explore students' basic understanding of an exoplanet.

2.3.3 Data Acquisition

Students in 13 ASTRO 101 sections were asked to respond to one of six SSR open-ended survey questions relating to the topic of planet formation. Students were answered only one question to ensure they would give a quality response while not taking up too much instructional time. This allowed us to survey the greatest number of students from eight Tier 1 and five Tier 2 courses to determine if the response quality was greater from individuals who had taken a previous astronomy or planetary science course. Since the goal of this work was to determine college students' understanding of planet formation before instruction, we administered the surveys during the first week of the Fall 2016 and Spring 2017 semesters before any relevant material was taught.

In the Fall 2016 semester, we administered SSR Questions 1-3, and in the Spring 2017 semester, we administered SSR Questions 4-6. Although the SSR questions had multiple parts, students were typically able to complete their answers in less than 10 minutes. The SSR questions were randomly distributed among the courses, and among the students within each course. Furthermore, the surveys did not request any information that would allow individual students to be identified. Each student answered one short answer question and provided information regarding whether or not they had taken any previous astronomy courses. By the end of the two semesters, we had received responses from a total of 1,050 students. The number of

responses to individual questions ranged from 167 to 192.

Students were not required to participate in the survey. Due to the anonymous nature of the survey, however, we do not know exactly how many students declined to participate. A comparison of course enrollments to the number of responses we received implies that fewer than 5% of students in attendance when the surveys were administered declined to participate.

2.3.4 Data Analysis

Once the surveys were collected, they were analyzed using a post-hoc coding process consistent with grounded theory (Glaser and Strauss, 1967). We closely followed the procedure outlined in Bailey et al. (2009). First, one of us (the lead author) read through every response to each individual SSR question and recorded common themes, ideas, and misconceptions. These were vetted with two additional education researchers as an independent check of the data. These themes, ideas, and misconceptions were then assigned a specific code, and this process continued until no additional themes emerged from the dataset. The frequency of each code was recorded. Many of the student responses were lengthy, and one response could often be coded for multiple themes. Since each question typically tackled a different aspect of planet formation, the six questions were coded separately.

Many of the broader themes that appeared in the dataset required sub-categories (e.g. Bailey et al. 2009). For example, when analyzing responses to SSR Question 1, we found that many students mentioned that the Solar System formed during the Big Bang. We created a larger umbrella code entitled "Big Bang," and then created a sub-category code, "After Big Bang" to note how many students were able to correctly identify that our Solar System's formation was not coincident with the formation of the Universe (see Table 2.3).

When analyzing each of the six SSR questions, we noted how many students had taken a prior astronomy course, how many responses we were unable to code due to the quality of response, and how many students answered the questions with phrases such as "No Idea" or "I Don't Know." These responses were assigned the

Table 2.2 General Themes for the Total Sample of Responses to Question 1

Code	**Total Responses** (N=170), n (%)
Prev. Astro	41 (24.1)
Not Codable	11 (6.5)
No Idea	9 (5.3)

codes "Prev Astro," "Not Codable," and "No Idea," respectively.

We were unable to code responses if the student did not attempt to answer the question in any meaningful way. For example, when one student was asked to describe the characteristics of the planets in our Solar System, and whether or not planetary composition changes with location (SSR Question 2), the response was, "There are many unique planets in our solar system. Each planet has something of their own that another planet does not. Each planet is effected in their own unique way when dealing with location and distance from the Sun" (SSR Question 2 – Student #182). Responses we were unable to code, and those given the code "No Idea," were not included when determining the frequency of each theme. Thus:

Codable Responses = Total Responses – (Not Codable + No Idea)

For more details, see the headers of Table 2.2 versus Table 2.3. Responses we were unable to code differed slightly from those coded as "miscellaneous." Responses were determined to be miscellaneous when the student attempted to meaningfully answer the question, but their response was not consistent with the larger themes identified from the dataset.

After coding the responses to each question, we performed a second level of analysis. At this stage, students' responses were compared to what would be considered a full credit, correct response on a final exam after learning about planet formation in an ASTRO 101 course. To generate these "correct" responses, we enlisted

Table 2.3 Most Common Themes Identified In Response to Question 1, "Describe how our Solar System (Planets) Formed to the Best of Your Ability. Include Drawings When Appropriate to Help With Your Explanation."

Code	**Codable Responses** (N=150), n (%)
Big Bang	66 (44.0)
After Big Bang	10 (6.7)
Accretion	54 (36.0)
Small particle accretion	38 (25.3)
Large object accretion	15 (10.0)
Gas accretion	12 (8.0)
Gravity/"Pulling" Force	52 (34.7)
Accretion due to gravity	33 (22.0)
Sun's gravity	14 (9.3)
Explosions	27 (18.0)
Star/Supernova explosions	13 (8.7)
Collisions	19 (12.7)
Planets are leftover from star formation	18 (12.0)
Mentioned advanced topics *(e.g. ang. momentum, protoplanetary disk, solar nebula)*	11 (7.3)
Energy	10 (6.7)
Condensation of particles	7 (4.7)
Religion	6 (4.0)
Just defined a solar system	5 (3.3)

Responses (especially lengthy responses) could be coded for more than one theme, so percentages do not necessarily add up to 100. Rows that are indented are subcategories. Responses deemed not codable or given the code "No Idea" were not included in the codable responses.

the help of an Associate Professor of Planetary Science at The University of Arizona who researches planet formation and teaches this topic in ASTRO 101 courses. These professor's responses served as the upper anchor of student responses, and were written in such a way as to mimic a student-level response.

Once the full credit responses were provided, each student response was compared to the full-credit response and subsequently put into one of four possible categories as outlined in Bailey et al. (2009): Correct (C), where the response was complete and did not contain any incorrect statements; Incomplete (I), where the response was missing one or more of the components necessary for a full credit response; Partial (P), where the response was partially correct, but also contained incorrect statements; and Wrong (W), where no part of the students' response matched any component of the full credit response.

For SSR Questions 1, 2, and 4, an additional category was introduced: True but insufficient (T). This category was used when a response included true statements which were off-topic, so they did not answer the question in any significant way (Bailey et al., 2009). Responses that we deemed not codable were either classified as "Wrong" or "True but insufficient" depending on the content of the response. Students who responded "No Idea" were classified as "Wrong" for this component of the analysis.

At first, it was not intended that any of the SSR questions would cover the basic definitions of planets, solar systems, and exoplanets. After coding the first three SSR questions from the Fall 2016 semester, however, it was clear that many students were using these fundamental terms incorrectly, and questions probing their understanding of these definitions were required. As a result, we developed SSR Questions 4 and 5, and administered just SSR Questions 4, 5, and 6 in the Spring 2017 semester.

2.4 Results

2.4.1 SSR Question 1: General Knowledge of Planet Formation

A total of 170 students responded to this question in the Fall 2016 semester, and 150 responses were classified as codable (see Table 2.2). Approximately 44% of those responses attributed solar system formation to the Big Bang in some capacity. Around 15% of students who mentioned the Big Bang claimed that the Solar System formed after the Big Bang, but only two students were able to provide the correct timescale, billions of years after. A substantial fraction (36%) of students mentioned the process of material coming together to form planets, which was coded as "accretion" despite the fact that no student actually used the word accretion in their response. Nearly the same percentage of students (35%) stated that gravity or a "pulling force" played a significant role in the formation of the Solar System.

Almost one quarter of students (22%) coupled the themes of accretion and gravity. A small percentage of students (≈5%) provided more complex responses that were coded for accretion, gravity, and collisions. One of these students stated, "A bunch of rocks drawn into the orbit of the Sun collided to make the rockier planets. The more gaseous planets were probably formed when a bunch of gas, possibly from the remnants of a dead star, got together because of gravity. I really don't know what specific raw materials were the origin, or where they came from exactly. Basically, a bunch of space stuff got together because of gravity" (SSR Question 1–Student #17).

Another student affirmed that, "Lots of cosmic dust starts colliding after a super nova/Big Bang creates a gravitational pull. More and more collide and the celestial objects grow. This continues for billions of years, eventually the clumps get big enough to attract everything near by, sort of 'cleaning it up' and eventually these [clumps] are big enough to be considered planets" (SSR Question 1–Student #140). Although these responses were not entirely correct, since these students were able to identify that collisions lend to accretion, and that the force of gravity plays a major role in the accumulation of material, these higher-level responses had components

Table 2.4 Numerical Results From the Classification of All Responses to Question 1

Classification	**Total Responses** (N=170), n (%)
Correct	3 (1.7)
Incomplete	25 (14.7)
Partial	36 (21.2)
True but Insufficient	12 (7.1)
Wrong	94 (55.3)

Responses that were deemed "Not Codable" were either classified as Wrong or True but Insufficient depending on the content of the response. Students who responded "No Idea" were classified as Wrong for this portion of the analysis.

consistent with an accurate description of planet formation.

Of the 150 codable responses, 11 students (7%) discussed more advanced topics when asked to explain how planets form. For example, one student responded, "It started as a flat disk from a nebula. The rocky planets formed closer to the middle because the material could withstand hot [temperatures], while gaseous planets formed past the freeze zone" (SSR Question 1–Student #136). These student responses were not complete, but they did introduce higher-level concepts that were found in only a small percentage of responses. Interestingly, of 11 students who mentioned more advanced topics in their response, only one student response was also coded for gravity, accretion, and collisions. This finding highlighted that although students may utilize more advanced terminology, they still lack a total understanding of the planet formation process. A more complete list of themes can be found in Table 2.3.[2]

For SSR Question 1, a Correct response included mentioning gravity, collisions, and accretion in addition to the basic understanding that gas giants and terrestrial planets follow slightly different formation processes in terms of what material is predominantly accreted. Only three students were able to incorporate all of the

[2]For ease of reading, the remainder of the tables for this chapter can be found in Appendix B.

components necessary for a Correct response. A typical response to SSR Question 1 was, "The Solar System was created by an explosion called the Big Bang resulting in the formation of our planets in the Solar System" (SSR Question 1–Student #67), and since nearly 50% of students mentioned the Big Bang in regard to planet formation, these responses were predominantly classified as Wrong. The classification breakdown for the entire question is presented in Table 2.4.

2.4.2 SSR Question 2: Planetary Composition and the Architecture of our Solar System

SSR Question 2 asked students to describe the composition and characteristics of the planets in our Solar System, along with whether or not planetary composition changes with location. A total of 192 students responded to this question in the Fall 2016 semester, and 187 responses were classified as codable (see Table B.1). Approximately a quarter of these responses (27%) stated that the rocky planets were closer to the Sun, while the gaseous planets were further away. A smaller fraction (15%) of students stated that there was a region with abundant ice even further from the central star.

This question had multiple components, and many students chose to answer only part of the question and left the other components blank. However, 94% of students answered the component of the question that asked them to explain the composition of the planets in our Solar System. The majority (68%) of students mentioned that the planets are made of a combination of rocks, asteroid fragments, and dust particles (all categorized as solids). Additionally, 60% of students stated that planets are made of gas, and 37% of students more vaguely stated that planets are made of small particles (e.g. molecules, elements, and atoms).

Sixteen students (9%) said that planets are a combination of rock and gas, and an additional 16 students went a step further and claimed that planets are made of a combination of rock, gas, and ice. Nearly a quarter of students (24%) separated the planets into two categories: rocky planets and gas giants, while 5% of students separated the planets into three categories: rocky planets, gas giants, and ice giants.

When asked whether or not planetary composition changes with location, 79% of students replied "Yes." Less than half of students (47%) provided an explanation as to why planetary composition changes with location, but those who did most commonly attributed planetary composition change to the amount of heat received from the Sun at each planet's location (25%). Only three students (2%) correctly attributed the transition from rocky to gas giant planets to the presence of the snow line.

The most complete student response to SSR Question 2 was, "The inner planets Mercury, Venus, Earth, and Mars are the terrestrial or rocky planets. They are composed of rock. The outer gas giant planets Jupiter, Saturn, Uranus, and Neptune are composed of ice and gas – mainly gas with icy cores. Composition changes with location because in the inner solar system, during formation, it was too warm for ices, so the planets formed from rock and accreted small gaseous atmospheres. In the outer solar system, past the snow line, the presence of ice allowed the planets to form bigger icy cores and accrete much larger gaseous atmospheres" (SSR Question 2–Student #190). This student response was significantly more complex than a typical student response to SSR Question 2, which was, "Planets are made of rock and gases. Yes, [their composition does change with distance from the Sun] because the amount of heat they receive changes with distance" (SSR Question 2–Student #151). A complete list of the common themes identified in each component of SSR Question 2 can be found in Tables B.2 - B.5.

For this question, a Correct response required students to distinguish rocky planets from gas giant planets, and ice giant planets. Students were also required to note that rocky planets were located closer to the Sun than the giant planets. Lastly, a complete answer included an explanation of the snow line and its role in separating the rocky planets from the gas giants. Since this question was particularly complex, only 2% of students answered the question completely. A majority of the responses were classified as Partial (51%) since almost every student was able to provide some explanation about the basic composition of the planets in our Solar System. The classification of all of the student responses to SSR Question 2 can be found in Table

B.6.

2.4.3 SSR Question 3: Planetary Motion and Migration

A total of 168 students responded to this question in the Fall 2016 semester, and 166 responses were classified as codable (see Table B.7). More than half (57%) of these responses correctly identified that the planets in our Solar System orbit the Sun in the same direction, and an additional 10% of students went on to say that these objects orbit in the same direction but at different speeds. Only one student was able to connect planets orbiting in the same direction to the planet formation process. This student stated, "Yes [planets orbit around the Sun in the same direction]. Due to the planetary formation process, in which planets form out of a swirling vortex of dust, gas, and ice around a new star, they orbit in the direction this vortex was spinning" (SSR Question 3–Student #168).

Six students (4%) mentioned that the planets orbit around the Sun on elliptical orbits, a concept that is taught at both the middle school and high school levels. A large majority (84%) of students affirmed that the planets likely did not form in their present locations, and nearly three quarters (73%) attempted to provide an explanation. The most common explanation (28%) was that planets were pulled into their current orbits due to the force of gravity, or the misconception that planets could not have formed in their current location because objects in space are constantly moving as the Universe is expanding (22%). A small percentage (8%) of students alluded to the concept of planetary migration, while an even smaller percentage of students attributed planetary motion to collisions with large objects (7%). A complete list of the common themes identified in each component of SSR Question 3 can be found in Tables B.8-B.10.

A Correct response to SSR Question 3 included a statement that planets orbit the Sun in the same direction on elliptical orbits. Additionally, Correct responses involved an understanding that planets likely did not form in the exact locations they are in now, and that planetary migration was responsible but not well understood.

There were very few Correct responses to this question because even though

nearly 10% of students alluded to migration in their responses, only 4% of students mentioned the elliptical nature of planetary orbits. It was surprising that twice as many students mentioned migration as mentioned the elliptical orbits. This could have been due to the phrasing of the question, and if this question were to be administered again, it would be beneficial to ask students about the shape of planetary orbits more explicitly. The classification of all of the student responses to SSR Question 3 can be found in Table B.11.

2.4.4 SSR Question 4: Basic Understanding of a Planet

A total of 167 students responded to this question in the Spring 2017 semester, and 155 responses were classified as codable (see Table 8a). More than half (57%) of these responses mentioned that a planet must orbit a sun or star. Nearly a quarter (23%) of students defined a planet in terms of its physical composition, claiming a planet must be made of rock or gas. Nearly the same percentage (22%) of responses stated that a planet must be a certain size, and 10% of students stated that a planet must be bigger than an asteroid, comet, or moon. Although a substantial percentage (19%) of students mentioned that a planet must have a distinct orbital path, only six students (4%) stated that a planet must clear its orbit.

One example of a particularly comprehensive answer to SSR Question 4 was, "A planet is an object that is formed during the creation of a solar system that is large enough to become spherical by its own gravity and has cleared its orbit of other objects. It is different than other objects like the Sun because it isn't large enough to start fusion. Asteroids and comets aren't large enough to become spherical by its own gravity and they haven't cleared their orbits of other objects. Planetoids such as Pluto are large enough to become spherical but they haven't cleared their orbits of other objects" (SSR Question 4–Student #146). Although this student had not yet taken a previous astronomy course, they were able to correctly pinpoint the reason Pluto is no longer classified as a planet. Furthermore, this student was able to provide scientifically accurate explanations when distinguishing a planet from other objects in the Solar System, in addition to correctly mentioning keywords and

phrases such as "spherical" and "self-gravity."

Another student directly addressed Pluto's demotion to dwarf planet status by stating, "A planet is a satellite around a star that is large enough to clean up the area around its orbit. For instance, Earth has cleaned up the surrounding materials while Pluto has not. This is why Pluto is not considered a planet" (SSR Question 4–Student #151). These responses were significantly more detailed than a typical response to SSR Question 4, which was, "A planet is a mass that orbits around a star." (SSR Question 4–Student #64). Of the 155 codable responses, only three of them (2%) addressed every component of the working IAU definition of a planet. A complete list of the common themes identified in SSR Question 4 can be found in Table B.13.

A complete response to SSR Question 4 included mentioning that a planet revolves around a sun (star), that it is massive enough to be roughly spherical in shape, and that a planet clears its orbit. Furthermore, a complete answer also discussed at least one characteristic of a planet that separates it from other celestial objects (e.g. planets do not fuse hydrogen, planets revolve around stars while smaller bodies revolve around planets, smaller bodies are not necessarily spherical in shape, etc.).

The majority of responses were classified as either Partial (33%) or Incomplete (22%), but a large percentage of responses (40%) were classified as Wrong. Responses were typically marked Wrong if students neglected to mention any of the components in the working IAU definition of a planet, and instead mentioned that planets must, for example, have an atmosphere, have moons, or have an environment potentially sustainable for life. The classification of all of the student responses to SSR Question 4 can be found in Table B.14.

2.4.5 SSR Question 5: The Solar System and Exoplanets

SSR Question 5 covered two distinct topics: the definition of a solar system (SSR Question 5a), and the definition of an exoplanet (SSR Question 5b). The original intention was to analyze both components of SSR Question 5 together, but only 60% of the students who were given SSR Question 5 attempted to answer 5b. Due to the

distinct nature of the topics covered, and the variation in the number of students that answered each component, we coded questions 5a and 5b separately as shown in Tables B.15-B.22.

SSR Question 5a: Basic Understanding of a Solar System

A total of 175 students responded to this question in the Spring 2017 semester, and 172 responses were classified as codable (see Table B.15). Slightly more than half (55%) of these responses stated that a solar system is a set of planets (or celestial bodies) orbiting a star. Nearly a quarter of students (22%) provided a more vague response and mentioned that a solar system is a set of objects close to each other in space. Seven students (4%) believed that the Milky Way Galaxy is part of the Solar System. When asked what objects students would expect to find in a solar system, the most common responses were planets (70%), multiple (many) stars (34%), moons (32%), asteroids (30%), and one central star/sun (23%). Thirteen students (8%) stated that galaxies and/or nebulae were part of a typical solar system. A complete list of the common themes identified in SSR Question 5a can be found in Tables B.16 and B.17.

A Correct response to SSR Question 5a included stating that a solar system is typically a system with a single star and planets orbiting around it. A correct response also included correctly identifying at least two additional objects that can be found in a solar system (e.g. comets, moons, asteroids, dwarf planets etc). This question had the largest percentage of Correct responses among all six SSR Questions. An example of a Correct response was, "The Solar System is comprised of objects, large and small that orbit a star. All of them are on the same plane normally. You would likely find planets moving around the sun and moons moving around the planets. Then there are asteroids, comets, and dwarf planets" (SSR Question 5a–Student #173). The majority of responses were classified as Partial (41%), but there were 24 Correct responses (14%), and only 29 responses were classified as Wrong (17%). The full classification schematic for SSR Question 5a can be found in Table B.18.

SSR Question 5b: The Introduction of Exoplanets

As mentioned in Section 2.4.5, a total of 175 students responded to Question 5 in the Spring 2017 semester. Of these 175, only 105 students (60%) attempted to answer Question 5b (see Table B.15). One-third of these students (33%) correctly defined an exoplanet as a planet outside of our Solar System. The most common misconceptions found in this sample were that an exoplanet is a planet orbiting at the edge of our own Solar System (15%), and that exoplanets and dwarf planets are synonymous (12%). Nearly 10% of students explicitly stated that Pluto is an example of an exoplanet. One student stated, for example, "An exoplanet is a celestial body which could be considered a planet, but doesn't quite meet all the scientific criteria, also known as, in our own solar system, Pluto" (SSR Question 5b–Student #162).

When asked directly if students would expect to find exoplanets in our own Solar System, 32% said 'Yes', only a slightly larger percentage (36%) said 'No,' and 29% of students did not provide a response. A more complete list of the common themes identified in SSR Question 5b can be found in Tables B.20 and B.21.

A Correct response to SSR Question 5b included defining an exoplanet either as a planet outside our Solar System, or a planet that orbits a star other than our Sun. A Correct response also implied that, by definition, we would not expect to find exoplanets in our own Solar System. For this particular question, student responses were typically classified as either Correct (23%) or Wrong (68%). There were very few Partial or Incomplete responses. The full classification schematic for SSR Question 5b can be found in Table B.22.

2.4.6 SSR Question 6: Solar System Formation and its Impact on Planetary System Architectures

The goal in developing SSR Question 6 was to take the themes addressed in previous SSR Questions and apply students' knowledge of planet formation to solar system architectures. A total of 178 students responded to this question in the Spring

2017 semester, and 172 responses were classified as codable (see Table B.23). This question was the most difficult to code, since the range of answers varied significantly and there was no 'typical' response to this question. Approximately one-quarter (26%) of students stated that gravity "helped" our Solar System form. A non-negligable percentage (19%) of students went on to explain in more detail that closest to the Sun, gravity was strong enough to pull the denser, rockier planets in. These students held the misconception that because terrestrial planets have higher densities, they are more massive than gas giant planets, and a greater deal of gravity was required to pull them into their current orbits around the Sun.

Nearly one-fifth (17%) of students stated that the Sun's temperature directly affects the layout of our Solar System, but could not state a particular reason. Ten students (6%) asserted that the layout of the planets in our Solar System was directly related to the order in which they formed. Only four students (2%) mentioned the snow line in their responses. One of these students asserted, "[The layout of our Solar System] tells us that planets inside the frost line formed from colliding rocks and metals and the gas giants formed outside the frost line collecting ices and hydrogen compounds that stayed frozen due to the distance from the Sun" (SSR Question 6–Student #113). When asked if all solar systems have to mirror the layout of our own, 34% of students said "Yes", 55% said "No," 9% of students did not provide a response, and 2% of students said "Both Yes and No." A complete list of the common themes identified in SSR Question 6 can be found in Tables B.24 and B.25.

Similar to SSR Question 2, a Correct response to SSR Question 6 included mentioning that the distinction between rocky and gas giant planets in our Solar System is due to the location of the snow line and the condensation temperatures of different elements during planet formation. Students were also required to mention that due to the differing condensation temperatures of metals, rocky minerals, and hydrogen compounds, we would expect that (in other solar systems) gas giant planets would be located further away from the central star while rocky planets would be located closer in, like in our Solar System. Due to the complexity of this question, if students said that the layout of other solar systems would likely follow a similar trend

to our own, their responses were classified as Correct even if they did not provide a fully comprehensive explanation.

One student who had *not* taken a previous astronomy course provided the response, "The idea right now is that the rocky planets formed close to the Sun because that was all that could survive the hotter temperatures. The gas planets formed further away where it was cooler. For the most part, gas planets have to form further out, but we now know that a bit of them move in closer to their star (e.g. Hot Jupiters)" (SSR Question 6–Student #91).

Science majors in upper level astronomy courses would be expected to know about exoplanetary systems with Jupiter-sized planets on orbits well within the orbit of Mercury, and be able to attribute this architectural difference to planetary migration in gaseous disks. Students in 100 and 200-level courses were not required to make such interpretations to have their responses marked Correct. For this question, only two students provided Correct responses. The vast majority of responses (85%) were classified as Wrong. The classification of all of the student responses can be found in Table B.26.

2.5 Discussion

2.5.1 Summary of Significant Results

We used the SSR questions listed in Table 2.1 to compile and analyze the frequency of (n = 1050) students' ideas on the topic of planet formation during the Fall 2016 and Spring 2017 semesters, before relevant instruction. The most common misconception students' had was that nearly 50% of students who answered SSR Question 1 asserted that our Solar System either formed directly from the Big Bang, or as a direct result of the Big Bang. These findings were consistent with previous studies that analyzed fundamental misconceptions in astronomy (Prather et al. 2002; Simonelli and Pilachowski 2003; Wallace et al. 2012; Bailey et al. 2012).

Furthermore, when probing students' understanding of the Big Bang specifically, Prather et al. (2002) found that 80% of college students asserted that the Big Bang

was an explosion of pre-existing matter. We found that nearly 20% of students who answered SSR Question 1 attributed the formation of the Solar System to a large-scale explosion (although we did not ask students to explain whether or not they believed matter existed before the Big Bang), which is a physically incorrect characterization of the Big Bang (Wallace et al., 2012). College students' commonly held belief that our Solar System formed from the Big Bang demonstrates that ASTRO 101 instructors need to provide students with a lesson on cosmological time before teaching planet formation. Students must understand that the formation of the Universe and the formation of the Solar System are independent events taking place on vastly different scales, and separated in time by nine billion years.

Over a third of students (36%) who were asked to describe the general process of planet formation (SSR Question 1) were able to correctly identify that planets form by accretion. Although students did not explicitly use the term "accretion," they were able to describe a process of material coming together due to the force gravity to form planets (see Section 2.4.1). Students described accretion as either the accumulation of small particles (25%), the accretion of rocks and asteroid-sized bodies (10%), the accretion of gaseous material (8%), or some combination of the three. Nearly a quarter (22%) of students asserted that accretion occurs due to the force of gravity (a pulling force) driving chunks of material towards each other.

Nearly 10% of students who answered SSR Question 1, and 8% of students who answered SSR Question 6 claimed that the Sun's gravity specifically acts as a catalyst for accretion. Since the Sun makes up the vast majority of our Solar System's mass, students tend to view the presence of the Sun as a significant factor in determining a planet's gravity (Williamson and Willoughby, 2012). When explaining the process of accretion, instructors should make it clear that a planet is massive enough to have its own gravity, and it is the gravity of the growing planet that attracts surrounding material to be accreted.

SSR Question 6 also illustrated that many students have a difficult time distinguishing mass and density. Nearly 20% of students who answered Question 6 claimed that the rocky planets in our Solar System are closer to the Sun because

they are denser, more massive, and thus experience a larger force of gravity. One student stated, "After the Big Bang, more dense and larger/more massive planets did not travel as far as those which are 'lighter.' This is explained with the gravity formula where larger mass means more attraction, holding 'heavier' planets closer to the Sun and 'lighter' ones further away" (SSR Question 6–Student #153). Another student claimed that, "Since the rocky planets are more dense and weigh more than the gas planets, they gravitate towards the Sun" (SSR Question 6–Student #108). These responses clearly demonstrate that students assume that higher density means higher mass without taking a planet's size into account (Williamson and Willoughby, 2012).

In the case of our Solar System's planets, the gas giant planets are significantly more massive than the terrestrial planets despite the fact that gas is less dense than rock, and in fact they almost certainly have rocky cores more massive than the terrestrial planets. This can be attributed to the fact that in the outer Solar System past the snow line (where the gas giant planets form), the surface density of solids increases by a factor of $\approx$3, and planets are able to grow large enough to accrete a gaseous envelope (Kennedy and Kenyon, 2008). The combination of large icy and rocky cores with significant gaseous envelopes makes the gas giant planets more massive than the inner, rocky planets.

Students' inability to distinguish mass and density can lead to an incorrect understanding of the role of gravity. This misconception is particularly difficult to address since the density of an object indirectly provides information about an object's mass (Williamson and Willoughby, 2012). As a result, students are not only conflating density with mass, but also misapplying the gravitational force law. In ASTRO 101 courses, it is important to clearly define mass and density before delving into the gravity equation. Furthermore, it is important for instructors to state that gravity is directly proportional to a planet's mass, and that the inner planets do not have more gravity just because they are located close the Sun. To do this, instructors could simply use our Solar System's planets to illustrate how higher density does not necessarily equal larger mass, and by extension, a stronger gravitational

force.

SSR Question 2 explored students' understanding of planetary compositions and solar system architectures. An in depth understanding of planetary composition is required before students are able to fully comprehend the process of planet formation and its application to planetary systems beyond our own. Most students were able to correctly identify that planets are made of primarily solid rocky material (68% of responses), gas (60%), and ice (26%). It is particularly interesting to note that over a quarter of students who answered SSR Question 2 mentioned ice as a primary component of a planet's composition, as "the notion of grouping planets as rocky, gaseous, and icy is relatively new to the field of astronomy" (Plummer et al. 2015, p. 1390).

When asked to explain if planetary composition changes with location, and why, less than half of students provided a response, and those who did primarily attributed compositional differences to the amount of heat given off by the Sun at each planet's location. Students who answered SSR Question 2 (and those who answered SSR Question 6) affirmed that the Sun's temperature affects the layout of our Solar System. What they fail to understand is the fact that it is the condensation temperature of elements rather than the Sun's temperature that governs our Solar System's architecture. Although students are correct that closer to the Sun the temperature is hotter, they seem not to understand that planetary composition is primarily determined by the condensation of refractory elements (like rocks and metals) at high temperatures and volatiles (e.g. hydrogen compounds) at lower temperatures past the snow line (Lodders, 2003).

Although condensation temperature is not a trivial concept to teach, it is important that the condensation of elements and the role of the snow line are discussed when teaching planet formation at the ASTRO 101 level. Otherwise, students will continue to leave ASTRO 101 courses with a superficial understanding of the physical characteristics of the planets, and be unable to explain the layout of our Solar System. This will limit them from being able to draw any parallels between the composition and locations of the planets in our own Solar System and those that

are being discovered around other stars.

Additionally, SSR Question 2 emphasized students' inability to take basic concepts introduced in ASTRO 101 and apply these concepts to explain more detailed processes or phenomena. SSR Question 2 was broken down into four parts for analysis (see Tables B.2-B.5). When students were asked, 'What are the planets [in our Solar System] made of?' 94% of students provided a response. When asked to explain why or why not planetary composition changes with distance from the Sun, however, less than half (47%) of students attempted a response.

Furthermore, with the exception of SSR Question 5b (on the topic of exoplanets), the questions that had the largest percentage of responses classified as 'Wrong' were SSR Questions 1 and 6 (see Figure 2.1). These were the two questions that required students to apply concepts like gravity, planetary composition, and temperature to explain the more complex process of planet formation. These findings shed light on the fact that there needs to be an emphasis on the application of physical principles in ASTRO 101 courses, and not simply an overview of basic astronomy concepts.

As previously mentioned in Sections 2.4.4 and 2.4.5, SSR Questions 4 and 5 were administered in the Spring 2017 semester after coding SSR Questions 1-3. It was clear from the Fall 2016 responses that many students were unable to differentiate a planet from a star, and others believed that the galaxy (or nebulae) exist[s] inside our Solar System. When asked to specifically define a planet, 3% of students who answered SSR Question 4 claimed that a planet and a star were analogous, and only 5% clearly stated that a planet must be smaller than a star. Bailey et al. (2009) found that 6% of students asked to respond to the question, "Is there a difference between a star and a planet?" selected 'No,' and an additional ten students ($\approx$5%) selected 'both yes and no' for their response.

ASTRO 101 students have a difficult time comprehending the basic definitions of celestial objects, as well as their size and scale relative to each other. This is made even clearer when analyzing students' understanding of the relationship between the Solar System, Milky Way Galaxy, and Universe (Simonelli and Pilachowski, 2003). Bailey et al. (2012) found that among nearly 200 introductory astronomy students,

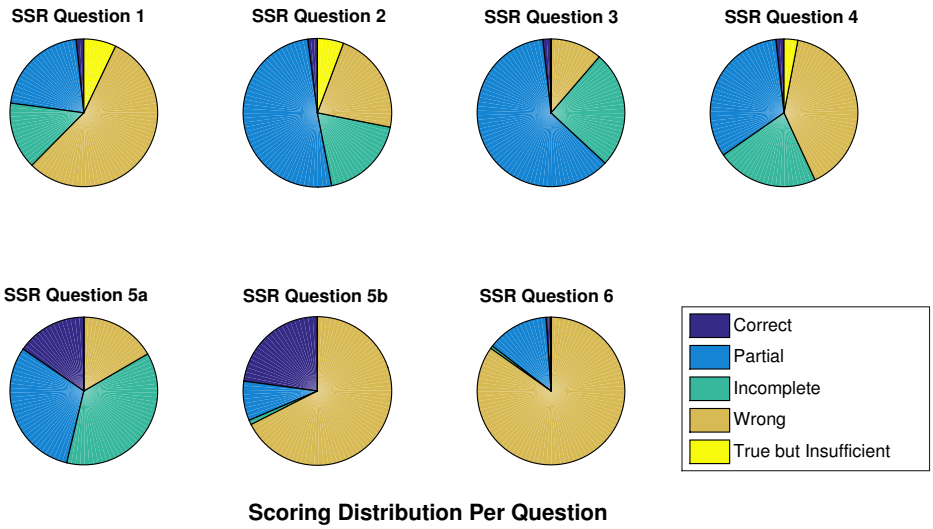

Figure 2.1 Classification breakdown for all six SSR Questions. Question 5 was split into two parts: 5a and 5b for coding purposes (see Section 2.4.5). Questions 1 and 6, which tested students' understanding of complex processes, and Question 5b, which tested students' understanding of exoplanets, had the largest percentage of responses classified as Wrong. Question 5a, which tested students' understanding of the basic definition of a solar system, had the largest percentage of responses classified as Correct and Incomplete. Questions 2, 3, and 4 had a substantial percentage of responses classified as Partial.

52 of them (26%) provided an incorrect response when asked to describe this relationship, and students often confused solar system and galaxy. Of the 172 codable responses to SSR Question 5, thirteen students responded that they expected to find galaxies or nebulae within our Solar System, and 7 students deliberately stated that the Solar System is a region that includes the Milky Way Galaxy.

Although these percentages (8% and 4% respectively) were not as high as those found by Bailey et al. (2012), there were additional student responses that mentioned the Solar System consists of many stars (34%), including specifically the constellations that make up our night sky (2%). It is crucial that instructors not assume that students are able to distinguish celestial bodies from each other, or that they have an even basic understanding of these definitions. Before lecturing on the topic of planet formation, instructors should provide an overview of basic definitions, as well as spend time discussing the size and scale of the Universe. Non-science majors do not have an intuitive grasp of the huge range of scales of time and space encountered in astronomy, so they need initial orientation.

SSR Question 5b asked students to define an exoplanet at the most basic level. As mentioned in Section 2.4.5, only 60% of students who answered SSR Question 5 even attempted to provide an answer to the exoplanet component. This was particularly surprising, given the high visibility of exoplanet discovery over the last decade. Furthermore, the discovery of potentially habitable exoplanets is often publicized on social media and online news platforms. Students' inability to even attempt SSR Question 5b highlights the need for professors to teach topics that are at the forefront of current astronomical research (Pasachoff, 2002). Since these topics appear in magazines and news reports, it is in the best interest of ASTRO 101 professors to help their students understand the significance behind these discoveries.

2.5.2 The Impact of Previous Exposure to Astronomy

Of the 1,050 students surveyed in the Fall 2016 and Spring 2017 semesters, 221 had taken a previous astronomy course at the high school, college, or community-college level. One limitation of this work was that we did not ask students if they had

studied planet formation in their previous astronomy course, so we were unable to track students' retention of the material. Since nearly a quarter of students who answered SSR Questions 1-6 had taken a previous astronomy course, we compared their level of understanding to students who had never seen the material at higher than an elementary school level. Almost one-tenth of students (9%) who had taken a previous astronomy course provided a response to their respective SSR Question that was classified as Correct. Students who had not taken a previous astronomy course provided a Correct response 4% of the time.

Approximately one quarter (22%) of students who had previous astronomy background knowledge provided Incomplete responses. A smaller percentage of students (15%) who had not taken a previous astronomy course provided responses that were classified as Incomplete. Interestingly, nearly identical percentages of students provided Partial credit responses (36% and 34%) whether they had previous astronomy or no previous astronomy, respectively. Students with no previous astronomy courses contributed a significantly larger percentage of responses classified as Wrong (44% versus 31%). Although the classification 'True but Insufficient' was not commonly used for either group, students who had not taken a previous astronomy course were twice as likely to provide a True but Insufficient response. A graphical representation of these percentage differences can be found in Figure 2.2.

It is not surprising that taking a prior astronomy course yielded a greater percentage of Correct and Incomplete responses when compared to students who were not familiar with the material. A portion of the SSR Questions did explore students' understanding of topics taught at the elementary school-level (the definition of a planet and a solar system, planetary orbits, gravity, etc.). Despite previous exposure to some of the material, the small fraction of Correct and Incomplete responses from both groups emphasizes instructors' need to incorporate classroom practices that promote retention of material from an early age. Furthermore, the limited number of Correct and Incomplete responses highlights the complex nature of the topic of planet formation, and the need to better familiarize students with the physical concepts behind the creation of their solar neighborhood.

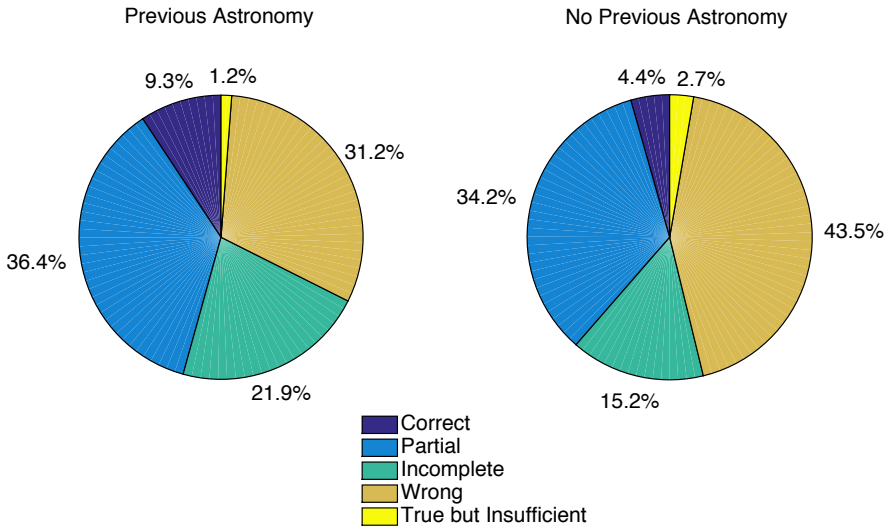

Figure 2.2 The percentage of students from each category (previous astronomy versus no previous astronomy) whose responses were classified as Correct, Partial, Incomplete, Wrong, or True but Insufficient. Students who had taken a previous astronomy course were more than twice as likely to respond correctly to their given SSR question when compared to students with no previous astronomy background. Students with no previous astronomy course (at higher than an elementary school level) typically provided responses that were classified as either Wrong or Partial. Due to the complex nature of SSR Questions 1, 5b, and 6, even with previous astronomy knowledge, student responses were still typically classified as either Wrong or Partial. Overall, there was a greater percentage of Incomplete and Correct responses amongst the six SSR questions from students with previous astronomy coursework.

2.6 Conclusion

The goal of this work was to evaluate college-students' comprehension on the topic of planet formation before any relevant instruction. We did this by providing 1,050 ASTRO 101 students with one of six short answer questions on relevant topics. After analyzing their responses, we learned that a substantial percentage of these students are missing fundamental information about planetary systems (basic definitions, an understanding of gravity, solar system architectures, timescales, physical processes associated with solar system formation), and this lack of foundational knowledge is preventing them from explaining the process of planet formation.

The most common themes, ideas, and misconceptions collected from the dataset are currently being used to develop the Planet Formation Concept Inventory (PFCI). This instrument will allow us to more efficiently measure how well students understand these concepts both before and after adequate instruction. This instrument will also allow instructors to test new pieces of interactive pedagogy that may be developed in the future to teach planet formation in ASTRO 101 and astrobiology courses. Before this pedagogy is developed, however, it is essential to identify the major holes in students' understanding. Students need a secure understanding of the physical and chemical processes that govern the creation of our own Solar System before being able to adequately address the fascinating but complex subject of the worlds being discovered beyond our Solar System.

3.0 THE DEVELOPMENT AND VALIDATION OF THE PLANET FORMATION CONCEPT INVENTORY (PFCI)

3.1 Introduction

A concept inventory is a multiple-choice style instrument that addresses a single topic or closely related set of topics. Concept inventories should be written in a way that emulates students' natural language, and, as a result, scientific jargon should be minimal. Most importantly, concept inventories can be distinguished from traditional multiple-choice tests in that they use students' preinstructional ideas and misconceptions as the basis of their distractors (incorrect answer choices) (Bailey, 2009). Concept inventories are particularly useful for assessing students' pre and post-instructional conceptual understanding of a specific topic, and the efficacy of pieces of pedagogy developed to teach that topic (e.g. Lopresto and Murrell 2009; Prather et al. 2004). In astronomy and planetary science, concept inventories have already been developed on the topics of: stars and their properties (Bailey et al., 2011), the greenhouse effect (Keller, 2006), light and spectroscopy (Bardar et al., 2006), lunar phases (Lindell and Olsen, 2002), and Newtonian gravity (Williamson et al., 2013).

The Planet Formation Concept Inventory (PFCI) explores the many conceptual and reasoning difficulties students face when learning about planetary origins (Simon et al. 2018; Plummer et al. 2015). The PFCI was developed, in particular, to assess student understanding of planet formation in general education undergraduate astronomy and planetary science courses, typically referred to as "ASTRO 101."

The topic of planet formation has become increasingly relevant to the introductory astronomy curriculum as the characterization and discovery of thousands of planets outside of our Solar System (exoplanets) becomes ever more prevalent. Teaching students about the formation of our Solar System (and the process of planet formation on a more general scale) lends to a better understanding of the origin and evolution of exoplanetary systems more generally. As a result, it is imperative that introductory students have a preliminary understanding of planet formation before they are able to draw comparisons between the thousands of solar systems discovered, and our own stellar neighborhood.

Prior research has shown that students come into their ASTRO 101 courses with a variety of preinstructional ideas on the evolution of planetary systems (Simon et al., 2018). These ideas can cloud their ability to develop a comprehensive understanding of the topic. While a thorough explanation of students' conceptual and reasoning difficulties is beyond the scope of this work, three common examples include:

- Students are frequently unable to distinguish the formation of the Universe and the formation of our Solar System - they assert that the Solar System formed as a direct result of the Big Bang.

- Students lack a model connecting the condensation temperature of specific elements (metals, silicates, and hydrogen compounds) to why planetary composition changes with location. Students more typically attribute the compositional differences between the planets in our Solar System to how much heat they are receiving from the Sun, and remark that the amount of gravity at their specific location directly affects planetary composition.

- Students have a difficult time explaining that a solar system typically consists of a single star with planets orbiting around it (and moons potentially orbiting those planets). Many students assert that the Milky Way Galaxy is part of our Solar System and that our Solar System has many stars, including the constellations visible in the night sky.

An in depth explanation of these pre-instructional ideas related to planet formation can be found in Simon et al. (2018) and the references therein.

The development and validation of the PFCI was motivated not only by the topic of planet formation's aforementioned relevance to ASTRO 101 curriculum, but also due to the fact that the astronomy education research literature is incomplete when it comes to studies that reflect our understanding of students' perceptions on planetary origins (e.g. Slater 2014). The PFCI is the first concept inventory that addresses topics central to an understanding of planet formation. The research question we aim to address through this work is to what extent can we quantitatively demonstrate that the PFCI is a reliable and valid instrument that can be successfully utilized to assess student learning on the topic of planet formation before and after instruction.

3.2 Methods

3.2.1 Concept Domain

The PFCI's concept domain was determined after an analysis of course materials from 34 undergraduate courses that covered planet formation as part of their curriculum; as well as after a thorough analysis of students' pre-instructional misconceptions on relevant topics (Simon et al., 2018). The concept domain covered by the PFCI addresses the following topics:

- the physical composition of the planets in our Solar System
- condensation temperature - and the role the condensation of elements plays in determining the physical characteristics of the planets in our Solar System
- the accretion process
- planetary motion
- a fundamental understanding of planetary systems (e.g. definitions of a planet, exoplanet, and solar system)

- the nebular theory (and the fact that the formation of the Universe and the formation of our Solar System are independent events)

Each of these topics are represented by at least two questions on the PFCI.

3.2.2 Test Question/Item Development

To evaluate students' ideas on the topic of planet formation most efficiently, and for ease of scoring and analysis, we selected a multiple-choice format for this instrument. All of the items on the PFCI originated from prior research into students' understanding of planet formation before instruction (Simon et al. 2018; Plummer et al. 2015). When developing each of the multiple-choice items on the PFCI, we commonly referred back to the 31 item writing guidelines for classroom assessment described in Haladyna et al. (2002). As a result, each of the multiple-choice items consisted of a question stem followed by either four or five answer choices. Each item had a clearly worded correct answer, and the rest of the answer choices consisted of common student naive ideas on the topic being addressed, and served as distractors. A good distractor "should appear incorrect to someone who fully understands the concept addressed by the item [stem] but should also appear reasonable to someone who does not understand the concept, therefore making them attractive response options" (Bardar et al. 2006, p. 105). We wrote each of the item distractors in students' natural language, and limited scientific jargon as much as possible. After the original set of test items were developed, they were reviewed by a faculty member whose research is planet formation-focused and who has experience teaching planet formation in general education undergraduate introductory courses.

3.2.3 Preliminary Versions of the PFCI

The PFCI was developed using an iterative design process over 4 semesters. The first version of the PFCI consisted of 20 multiple-choice questions and 3 demographic questions (major, gender, previous planet formation exposure). It was administered to six introductory and planetary science courses (N = 455 students) at The Uni-

versity of Arizona at the beginning of the Fall 2017 semester before any relevant material was taught (this version was only administered as a pre-test). Students enrolled in these courses were overwhelmingly non-majors fulfilling their college's natural science requirement. The PFCI was administered to students in both 100 and 200 - level courses, but considering neither course has a science pre-requisite, we refer to *both* the 100 and 200 - level courses as ASTRO 101 for the remainder of this work.

For the first administration of the PFCI, we broke the 20 content questions into three "mini" concept inventories. Students (at random) either answered questions 1-7, 8-14, or 15-20 (along with the three demographic questions). Students were instructed not to put their names on the concept inventory in order to preserve their anonymity. In addition to selecting an answer choice, students were asked to provide 1-2 sentences explaining why they selected a particular answer (Bailey et al. 2011; Keller 2006). Students were also encouraged to provide feedback regarding the clarity of the question stem and the different answer choices. This multiple-choice with explanation of reasoning (MCER) approach allowed us to determine whether the students were interpreting the questions on the PFCI as we intended. Our analysis of students' MCER responses also allowed us to better determine the clarity and quality of the test questions, and to gage if students were using prior knowledge correctly or incorrectly when selecting an answer choice. We did not perform a statistical analysis of the PFCI Version 1 since it was broken into three mini concept inventories. Instead, we coded students' MCER responses using the same post-hoc coding method described in detail in Simon et al. (2018). The MCER responses did not lend to any additional content codes from those uncovered in Simon et al. (2018), but our analysis of student responses did lead to the revision of seven test items and the creation of one additional test item. Of the seven test items we amended at this stage: three items had distractor(s) that were revised for clarity/use of less technical jargon, one item had the stem reworded for clarity, and three test items required a distractor to be eliminated completely. These revisions and the addition of a 21^{st} item lent to the second version of the PFCI.

Version 2 was administered to two ASTRO 101 courses (N = 141 students) during the Spring 2018 semester. This version was administered in its entirety in typical multiple-choice format at the end of the semester (just post-test). Once again, students were instructed not to put their names on the concept inventory in order to preserve their anonymity. The second version of the PFCI consisted of 21 content items, and the same 3 demographic questions from Version 1. The average score on the PFCI Version 2 was 10.4/21 (49%) with a standard deviation of 3.6 (17%). We performed a brief statistical analysis on this version, including calculating the instrument Cronbach's alpha (α) = 0.681. Item difficulty values (p) for the PFCI Version 2 ranged from 0.18 - 0.81 with an average $p = 0.49$. Item discrimination (ρ_{pbis}) values ranged from 0.01 - 0.43 with an average $\rho_{pbis} = 0.25$. A detailed explanation of these statistical tests and their interpretations can be found in Sections 3.3.2, 3.3.3, and 3.3.5. The results of our statistical analysis lent to the revision of seven test items: five items were revised due to low item discrimination values, one item was revised due to a low item difficulty value (indicating the question was too difficult even after adequate instruction), and an additional item was revised due to a poor item discrimination *and* item difficulty value.

At this phase of the iterative revision process, we solicited the feedback of three planetary science professors, one astronomy professor, and two science education researchers. The planetary science/astronomy professors provided feedback on the questions' scientific accuracy, as well as whether or not they all could converge on the same correct answer choices. The education researchers analyzed the language used in the instrument to determine whether or not it was appropriate for undergraduate ASTRO 101 students. The professors provided minor content/clarity suggestions to 4 of the test items on the PFCI Version 2. We then received more detailed feedback from an *additional* astronomy education-research specialist with years of experience writing concept inventories in particular. The astronomy education specialist was able to provide a great deal of assistance with regards to making sure the PFCI was written using language accessible to the target population. The combination of our statistical analysis and the in-depth feedback

from the education research specialist ultimately lead to the revision of 15 of the PFCI's 21 content items in total. A majority of the revisions were relatively minor (removal of a poorly-written distractor, revision of a question stem or distractor's wording, etc...) with the exception of item #20, which was removed entirely. The completion of these revisions lead to Version 3 of the PFCI.

A visual depiction of the revision process for one of the PFCI's content items can be found below:

PFCI Version 1: Item #14

In our Solar System, why did rocky planets form close to the Sun while the gaseous planets formed further away?

A. Close to the Sun, gravity was strong enough to pull the denser, rockier planets close in

B. Close to the Sun, gravity was too weak to pull the denser, gaseous planets close in

C. Close to the Sun, planets composed of mainly gas were incapable of remaining stable and exploded due to strong pressure forces

D. Close to the Sun, only heavy elements (like rocks and metals) could solidify and eventually form a planet

E. Close to the Sun, gaseous material was used to create the young Sun, so there was no material left to form planets

The correct answer choice is D. Between versions 1 and 2, we removed the original option B, as we found this to be an unnecessary distractor since the naive idea we wanted to address was students' thinking that (in our Solar System) rocky planets are close to the Sun because they are denser, and, as a result, more massive and experience a larger force of gravity (Simon et al., 2018). After analyzing students' responses to Version 1, we felt that option A was an adequate distractor on its own. We also removed the words 'and exploded' from option C because these

words did not add to the validity of the distractor and were making the answer choice longer than it needed to be. We added the phrase 'at such high temperatures' to option D to encourage students to think of condensation temperature when selecting this answer choice. Finally, we revised option E to increase its clarity. We did not create a new distractor for this item even after removing choice B, since there is no evidence in favor of an additional distractor when there are already at least three well-written answer choices (Haladyna et al., 2002).

The revised question #14 was as follows:

PFCI Version 2: Item #14

In our Solar System, why did rocky planets form close to the Sun while the gaseous planets formed further away?

A. Close to the Sun, gravity was strong enough to pull the denser, rockier planets close in

B. Close to the Sun, planets composed of mainly gas were incapable of remaining stable due to strong pressure forces

C. Close to the Sun, only heavy elements (like rocks and metals) could solidify at such high temperatures and eventually form a planet

D. Close to the Sun, all of the gaseous material was used to create the young Sun, so there was no material left to form the gas planets close in

The correct answer choice is now C. Between versions 2 and 3 there were limited changes made to item #14. We did, however, add the word 'only' to option A for emphasis. We also removed the phrase 'due to strong pressure forces' from option B to increase the brevity of the answer choice, and because there was no evidence in our earlier research that students associated gas planet instability with any type of pressure force.

Item #14 as it appeared on the PFCI Version 3 was:

PFCI Version 3: Item #14

In our Solar System, why did rocky planets form close to the Sun while the gaseous planets formed further away?

A. Close to the Sun, gravity was only strong enough to pull the denser, rockier planets close in

B. Close to the Sun, planets composed of mainly gas were incapable of remaining stable

C. Close to the Sun, only heavy elements (like rocks and metals) could solidify at such high temperatures and eventually form a planet

D. Close to the Sun, all of the gaseous material was used to create the young Sun, so there was no material left to form the gas planets close in

The correct answer choice is C.

After the development of the PFCI Version 3, we held a student 'round-table' with four undergraduate non-majors who were employed by a professor in The University of Arizona's Department of Astronomy/Steward Observatory. These students participated in the round-table on a volunteer-basis and had no previous relationship with M. Simon. Although the round-table was recorded, students were not permitted to give their names and instead were required to describe themselves by indicating their academic major[s], their previous astronomy experience, and their class year. At this point in the revision process, the purpose of the round-table was to ensure that the PFCI was being interpreted as intended by a subset of the undergraduate population. All of the student participants had previous experience with introductory astronomical content as a result of their work with Active Galactic Videos (AGV) - an educational YouTube series run by undergraduate students that highlights important topics in astronomy. Two of the four students had taken at least one ASTRO 101 course during their educational tenure, but none of the students were science majors. During the round-table,

each of the students took the PFCI individually, and then re-convened and had a discussion regarding the clarity of each of the content items and their motivation for selecting the answer choice they did. When a students converged on a distractor rather than the correct answer choice, there was a discussion lead by M. Simon aimed to steer the students toward the correct answer choice after providing the required context. After all of the correct answer choices were revealed, students had an additional discussion regarding whether or not the correct answer choice had become clearer after an adequate explanation from the PFCI's developer. At this point in the revision process, the PFCI Version 3 had already undergone extensive content and language revisions. As a result, the student round-table did not lead to the revision of any test items. After their group discussions, the student participants unanimously agreed that the PFCI Version 3 was being interpreted as intended.

One potential limitation of our study was the lack of student interviews held earlier on in the revision process. It would have been beneficial to conduct either individual or group interviews with a larger number of students with a wide variety of academic majors. Additionally, it would have been advantageous to interview students who had previously taken the PFCI in class to see if their answer choices were consistent in a written versus out-loud reasoning format (see e.g. Keller 2006). Despite skipping the traditional student-interview process, the PFCI was vetted extensively by over 400 students utilizing the MCER technique, by four faculty content reviewers, three science-education research specialists (one with experience developing multiple concept-inventories), and, ultimately by the student round-table.

Version 3 of the PFCI consisted of 20 content items and 3 demographic items. It was *this* version that was administered to ASTRO 101 students in a pre and post-test fashion, and underwent an in-depth reliability, validity, and item analysis as described in Sections 3.3.1 - 3.3.6. Our analysis resulted in moderate revisions to one of the test items on the PFCI Version 3 (see Section 3.4.1). The final and most robust version of the PFCI can be found in Appendix C.

3.3 Results

We performed an in-depth quantitative analysis of the PFCI Version 3 using methods consistent with classical test theory (CTT). CTT is typically utilized as a means to determine the statistical properties of test item scores and, if necessary, eliminate or revise the test items that do not meet pre-established criteria. CTT methods also outline a procedure to conduct a statistical analysis of an instrument's reliability and validity (Crocker and Algina 1986; Bardar et al. 2006). The results from our CTT analysis of the PFCI's third iteration are presented in the subsequent sub-sections.

3.3.1 PFCI Version 3 Sample

Version 3 of the PFCI was administered during the Fall 2018 semester to seven ASTRO 101 courses before any relevant material was taught (pre-test), and to six of those same classes *again* at the end of the semester (post-test). Each student received the same version of the PFCI, and students recorded their answers directly onto the instruments. Student scores were recorded manually by M. Simon and verified by additional group members. For our analysis of the PFCI Version 3, we removed any students from the dataset who selected the same answer for all 20 questions or who answered the questions in a specific visual pattern - indicative of the fact that they did not put any effort into completing the PFCI. Following the procedure outlined in Bailey et al. (2011), we also removed data from students who left more than two questions blank in order to avoid early question bias. We then matched students who took both the pre and post-test (matched pairs) when available. The final distribution of test takers can be found in Table 3.1.

3.3.2 Item Analysis I: Item Difficulty

Item difficulty, p, is defined as the proportion of students who answered a specific question correctly (Crocker and Algina, 1986). As a result, items with lower difficulty values are considered *more difficult* than items with higher difficulty values. According to Bardar et al. (2006), the range of acceptable p-values is typically be-

Table 3.1 PFCI Version 3 Participant Distribution

Administration	Number of Students (N)
Pre-Test	
All	582
Revised	561
Post-Test	
All	383
Revised	374
Matched-Pairs	287

'All' = all participants, 'Revised' = sample where we removed select students from the dataset for the reasons mentioned in Section 3.3.1.

tween $0.2 < p < 0.8$, with an average item difficulty of ≈ 0.5. Our pre-test item difficulty values ranged from 0.17-0.81 with an average $p = 0.46$. After instruction (post-test), our item difficulty values ranged from 0.34-0.81, with an average $p = 0.58$ (see Table 3.2).

Although two of the items (#1 and #13) had lower than desirable p-values on the pre-test, their corresponding p-values on the post-test were within the acceptable range. Item #1 deliberately asked students, *'How did the planets in our Solar System form?'* Pre-instruction, 54% of students selected the answer choice that corresponded to the Solar System forming at the time of the Big Bang, but after instruction only 28% of students selected the same response. Item #13 asked students, *'Why do the planets in our Solar System orbit the Sun in the same plane?'* Pre-instruction 45% of students selected the answer choice that used the 'buzz-words' retrograde motion. After instruction, however, only 25% of students selected the retrograde motion answer choice, and 60% of students selected the correct answer (*'The planets formed from a flattened disk-like structure, which caused the planets to orbit in this configuration'*). These examples demonstrated that items #1 and #13 addressed wide-spread misconceptions that were reversed (for a significant

percentage of students) after adequate instruction.

Additionally, items #3 and #12 had p-values on the cusp of indicating that these questions were 'too easy.' This was unsurprising, however, since these items were developed to act as the instrument's 'baseline.' These questions addressed the topics of terrestrial planet composition and the most basic definition of a planet; and were developed to make sure students had a grasp on general content knowledge before delving into more complex topics. Since both of these items had acceptable point-biserial values (discussed in the next section), and their p-value of 0.81 was within 1% of the conventionally acceptable range, we did not flag these items for further revision.

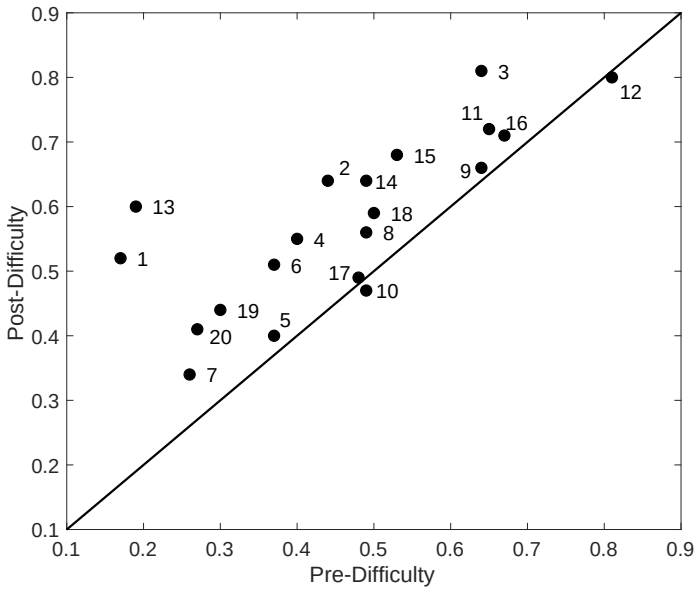

Figure 3.1 Pre-instruction item difficulty versus post-instruction item difficulty. Ideally, item difficulty values should be higher (a greater proportion of students answered the item correctly) post-instruction. Items following the desired trend are plotted above the diagonal line.

Ideally, students should preform better on the PFCI after adequate instruction. As a result, item difficulty values should be higher (a greater proportion of students answered the item correctly) for all of the PFCI's post-test items. This is true

Table 3.2 PFCI Version 3 Item Difficulty

Item Number	**Pre-*p*** (N=561)	**Post-*p*** (N=374)
1	**0.17**	0.52
2	0.44	0.64
3	0.64	**0.81**
4	0.40	0.55
5	0.37	0.40
6	0.37	0.51
7	0.26	0.34
8	0.49	0.56
9	0.64	0.66
10	0.49	0.47
11	0.65	0.72
12	**0.81**	0.80
13	**0.19**	0.60
14	0.49	0.64
15	0.53	0.68
16	0.67	0.71
17	0.48	0.49
18	0.50	0.59
19	0.30	0.44
20	0.27	0.41

Item difficulty (p-values) for the PFCI Version 3 pre and post-test administration. Values that are outside of the conventionally accepted range are in bold.

for all but two items (#10 and #12) as shown in Figure 3.1. Item 10 addressed the role of gravity during the accretion (planet formation) process. Although all of the course instructors surveyed (see Section 3.4.2) claimed to have discussed the accretion process in class, we failed to inquire the extent to which their instruction gave a full explanation of the role of gravity. The formation of planetesimals into planets can be simplified using terms like 'collisions' or 'material is pulled together.' If students do not know gravity is the attractive force responsible for the collisions, there may not be a change in the proportion of students answering #10 correctly post-instruction. Since #10 had such a minimal decrease in p-value, and since its point biserial value is within the acceptable range (see Section 3.3.3), we argue in favor of keeping item #10 as is for the final version of the PFCI.

As mentioned above, item #12 covered the most basic definition of a planet. Due to its relatively trivial nature, this question had one of the highest item difficulty values both pre and post-instruction. We did not flag this item for further revision due to its favorable point biserial value, and the fact that the difficulty value post-instruction only fell by 1%. Ultimately, none of the items on the PFCI Version 3 were removed or deemed to be in need of modification based on their item difficulty (p) value.

3.3.3 Item Analysis II: Item Discrimination

Item discrimination is used to measure how effectively an item differentiates between test takers who do well and those who do poorly on the entire test. It is defined using an item's point biserial,

$$\rho_{pbis} = \frac{(\mu_+ - \mu_X)}{\sigma_X} \cdot \sqrt{\frac{p}{q}} \tag{3.1}$$

where μ_+ is the mean test score for those who answered the question correctly, μ_X is the mean test score for the entire sample, σ_X is the standard deviation of all of the test scores, p is the item difficulty, and q = (1-p). Values of ρ_{pbis} can range from -1.00 to +1.00 with a value of 0 indicative of zero correlation. A positive ρ_{pbis} value

indicates that there is a positive correlation between the item score and the test score overall, thus, students scoring higher on the exam were more likely to answer that particular item correctly when compared to students whose test scores were low. This indicates that the item successfully discriminated between high- and low-scoring students (Bardar et al., 2006). Similarly, a negative ρ_{pbis} value indicates that students who are performing well on the exam are answering that item *incorrectly* more often than students performing poorly on the exam. Items with negative item discrimination values need to be analyzed further to ensure there is not a problem with the question.

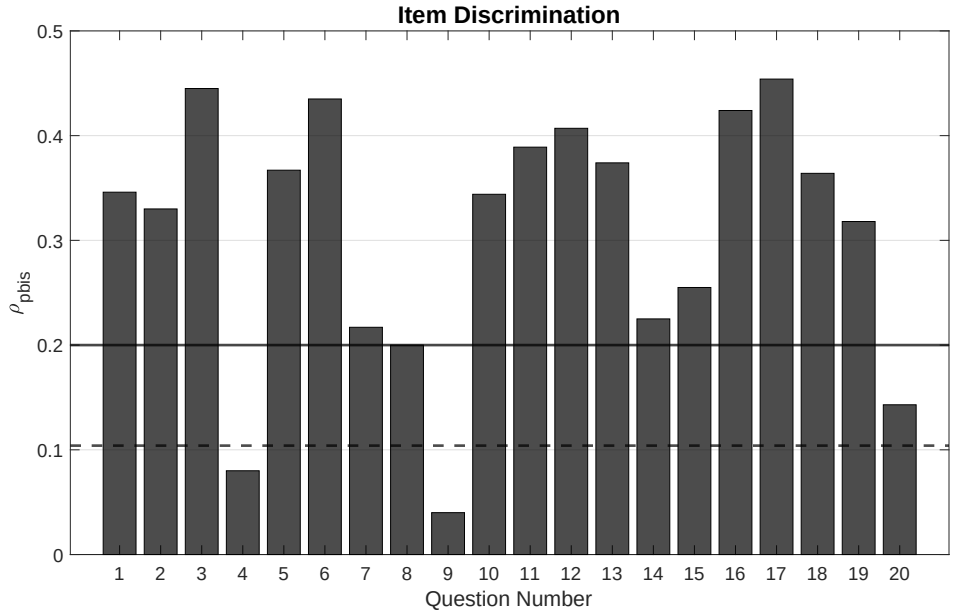

Figure 3.2 Post-instruction item discrimination (ρ_{pbis}) values. ρ_{pbis} values between 0.2-0.7 are desired, while values greater than 0.104 are acceptable. The horizontal black line is at 0.2, while the dashed line is at 0.104. All of our items excepts #4 and #9 have ρ_{pbis} values within the acceptable range.

For the post-test administration of the PFCI Version 3, our ρ_{pbis} values ranged from 0.04-0.45 with an average of 0.31 (see Table 3.3). Our average ρ_{pbis} value was consistent with other concept inventories within this topical domain and with this population of test-takers (see e.g. Bardar et al. 2006; Bailey et al. 2011). The

Table 3.3 PFCI Version 3 Item Discrimination

Item Number	ρ_{pbis} (N=374)
1	0.35
2	0.33
3	0.45
4	**0.08**
5	0.37
6	0.44
7	0.22
8	0.20
9	**0.04**
10	0.34
11	0.39
12	0.41
13	0.37
14	0.23
15	0.26
16	0.42
17	0.45
18	0.36
19	0.32
20	**0.14**

Point biserial (ρ_{pbis}) values for the PFCI Version 3 post-test administration. Values that are outside of the conventionally acceptable range are in bold.

minimum desired point biserial value is 0.2, with an ideal range between 0.3-0.7 (Ding and Beichner 2009; Allen and Yen 1979). All but three of our items had point biserial values within the desirable range. Items with point biserial values less than 0.20 can still be considered acceptable if the point biserial coefficient is two standard deviations above 0.00 and the sample size (N) is ≥ 50. The standard deviation is defined as:

$$\sigma_\rho = \frac{1}{\sqrt{N-1}} \tag{3.2}$$

(Bardar et al., 2006). For a sample size of N = 374, the standard deviation of the point biserial coefficient is 0.052, and two standard deviations is 0.104. All of our items except #4 and #9 were above $\rho_{pbis} = 0.104$ (see Figure 3.2). These two items underwent additional review to determine whether they should be discarded or modified before publishing the final version of the PFCI. A detailed explanation of our review process can be found in Section 3.4.1.

3.3.4 Student Learning Gains

To measure average learning gains, we first calculated normalized gain scores for each individual student ($g_{student}$) in the matched-pairs dataset (N = 287 students). We used the equation developed by Hake (1998) to calculate each student's individual gain score:

$$g_{student} = \frac{(post\%) - (pre\%)}{100 - (pre\%)} \tag{3.3}$$

where ($pre\%$) and ($post\%$) in this case were each individual student's pre and post-test score.

Using the student data, we then calculated the average normalized gain score for each class, g_{class}. According to Hake (1998), the average learning gain is defined as:

Table 3.4 Measured Learning Gains

Course Number	**# of Students** (N)	**Pre-Test** $< M >$ %	**Pre-Test** $< SD >$ %	**Post-Test** $< M >$ %	**Post-Test** $< SD >$ %	g_{class}
PTYS 206	24	48.1	19.6	61.5	20.2	0.295
PTYS 214	9	59.4	27.2	77.2	16.2	0.377
PTYS 170B2 (1)	52	43.8	17.1	58.1	20.5	0.269
PTYS 170B2 (2)	40	51.0	14.9	60.1	20.2	0.170
PTYS 170A1	92	48.0	16.0	60.4	15.1	0.227
ASTR 170B1	70	41.5	15.7	53.0	20.5	0.203
Whole Sample	**287**	**46.4**	**17.1**	**58.7**	**19.1**	**0.231**

$$g_{class} = \frac{< post\% > - < pre\% >}{100 - < pre\% >} \tag{3.4}$$

where $< pre\% >$ and $< post\% >$ were the averaged pre and post-test scores for each class. Hake (1998) and Prather et al. (2009) split g_{class} into three categories: low g_{class} ($g_{class} < 0.3$), medium g_{class} ($0.3 < g_{class} < 0.7$), and high g_{class} ($g_{class} > 0.7$). We followed the same metric when analyzing the gain values for each of the six classes that were surveyed at both the beginning and end of the Fall 2018 semester. For our matched-pairs sample, skewness and kurtosis absolute values were below the accepted value of 1, indicative of normal distributions (George and Mallery 2010; Bailey et al. 2011). The mean (M), standard deviation (SD), and normalized gain values for the entire matched-pairs dataset, as well as those measured for each individual class are reported in Table 3.4.

Up until this point, we have been discussing the average normalized gain score for each of the six classes. We now transition into analyzing the entire matched pairs dataset by looking at the individual scores of students. A paired-sample t-test comparing individual students' pre and post-test scores showed that students' scores after instruction were significantly higher than their scores on the pre-test, t(286) = -14.426, p <0.001. Despite the fact that the normalized gain for the whole sample was classified as low gain ($< g > = 0.231$), 76% of students performed better on the post-test, as shown in Figure 3.3. This indicates that the overwhelming majority of

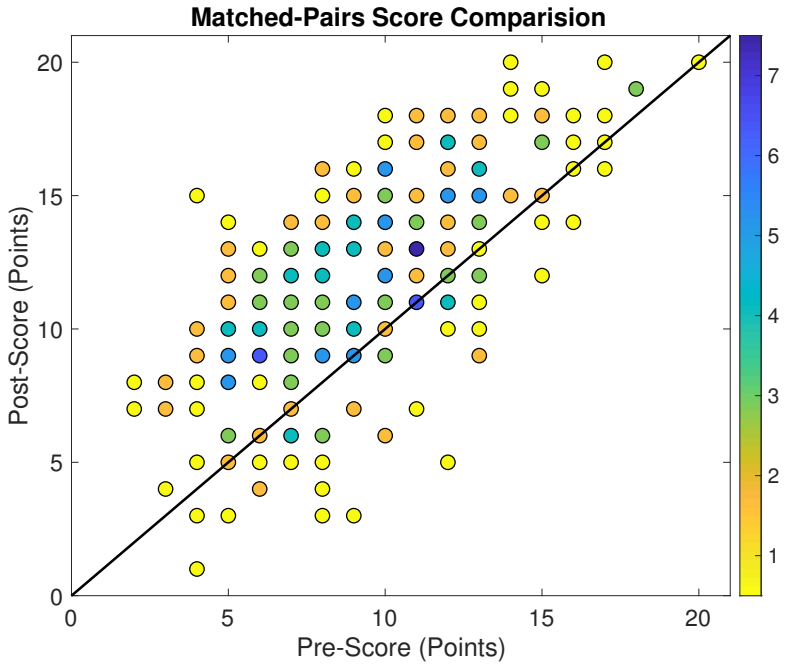

Figure 3.3 The pre-test scores versus post-test scores for the 287 students with matched pairs data. The diagonal line represents students who got the same score on both the pre- and post tests. Students above the diagonal line performed better on the PFCI after instruction. The number of students represented by each datapoint is denoted on the colorbar (up to seven students).

students demonstrated a better understanding of planet formation after instruction.

Following the procedure outlined in Schlingman et al. (2012), we conducted an analysis of the normalized gain score for each student to better understand their individual performance when compared to overall class performance. Figure 3.4 further demonstrates that the overwhelming majority of students performed better on the PFCI after instruction. Similar to Schlingman et al. (2012), we found that the range of normalized gain scores achieved by individual students (-0.875 $< g_{student}$ < 1.0) was significantly greater than the range of gain scores we observed for the six classes we surveyed ($0.170 < g_{class} < 0.377$). Over one-third of students (38%) scored within the medium gain range (0.3 - 0.7), and an additional 4% of students had normalized learning gain scores in the high range ($g_{student} > 0.7$). We explored

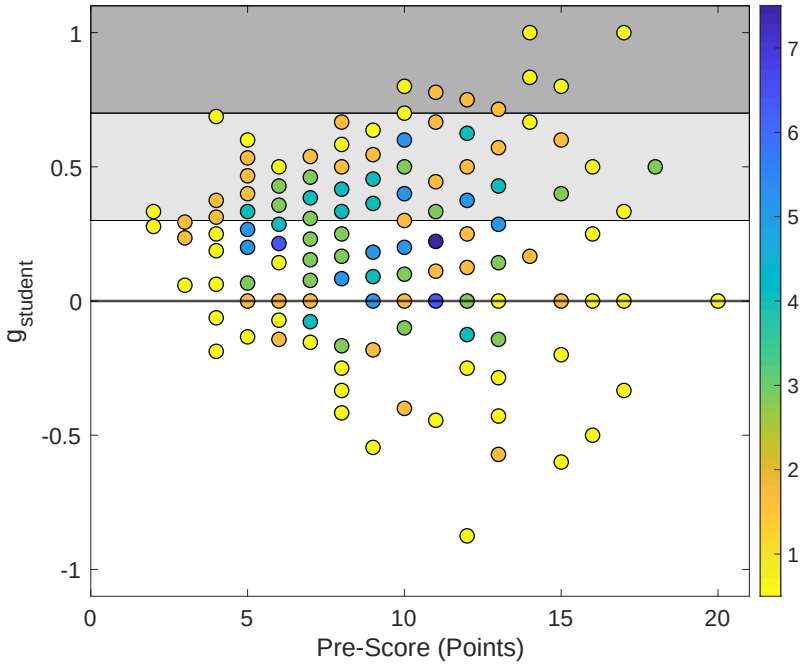

Figure 3.4 The pre-test scores versus normalized learning gain scores ($g_{student}$) for the 287 students with matched pairs data. The horizontal line represents zero normalized gain. Points below the horizontal line correspond to students who performed worse on the post-test than on the pre-test. The number of students represented by each datapoint is denoted on the colorbar (up to seven students). The regions corresponding to medium gain (0.3 - 0.7) and high gain (> 0.7) are shaded in light gray and darker gray, respectively.

the possibility that higher gain scores could be attributed to college major, gender, previous planet formation exposure, or type of instruction in Section 3.4.2.

3.3.5 Instrument Reliability

We assessed the reliability of the PFCI by calculating Cronbach's alpha (α). Cronbach's alpha is a standard measurement of an instrument's internal consistency, which, simply stated, indicates that students who do well on the entire test should do well on each test item, and students who perform poorly on the entire test should perform poorly on each individual test item. Cronbach's alpha is defined using the following formula:

$$\alpha = \frac{K}{K-1} \cdot (1 - \frac{\sum \sigma_i^2}{\sigma_x^2}) \tag{3.5}$$

where K = the number of test items, σ_i^2 is the variance of each item, and σ_x^2 is the variance of the entire test (Bardar et al., 2006). A reliability coefficient of 0.70 or higher is considered acceptable (Nunnally, 1978). We used the sample of matched pairs (N = 287 students) to calculate the PFCI's internal consistency both before and after instruction. Before instruction, $\alpha = 0.658$, which was slightly lower than what is deemed acceptable. For the post-test, however, $\alpha = 0.726$. This increase in α indicates that students answer more reliably to the items on the PFCI after instruction. Furthermore, this increase in α demonstrates that Version 3 of the PFCI is sensitive to increased student understanding of this topic area.

3.3.6 Instrument Validity

Validity refers to how well a scientific test (and the test items within) measure what the instrument intends (Crocker and Algina, 1986). Following the procedure outlined in Bardar et al. (2006), we evaluated three types of validity for the PFCI: content validity, face validity, and concurrent validity.

Content Validity

Content validity measures the extent to which the test questions are scientifically accurate - and whether or not the test items are representative of the concept domain the instrument seeks to evaluate (Markus and Smith, 2012). To evaluate the PFCI's content validity, we solicited the help of three planetary science professors, one astronomy professor, and two science education researchers (see Section 3.2.3). Their suggested language/content changes were implemented before Version 3 was administered during the Fall 2018 semester. Overall, the professors assessing the PFCI were in strong agreement that the instrument was well written and scientifically accurate, indicative of satisfactory content validity.

Face Validity

Face validity is utilized to determine whether the concept domain addressed by the instrument covers the topics most appropriate for assessing students' knowledge (Bardar et al., 2006). To assess the face validity of the PFCI, we conducted an analysis of course syllabi (and lecture slides, when available) from 34 undergraduate introductory astronomy and planetary science courses that covered the topic of planet formation (refer to Simon et al. 2018). Our investigation supported the claim that the PFCI does have face validity, and our instrument addresses the planet formation content most prevalently taught in ASTRO 101 courses.

Concurrent Validity

Concurrent validity in an instrument's ability to distinguish between distinct populations of test takers (Trochim 2006; Bardar et al. 2006). To evaluate the PFCI's concurrent validity, we administered the PFCI to a set of 12 planetary science graduate students, and two postdoctoral researchers ($M = 19.14/20$, 95.7%, $SD = 0.949/20$, 4.74%). We performed a t-test to determine whether the PFCI was able to measure a statistically significant difference in post-test scores between the graduate students/post-docs (experts) and the undergraduates (novices).

An independent sample t-test confirmed that the PFCI was successfully able to distinguish between the two test taking populations, $t(386) = -7.215$, $p < 0.001$.

Due to the fact that Version 3 of the PFCI satisfies the criteria outlined for content, face, and concurrent validity, we conclude that our instrument can be used in a classroom setting to distinguish between different levels of understanding amongst our target population on the topic of planet formation.

3.4 Discussion

3.4.1 Items Requiring Justification

As mentioned in Section 3.3.3, items #4 and #9 were flagged for having ρ_{pbis} values outside of the desirable range. These items were originally included in the PFCI because they attempted to address known student learning difficulties on the topics of planetary migration and condensation temperature, respectively.

On Version 3 of the PFCI, item #4 read as follows:

4. Which describes how the locations (relative to the Sun) of the planets in our Solar System may have changed over time?

A. They changed because space is constantly moving and expanding
B. They changed because the planets are constantly colliding with each other
C. The larger planets may have changed locations early in the Solar System's history because of the gravitational interactions between them
D. The locations of the planets have not changed over time; they formed in the same locations they are in now

The correct answer choice is C. Before instruction, 40.1% of students picked answer choice A, and 39.9% selected answer choice C. After instruction, however, only 24.1% of students picked answer choice A, and 55.1% chose answer choice

C. The results of an independent sample t-test showed that the percentage of students who answered #4 correctly after instruction was significantly higher than the corresponding percentage before instruction, $t(933) = -4.600$, $p < 0.006$.

Since we saw a statistically significant increase in the percentage of students selecting the correct answer after instruction, we assert this item measures a concept (giant planet migration) that adequate instruction on this topic is able to address. The fact that the ρ_{pbis} value is low simply indicates that while some students *do* learn the concept covered in this particular item, many of the students who answer this question correctly are still struggling with content related to other items on the instrument. A low ρ_{pbis} value could also be indicative of a test item that is being answered incorrectly by high performing students. This is illustrative of a topic that needs to be covered in greater depth when discussing planet formation. Due to the significant increase in the percentage of students answering this item correctly after instruction, we did not modify or remove item #4 from the final version of the PFCI.

Item #9 was flagged due to its less than desirable ρ_{pbis} value compounded with its nearly negligible increase in item difficulty post-instruction. Item #9 read as follows:

9. In the outer Solar System, which materials were able to become a solid?
   A. Only metals (e.g. iron)
   B. Only rocky (silicon-based) minerals
   C. Only hydrogen compounds (e.g. water and ammonia)
   D. Metals, rocky minerals, and hydrogen compounds
   E. Neither metals, silicon based minerals, nor hydrogen compounds

The correct answer choice is D. Prior to instruction, 16.6% of students selected C while 64% chose D. After instruction, the numbers remained relatively unchanged, with 17.9% of students picking C and 65.5% selecting D. The intent of this item was to measure whether or not students had a robust understanding of the role the condensation of elements plays in determining the compositional

differences between the terrestrial and jovian planets. As discussed in detail in Kennedy and Kenyon (2008), the surface density of solids increases by a factor of ≈3 in the outer Solar System past the snow line (where gas giants form). At these locations, condensed hydrogen compounds (icy solids) exist in much greater abundance than metals and rocky minerals. Ultimately, however, the availability of all three (metals, rocky minerals, and hydrogen compounds) is what leads to the accretion of cores large enough to attract a gaseous envelope.

It was clear from our pre-post analysis of question #9 that a majority of students were likely guessing the correct answer both before and after instruction. As a result, we developed a question with distractors more aligned with known student reasoning difficulties on the topic of condensation temperature/planetary composition (see Simon et al. 2018). These reasoning difficulties included but were not limited to: planet size and the force of gravity, the role of the Sun in the distribution of matter throughout the disk, and the relative abundance of solids versus icy material in the outer Solar System. We propose the following question as a replacement for item #9 in the final version of the PFCI.

9. Jupiter, Saturn, Uranus, and Neptune (the outer planets) were able to grow much larger than Mercury, Venus, Earth, and Mars because:

A. In the locations where the outer planets formed metals, rocky minerals, and icy minerals were all able to solidify. As a result, all of these materials could be used to form the outer planets.

B. The gravitational force far from the Sun was much weaker, allowing the outer planets to grow to much larger sizes.

C. In the outer Solar System there was much more rocky material than icy material. This made it possible for the outer planets to attract their large gaseous envelopes.

D. During the Solar System's formation, the Sun ejected additional solids into the outer Solar System. These solids were eventually used to form the outer planets.

The correct answer choice is A.

3.4.2 Further Exploration of Learning Gains

Section 3.3.4 illustrated that the range of normalized gain scores achieved by individual students ($g_{student}$) was very wide. As a result, we explored the possibility that higher gain scores could be attributed to college major, previous planet formation exposure, gender, or type of course instruction (e.g. interactive versus lecture based). Of the 109 students (38% of the entire matched-pairs sample) whose normalized gain scores were within the 'medium gain' range, 15.6% were science majors, the gender distribution was approximately 50-50, and 32.1% of these students had learned about planet formation previously in some capacity (either in high school or college). For the small sample of students (N = 11) whose normalized gain scores were within the 'high' range 54.5% were science majors, 63.7% were female, and 45.4% had previous exposure to the topic of planet formation. Histograms of these demographic breakdowns for the entire matched pairs sample as well as the medium and high gain subsamples can be found in Figure 3.5.

Due to the increase in the percentage of science majors between the medium and high normalized gain subsamples, we decided to explore whether or not the PFCI could differentiate between science and non-science majors for the entire matched pairs dataset. An independent sample t-test confirmed that science majors' normalized gain scores were significantly higher than those of non-science majors, $t(275) = 3.973$, $p < 0.001$. The same result could not be found, however, between male and female test-takers or between students who had previous exposure to planet formation and those who did not. The normalized gain scores between those demographic populations were statistically indistinguishable. It was particularly perplexing that the instrument was not biased towards students with previous exposure to planet formation. This finding could be indicative of the fact that planet formation is not adequately taught at the high school or introductory college level, and that there may be a discrepancy between the concepts covered in students' previous courses

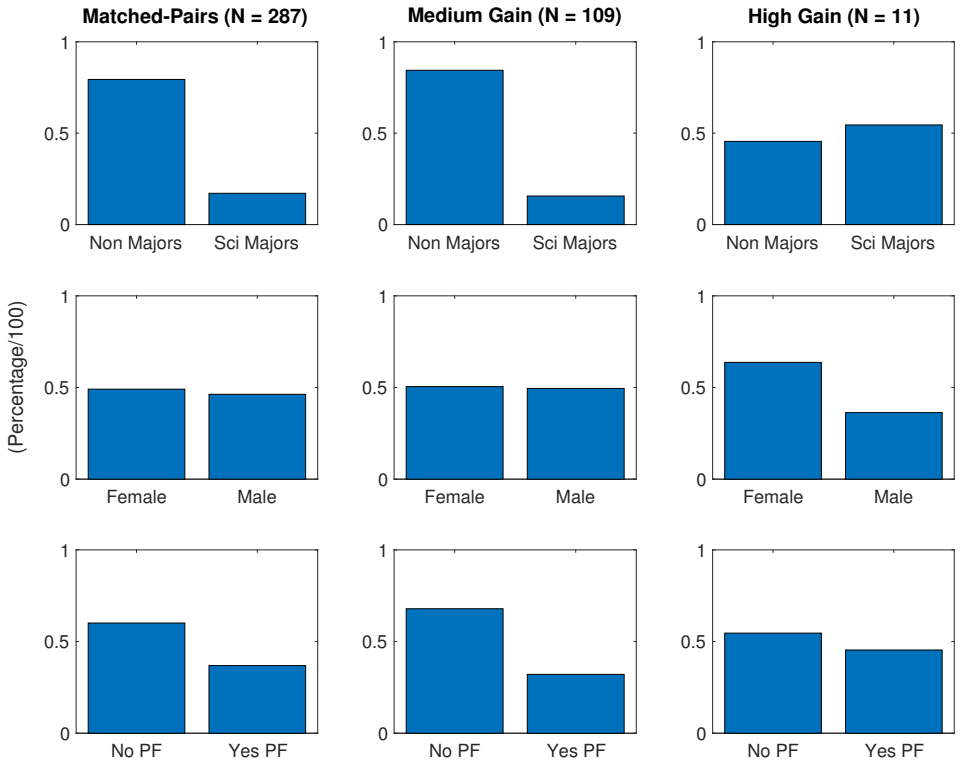

Figure 3.5 The demographic breakdown for the entire matched-pairs sample, the sample of students whose normalized gain scores were classified as 'medium gain', and the sample of students whose gain scores were classified as 'high gain'. There is little difference between the entire matched-pairs sample and students with medium gain scores. For the students with high normalized gain scores, however, there is a noticeable bias toward science majors. There is also an apparent difference in the percentage of female students and students with previous exposure to planet formation in the highest normalized gain score population.

and those emphasized on the PFCI.

We also explored the possibility that type of course instruction (interactive versus lecture based) played a role in helping students achieve higher normalized gain scores. In physics and astronomy courses specifically, the benefits of supplementing traditional lecture with active (interactive) learning strategies has been studied extensively (see e.g. Sokoloff and Thornton 1997; Prather et al. 2004; Prather et al. 2009). Typically, implementing active learning strategies into the classroom (such as Lecture Tutorials or Think-Pair-Share/peer instruction questions), allows students to "explore the reasoning behind their answers. In doing so, they improve their reasoning skills and their understanding of core topics. Systematic studies have shown that [active learning] strategies can improve students' understanding by two full letter grades beyond what traditional lectures accomplish" (Prather et al. 2009, p. 44).

Table 3.5 Course Interactivity

Course Number	Interactivity Level	g_{class}
PTYS 206	Interactive	0.295
PTYS 214	Interactive	0.377
PTYS 170B2 (1)	Partially Interactive	0.269
PTYS 170B2 (2)	Lecture Only	0.170
PTYS 170A1	Partially Interactive	0.227
ASTR 170B1	Interactive	0.203

In order to evaluate how interactive the six courses were, we administered a questionnaire at the end of the semester that asked the course instructors to describe what active learning strategies (if any) they used to supplement traditional lecture when teaching planet formation. Of the six courses surveyed, three were classified as 'interactive,' meaning the instructors used two or more interactive learning strategies when teaching planet formation, two were classified as 'partially inter-

active' meaning the instructors used one active learning strategy, and one course was classified as 'lecture only', since the instructor indicated that no active learning strategies were used when teaching planet formation in their course. Types of interactive learning strategies could include but were not limited to: the use of lecture tutorials, think-pair-share questions, clicker questions, group discussions, and in-class demonstrations relevant to the topic of planet formation or the subtopics therein. Table 3.5 shows the course number, level of interactivity, and average gain score for each of the six courses we surveyed both before and after instruction.

It was unsurprising that two of the three classes with the highest average gain scores were classified as 'Interactive' and the course with the lowest average gain score utilized only traditional lecture. Unfortunately, however, an independent sample t-test used to compare students' individual gain scores could not distinguish between students in interactive classes, and those in partially interactive or lecture only classes. This finding supports the idea that there are insufficient interactive instructional strategies that specifically target the topics covered in Version 3 of the PFCI at a level sufficient enough to aid students in the development of mental models necessary to reliably answer the test items. Furthermore, even when interactive curriculum does exist, the mere implementation of active learning strategies is not enough.

Although implementation of these strategies *generally* leads to higher individual student (and as a result, class averaged) normalized gain scores, what is really crucial is the successful implementation of these strategies. Instructors are typically encouraged to utilize a variety of active learning strategies without receiving any "significant pedagogical training" prior to implementation (Prather et al. 2009, p. 46). As a result, instructors may not execute these strategies successfully. Furthermore, if an active learning strategy *is* implemented successfully, it may cover topics outside of the PFCI's content domain (or cover only a small portion of what is covered in the PFCI's content domain). Instructors were not given a copy of the PFCI until after the post-test was administered, as we did not want them to teach towards the test. Since planet formation covers a broad array of concepts, there is no

uniformly accepted way to teach it, and according to the instructor questionnaires, basic definitions (planet, exoplanet, dwarf planet), planetary motion/migration, and the origin of the Universe (Big Bang) were not covered by 50% of the courses we surveyed. Based on these findings, we recommend re-analyzing the PFCI's ability to distinguish between interactive and lecture-only courses with a significantly larger sample size of participating courses, and with courses that teach topics with a greater amount of content overlap with the PFCI.

3.5 Conclusions & Future Work

In this work, we have provided the AER community with a detailed description of the Planet Formation Concept Inventory's (PFCI) development process. We have also utilized Classical Test Theory (CTT) to conduct a thorough statistical analysis of the PFCI's reliability, validity, and item statistics (difficulty and discrimination). Based on our findings, we conclude that Version 3 of the PFCI is a reliable and valid instrument that can measure change in ASTRO 101 students' conceptual understanding of planet formation before and after instruction.

There are several additional research avenues to explore based upon the results of this project. First and foremost, it would be beneficial to conduct a nationwide study of the PFCI. During this national study, we plan to investigate the instrument's reliability and validity when administered to students at different types of academic institutions (2 year colleges, 4 year colleges, private colleges, public colleges, etc...) with a larger sample of course instructors. With a more generalizable dataset, we could revisit whether or not the PFCI is able to differentiate between courses where active engagement is prevalent and those where instructors use predominantly lecture-based practices (e.g. Prather et al. 2009). Additionally, we hope to corroborate our CTT findings through an analysis of the PFCI using Item Response Theory (IRT). Item response theory has the ability to provide a more in-depth analysis of each of the PFCI's content items, and we plan to utilize *both* IRT and CTT when analyzing the data from the aforementioned national study.

The results of a national study could also potentially shed light on specific cases where instruction is not resulting in greater student understanding. By looking at a more robust sample of post-test results, we would be able to identify and address specific naive ideas that are resistant to change even after adequate instruction (see e.g. the suggestions of Bailey et al. 2011). These findings would allow us to develop new pieces of interactive pedagogy to be utilized as a means to target these more complex reasoning difficulties. The future development of learner-centered activities has the ability to promote a much deeper degree of learning on the topic of planet formation and the subtopics therein.

4.0 EVIDENCE FOR MAGNETICALLY DRIVEN PROTOPLANETARY DISK WINDS

The contents of this chapter were published in Simon et al. (2016).

4.1 Introduction

Low excitation forbidden lines of [O I] and [S II] are some of the defining spectroscopic characteristics of the low-mass, pre-main sequence stars known as T Tauri stars (TTS, Herbig, 1962). Their broad, blueshifted emission profiles were originally interpreted as arising in winds with receding flows occulted by the circumstellar disk (Appenzeller et al., 1984; Edwards et al., 1987), and the correlation between their luminosity and the luminosity of infrared emission from the disk demonstrated that the forbidden line emission was powered by accretion (Cabrit et al., 1990). Studies of large samples of TTS conducted by Hamann (1994), Hartigan et al. 1995 (hereafter HEG), and Hirth et al. (1997) showed that forbidden lines in these stars are characterized by two distinct components: a high velocity component (HVC) and a low velocity component (LVC).

The HVC forbidden emission, typically blueshifted by 30 to 150 km/s, was demonstrated to be formed in microjets, small-scale analogs to the parsec-long collimated jets emerging from more embedded Class I young stellar objects (YSOs) (Ray et al., 2007; Hartigan et al., 1994). A correlation between mass loss rates, derived from the luminosity of the HVC in the strongest [O I] 6300 Å forbidden line

and the accretion luminosity and/or disk accretion rate has been the foundation of the accretion-outflow connection in young accreting stars (HEG, Cabrit 2007). The origin of the outflows traced by the HVC is not yet fully understood, but is likely tied to mass and angular momentum loss in the accretion disk and/or the accreting star through magnetized magnetohydrodynamic (MHD) winds (Ferreira et al., 2006).

The origin of the LVC forbidden emission is even less well understood. HEG found the LVC to be present in all TTS with near infrared (NIR) excess at K-L (Class II sources, e.g. Lada and Wilking 1984), typically with small blueshifts $\sim$ 5 km/s. They considered the possibility the LVC might arise in a slow wind on the surface of a disk in Keplerian rotation with the LVC surface brightness decreasing as $\sim r^{-2.2}$. This possibility was investigated more thoroughly by Kwan and Tademaru (1995) who used line luminosities and line ratios to evaluate the physical conditions in the wind, and estimated disk wind mass loss rates as $\sim 10^{-8} M_{\odot}$/yr. The possibility that the LVC emission might trace thermally driven disk winds powered by photoevaporative heating due to extreme ultraviolet (EUV) radiation from the central accreting star was investigated by Font et al. (2004). However, the EUV heated flows produced very little neutral oxygen and thus could not account for the LVC observations.

More recently, the growing realization that photoevaporative flows are likely an important means of disk dispersal during the era of planet formation has led to renewed interest in additional sources of heating for photoevaporation, i.e. X-ray and far ultraviolet (FUV) radiation. These have the potential of producing significant amounts of neutral oxygen in the flow and accounting for the LVC forbidden emission (Hollenbach and Gorti, 2009; Ercolano and Owen, 2010, 2016; Gorti et al., 2011).

Another new development is the acquisition of high resolution spectra of [Ne II] at 12.8 μm. To date, 24 high-resolution profiles of [Ne II] in TTS have been acquired, showing, like the optical [O I] profiles, a mixture of high velocity and low velocity components. Low velocity components of [Ne II], blueshifted from -2 to -12 km/s, are seen in 13/24 of the high resolution spectra, and have been interpreted as direct

tracers of photoevaporative flows (see the recent review by Alexander et al. 2014 and references therein). Although the ionization required to produce substantial [Ne II] emission in a photoevaporative flow could arise either from EUV or X-ray heating, Pascucci et al. (2014) compared the measured [Ne II] luminosities with upper limits on the EUV radiation reaching the disk and demonstrated that, at least in three systems, this emission probes the X-ray rather than EUV-ionized surface. Due to the fact that X-rays penetrate deep in the disk and drive flows that are mostly neutral, blueshifted [Ne II] emission signals mass loss rates that are considerably higher than if the heating is from EUV, possibly as high as $\sim 10^{-8}\,M_{\odot}$/yr. Such mass loss rates are comparable to those estimated by Kwan and Tademaru (1995) from the LVC optical lines. If these mass loss rates are characteristic of photoevaporative flows, their similarity to TTS disk accretion rates (e.g. Alcalá et al. 2014), suggest that photoevaporation may play a major role early in the evolution and dispersal of protoplanetary material.

Photoevaporation can drastically change the disk surface density by opening gaps in planet-forming regions that widen with time, thus setting the timescale over which [giant] planet formation must occur. The implication this would have on the final architecture of planetary systems, the chemistry of the disk, planet interactions (such as the delivery of volatiles to planets located in the inner solar system), and the final mass and location of giant planets specifically, would be critical to enhancing our understanding of planet formation more generally.

A better understanding of the empirical properties of the forbidden LVC in TTS is needed to assess whether it arises in photoevaporative flows. Two recent works, Rigliaco et al. 2013, (hereafter R13) and Natta et al. 2014, (hereafter N14) have begun this process and provide the motivation for the present study. R13 introduced two changes in interpreting the LVC. Firstly, R13 revisited the forbidden line data from HEG with modern estimates for the accretion luminosity. Gullbring et al. (1998) demonstrated that the mass accretion rates in HEG were too large by nearly an order of magnitude due to uncertain bolometric corrections to the continuum excess measured in the R band, and from the simplistic assumption that

the accretion luminosity was produced in a boundary layer at the stellar surface. R13 re-derived the accretion luminosity for 30 of the HEG stars from Hα emission lines, observed simultaneously with the forbidden lines, which appeared in Beristain et al. (2001). They found correlations between the LVC luminosity from HEG with the improved accretion luminosities as well as with published values for FUV and stellar luminosities, but not with literature values for the X-ray luminosity. This led to the suggestion that *if* the LVC is from a photoevaporative flow, FUV heating may be more important than X-ray radiation in generating [O I] emission, although if [Ne II] emission were also present then X-rays would need to be a contributor as well. A further implication would be that photoevaporative flows might be prevalent throughout the T Tauri phase, decreasing in proportion to the disk accretion rate.

Secondly, R13 demonstrated, with a small set of new high resolution spectra, that the LVC itself may have two kinematic components. Focusing on only two [O I] LVC that were well separated from any HVC emission, the profiles were decomposed into a broad and a narrow contribution, with the suggestion that the broad feature may be formed in bound material in the disk and rotationally broadened, while the narrow feature may be associated with material from further out in the disk, possibly in a photoevaporative flow.

The study of N14 provided further refinement of the definition of the LVC for 44 TTS in Lupus and σ Ori. In HEG the LVC was defined very simply, assigning any emission within 60 km/s of line center to the LVC and outside of that to the HVC, using profiles from echelle spectra with a velocity resolution of 12 km/s. N14 improved on this by applying Gaussian fitting techniques to separate HVC from LVC emission, although their low spectral resolution of 35 km/s meant that a clear separation between these two components was not always possible, nor could they resolve the LVC into a broad and narrow component as done in R13. Nevertheless, they found good correlations between the total LVC luminosity and both the stellar luminosity and the accretion luminosity, but not the X-ray luminosity. They interpret the LVC as arising in a slow wind (< 20 km/s) that is dense ($n_H > 10^8\,cm^{-3}$), warm ($T \sim 5,000 - 10,000\,K$), and mostly neutral.

In this paper, we continue the investigation of the empirical properties of the LVC forbidden lines in TTS in order to elucidate their origin. While the possibility that they may provide a direct tracer of photoevaporative flows that are responsible for protoplanetary disk clearing is intriguing, other potential contributors are the base of MHD centrifugal winds and heated, bound gas in the disk itself. Our study differs from previous ones in two major ways. First, our sample of TTS spans a larger range of evolutionary stages when compared to the sample of HEG (Sects. 4.2.1 and 4.3). Secondly, using Keck/HIRES we reach a spectral resolution that is more than five times higher than N14 and about two times higher than HEG (see Section 4.2.2). This high spectral resolution enables us to define the kinematic structure of the LVC, where about half the detected sources show two kinematic components and the remaining LVC are separated into either broad or narrow profiles (Sects. 4.4 and 4.5). We discuss the relation of these components to MHD and photoevaporative winds in Section 4.6.

4.2 Observations and Data Reduction

For this project, we focus on the kinematic properties of several forbidden lines in T Tauri stars: [O I] 6300.304 Å, [O I] 5577.339 Å, and [S II] 6730.810 Å. We also searched for [O II] 7329.670 Å but did not detect it in any source. In addition, we use Hα as a tracer of the accretion luminosity and disk accretion rate (Alcalá et al., 2014). In the following subsections we describe our sample (4.2.1), the observations (4.2.2), the methodology to create forbidden line profiles free from telluric and photospheric absorption (4.2.3), and the evaluation of line equivalent widths and upper limits (4.2.4).

4.2.1 Sample

All of our science targets, with the exception of TW Hya, belong to the well-characterized star-forming region of Taurus-Auriga (age $\sim$1 Myr and average distance 140 pc; Kenyon et al. 2008). Our sample represents the spread of disk prop-

erties and disk accretion rates, but not the statistical distribution of mass, age, or other properties in this star formation region. The required high S/N precluded observing late M dwarfs and brown dwarfs, and disk inclination was not one of the criteria used to select our targets. Our sample is presented in Table 4.1 and consists of 33 mostly single and bright (B≥16) T Tauri stars (TTS) with disk spectral energy distributions encompassing: 26 Class II, full disks with optically thick inner regions; 5 transition disks, with absent or low NIR to mid-infrared (MIR) excess emission from the inner disk but large far-infrared (FIR) emission; and, 2 Class II/III evolved disks with weak NIR to FIR excess. Additional information on this sample can be found in Pascucci et al. (2015), who analyzed the Na D and K profiles (at 5889.95 and 7698.96 Å, respectively) from the same spectra presented here. The spectral types (SpTy), extinctions ($A_{\rm v}$), stellar bolometric luminosities (L_*), and stellar masses (M_*) in Table 4.1 are all taken from Herczeg and Hillenbrand (2014) who derived them in a homogeneous way from spectrophotometric data, while taking into account excess continuum emission (veiling) and extinction when deriving the stellar properties.[1]

Table 4.1 also gives disk inclinations for 22 stars taken from the literature based on spatially resolved disk images, shown by Appenzeller and Bertout (2013) to be the most reliable means of determining system orientations. For most sources uncertainties are reported to be $\sim 10\%$. However, for one source, DR Tau, nominally reliable techniques for estimating inclination range from close to face-on to almost edge-on and suggest that the inner and outer disk (>10 AU) have different orientations (Banzatti and Pontoppidan, 2015). Resolved millimeter continuum images point to a highly inclined outer disk (∼70°, Andrews and Williams 2007 and ∼35°, Isella et al. 2009). However, MIR interferometric visibilities coupled with spectral energy distribution (SED) fitting, as well as modeling of the spectroastrometic signal in the CO ro-vibrational line, suggest a much smaller inclination for the inner disk ($\sim 20°$, Schegerer et al. 2009 and $\sim 9°$, Pontoppidan et al. 2011). Additional

[1]The only source that did not have a stellar mass reported in Herczeg and Hillenbrand (2014) is HN Tau. The mass reported in Table 4.1 is taken from Keane et al. (2014).

Table 4.1 Source Properties

Source	SpTy	SED	A_v	log L_* [$L_\odot$]	M_* [$M_\odot$]	i [deg]	REF (i)	log L_X [$L_\odot$]
AA Tau	M0.6	II	0.40	-0.35	0.57	71	C13	-3.49
BP Tau	M0.5	II	0.45	-0.38	0.62	39	G11	-3.45
CI Tau	K5.5	II	1.90	-0.20	0.90	44	G11	-4.30
CoKu Tau 4	M1.1	T	1.75	-0.50	0.54	46†	—	—
CW Tau	K3	II	1.80	-0.35	1.01	65	P14	-3.13
CY Tau	M2.3	II	0.35	-0.58	0.41	34	G11	-4.37
DF Tau	M2.7	II	0.10	-0.04	0.32	52†	—	—
DG Tau	K7	II	1.60	-0.29	0.76	38	G11	-4.18*
DH Tau	M2.3	II	0.65	-0.66	0.41	$\sim$90†	—	-2.66
DK Tau	K8.5	II	0.70	-0.27	0.68	41	AJ14	-3.62
DL Tau	K5.5	II	1.80	-0.30	0.92	38	G11	—
DM Tau	M3	T	0.10	-0.89	0.35	35	AN11	-4.33*
DN Tau	M0.3	II	0.55	-0.08	0.55	39	I09	-3.52
DO Tau	M0.3	II	0.75	-0.64	0.70	37†	—	—
DR Tau	K6	II	0.45	-0.49	0.90	20	S09	—
DS Tau	M0.4	II	0.25	-0.72	0.69	65	AJ14	—
FM Tau	M4.5	II	0.35	-1.15	0.15	$\sim$70	P14	-3.86
FZ Tau	M0.5	II	3.5	-0.48	0.63	69†	—	-3.78
GH Tau	M2.3	II	0.40	-0.19	0.36	80†	—	-4.55
GI Tau	M0.4	II	2.55	-0.25	0.58	83†	—	-3.66
GK Tau	K6.5	II	1.50	-0.03	0.69	73	AJ14	-3.42
GM Aur	K6	T	0.30	-0.31	0.88	50	G11	—
GO Tau	M2.3	II	1.5	-0.70	0.42	66	AW07	-4.19
HN Tau	K3	II	1.15	-0.77	0.70	52	AJ14	-4.40*
HQ Tau	K2	II	2.6	0.65	1.53	20†	—	-2.86
IP Tau	M0.6	II	0.75	-0.41	0.59	33†	—	—
IT Tau	K6	II	3.1	-0.01	0.76	42	AJ14	-2.77
TW Hya	M0.5	T	0.00	-0.72	0.69	6	R12	-3.85
UX Tau A	K0	T	0.65	0.22	1.51	35	AN11	—
VY Tau	M1.5	II/III	0.6	-0.41	0.47	—	—	—
V710 Tau	M3.3	II	0.8	-0.43	0.30	44	AJ14	-3.45
V773 Tau	K4	II/III	0.95	0.48	0.98	34†	—	-2.61
V836 Tau	M0.8	II	0.6	-0.52	0.58	48	P14	—

Akeson and Jensen 2014 (AJ14); Andrews et al. 2011 (AN11); Andrews and Williams 2007 (AW07); Cox et al. 2013 (C13); Güdel et al. 2007; Guilloteau et al. 2011 (G11); Herczeg and Hillenbrand 2014; Isella et al. 2009 (I09); Keane et al. 2014; Piétu et al. 2014 (P14); Rosenfeld et al. 2012 (R12); Schegerer et al. 2009 (S09)

SED entries are taken from Pascucci et al. (2015). SpT, Av, L_*, and M_* values were taken from Herczeg and Hillenbrand (2014).

A † indicates sources where inclinations were derived in this work as described in Section 4.5.5.

L_X values were taken from Güdel et al. (2007) who used DEM fits. If the L_X value is marked with an * then it was derived using 1-T, 2-T fits instead. The one exception is TW Hya, in this case the L_X value was taken from Stelzer and Schmitt (2004).

evidence for a small inclination to the inner disk comes from exceptionally deep and broad sub-continuum blueshifted absorption at both He I 10830 Å and Hα (Edwards et al., 2003), requiring absorption along a line of sight through a wind that emerges radially from the stellar poles. From these considerations, we adopt a disk inclination of 20° for DR Tau, since, as will be shown in Section 4.5.5, the LVC forbidden line emission is likely to arise within just $\sim$5 AU of the star. For an additional 10 targets with no reliable inclination reported in the literature, we calculate potential disk inclinations based on forbidden line widths, as described in Section 4.5.5 and noted in Table 4.1 with a dagger.

4.2.2 Observations

We observed all targets using the Keck/HIRES spectrograph (Vogt et al., 1994) with the C5 decker and a 1.1″ x 7″ slit, which covers a wavelength range of 4,800-9,000 Å at a nominal resolution of 37,500. Pascucci et al. (2015) independently calculated the spectral resolution achieved by HIRES in this setting and found a slightly better resolution of $\sim$45,000 corresponding to 6.6 km/s. The targets were observed in two campaigns with the same instrumental setting, one in 2006 and another in 2012. Two of the targets, UX Tau A and IP Tau, were observed in both campaigns. In addition to the science targets, we observed 5 late type stars that are used as photospheric standards and a set of O/B type stars which are used as telluric standards. Spectra were acquired in the standard mode which places the slit along the parallactic angle to minimize slit losses. Slit position angles with respect to disk position angles are discussed in Appendix D and the table therein.

The data reduction was carried out using the highly automated Mauna Kea Echelle Extraction (MAKEE) pipeline written by Tom Barlow. In addition to bias-subtraction, flat-fielding, spectral extraction and wavelength calibration, the pipeline automatically subtracts the sky. An example of a spectrum before and after sky subtraction is discussed in Appendix D and the figure therein. Further details about the data reduction and source exposure times are given in Pascucci et al. (2015).

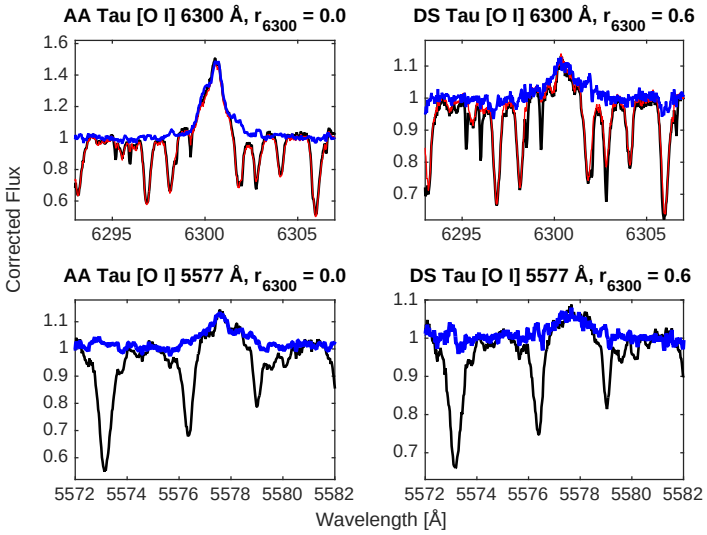

Figure 4.1 An example of the technique used to correct [O I] line profiles for two sources: AA Tau and DS Tau. The original spectrum (in black) includes the emission feature plus telluric and photospheric absorption lines that have not yet been subtracted. Once the telluric lines are removed the spectrum in red is produced. The spectrum in blue depicts the final corrected line profile after the telluric and photospheric lines have been removed. For the [O I] 5577 Å feature, no telluric correction is required.

4.2.3 Corrected Forbidden Line Profiles

In order to identify weak intrinsic emission in the forbidden lines we first remove any telluric and/or photospheric absorption contaminating the spectral order of interest. Telluric absorption is prevalent in the orders containing [O I] 6300 Å and [O II] 7330 Å, but minimal for [O I] 5577 Å and [S II] 6731 Å. We remove the atmospheric features by matching the telluric lines in an O/B standard star to those in the target spectrum and then dividing the target spectrum by the telluric standard. In order to remove photospheric lines, we follow a procedure motivated by the approach of Hartigan et al. (1989).

First, we select a photospheric standard with a spectral type that closely matches the spectral type of the target star. If need be, we broaden the absorption lines of the photospheric standard to match the width of the lines present in the target spectrum. We then apply a cross-correlation technique to shift the photospheric standard to

align with the photospheric lines in the target spectrum, and if necessary, we add a flat continuum to the photospheric standard to match veiled photospheric lines in the young accreting stars. The veiling (r_λ) is defined as the ratio of the excess to the photospheric flux, and r_{6300} is included in Table 4.2, with values ranging from 5.6 (DR Tau) to 0 (5 sources). The final corrected profile is created by dividing the target spectrum by the veiled photospheric spectrum of the standard. This method for correcting the line profiles is illustrated in Figure 4.1 for the [O I] emission features at 6300 and 5577 Å for two sources. One of them, DS Tau, has a moderate veiling, while the other, AA Tau, has zero veiling. No corrections are made for Hα, which has no telluric absorption and is a strong emission feature in all sources.

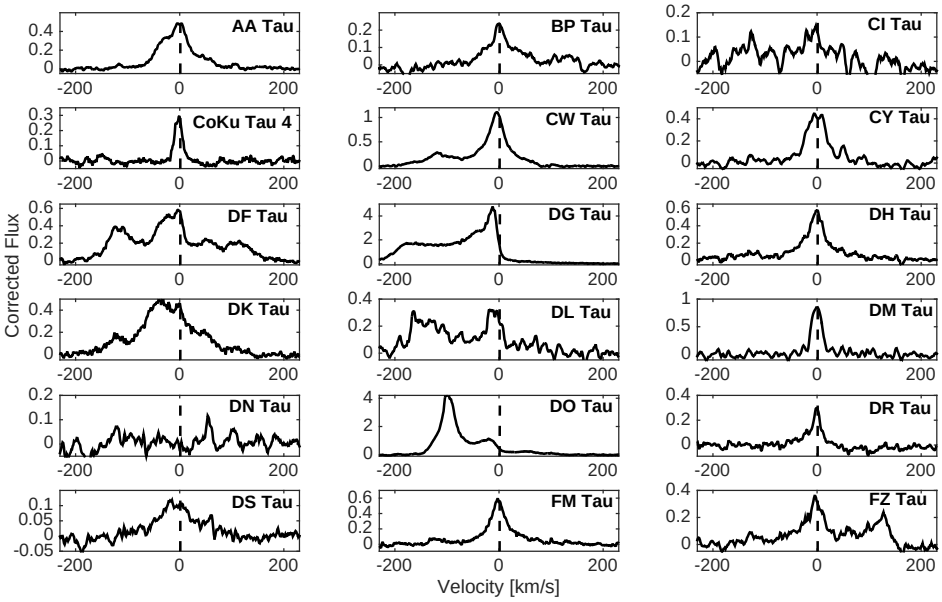

Figure 4.2 Corrected [O I] 6300 Å profiles with the stellar continuum subtracted for half of the sample.

Four of the five photospheric standards are luminosity class V and one is the weak lined T Tauri star (WTTS) V819 Tau, with no infrared excess from a disk. As discussed elsewhere (see Herczeg and Hillenbrand 2014), WTTS are ideal candidates for matching photospheric features in TTS, and V819 Tau was used whenever it was

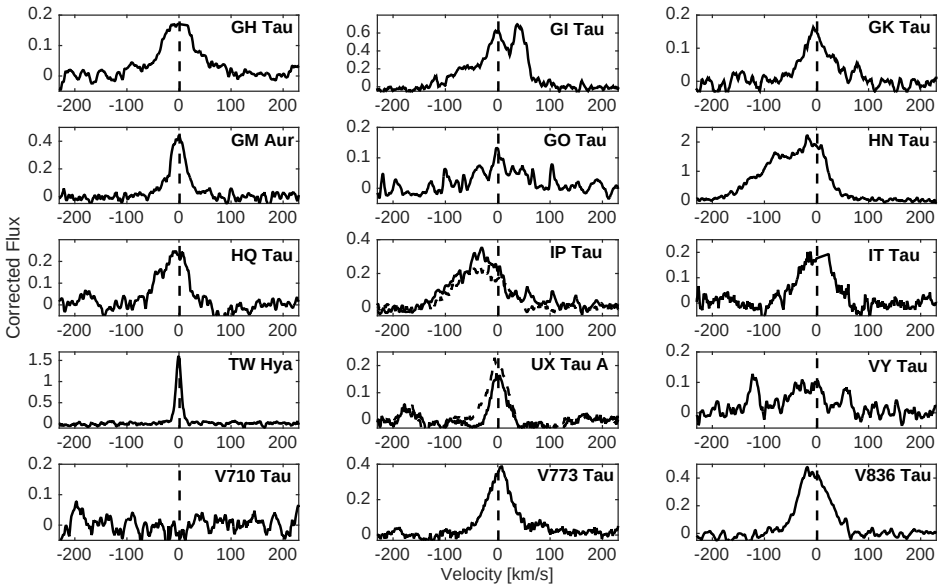

Figure 4.3 Corrected [O I] 6300 Å profiles with the stellar continuum subtracted for the second half of the sample. For IP and UX Tau A, the profiles from both observing campaigns are plotted. The solid line corresponds to the spectrum we analyzed in the paper (2006 for IP Tau and 2012 for UX Tau A).

a good match to the spectral type of the target. The five photospheric standards and their spectral types are: HR 8832 (K3), HBC 427 (K6), V819 Tau (K8), GL 15a (M2), V1321 Tau (M2). The standard applied to each target and line of interest is included in Table 4.2.

Final corrected line profiles are presented in Figures 4.2 and 4.3 for [O I] 6300 Å for all 30 stars, including the 3 non-detections (see next section). Final corrected profiles for the other two forbidden lines are shown only for the detections, in Figure 4.4 for [O I] 5577 Å and in Figure 4.5 for [S II] 6731 Å. They are plotted as corrected flux above the continuum versus radial velocity. The velocity is relative to the stellocentric frame, as determined from photospheric line centroids. The stellar radial velocities of our sources are given in Tables 5 and 6 of Pascucci et al. (2015) and have a 1σ uncertainty of $\sim$1 km/s.

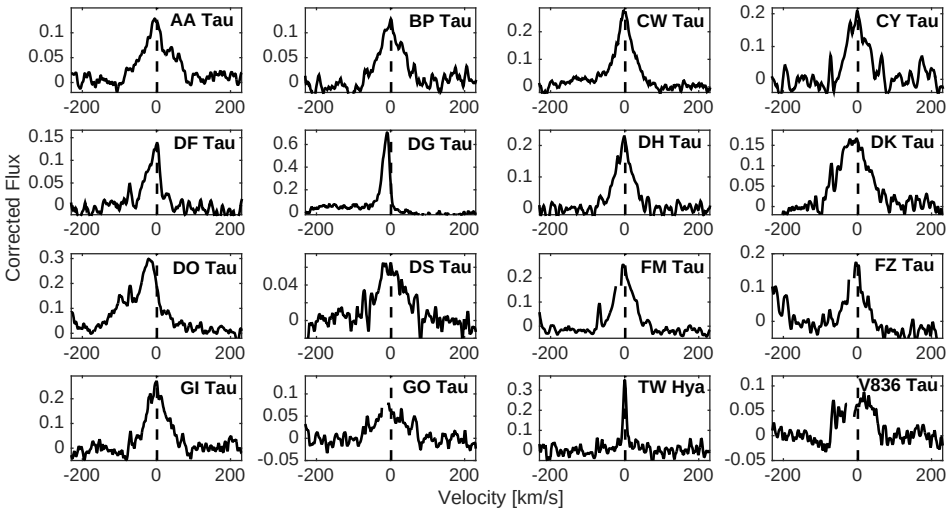

Figure 4.4 Corrected [O I] 5577 Å profiles for the 16 sources with detections.

4.2.4 Equivalent Widths

A number of our sources have weak or absent forbidden lines. The procedure used to identify a detection is to calculate the standard deviation of the residuals (RMS) from a linear continuum fit to a region $\sim$ 3 Å outside the line of interest. Any emission near the wavelength of interest, with a peak higher than 3 times the RMS and equal or broader in width than the 6.6 km/s of an unresolved line, is deemed a detection. Based on this method we find detections in the [O I] 6300 Å transition for 30/33 TTS. Non detections are DN Tau, VY Tau and V710 Tau, all with measured veilings very near or at zero. Both detections and non-detections are included in Figures 4.2 and 4.3 for [O I] 6300 Å. Additionally, we detect [O I] 5577 Å for 16 stars and [S II] 6731 Å for 8 stars. Detections are shown for these lines in Figures 4.4 and 4.5. The [O II] transition at 7330 Å is never detected.

For detected lines we calculate the line equivalent width (EW) by integrating over the wavelength range where there is emission above the continuum. In addition to measuring the line EW, we compute its uncertainty using a Monte Carlo (MC) approach (e.g. Pascucci et al. 2008). We do this by adding a normally distributed noise to each spectrum with the noise being the RMS on the continuum next to

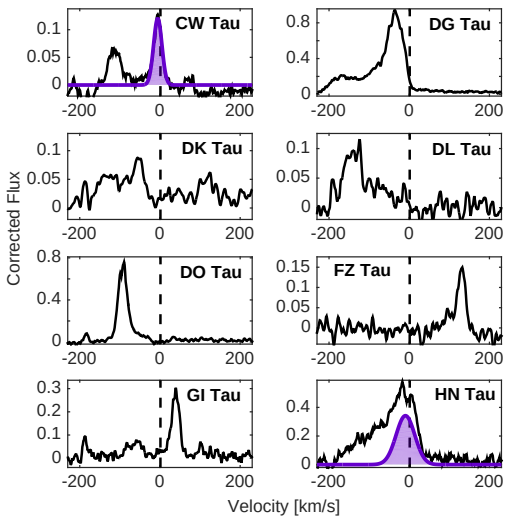

Figure 4.5 Corrected [S II] 6731 Å profiles for the 8 sources with detections. The LVC is only detected in two sources (CW Tau and HN Tau), and is shaded in purple.

the line of interest. We compute the EWs of 1,000 individual spectra generated by the MC approach and assign as the uncertainty the standard deviation of the distribution of EWs.

For lines we determine to be non-detections, we compute a 3σ upper limit (UL) on the EW assuming a Gaussian unresolved profile, $UL = (3 \times RMS) \times \sigma_\circ \times \sqrt{2\pi}$ where the RMS is calculated from the standard deviation of the residuals on a ~ 3 Å continuum, $\sigma_\circ$ in Å is defined as $(\lambda \times \Delta v)/(c \times 2.355)$ where λ is the wavelength of the line of interest, Δv is the FWHM of an unresolved line (6.6 km/s) and c is the speed of light in km/s.

Table 4.2 presents the EW for the detected forbidden lines and the upper limits for the non-detections for our 33 sources.

4.3 Accretion Luminosities and Disk Accretion Rates

In accreting TTS, most of the UV and optical excess continuum emission derives from energy released through accretion, attributed to magnetospheric accretion shocks on the stellar surface (Hartmann et al., 1998). Ideally accretion luminosities

Table 4.2 Forbidden Line Equivalent Widths

Source	Photospheric Standard	r_{6300}	EW ([O I] 6300) [Å]	EW ([O I] 5577) [Å]	EW ([S II] 6731) [Å]
AA Tau	V819 Tau	0	0.74 ± 0.03	0.21 ± 0.03	<0.005
BP Tau	V819 Tau	0.6	0.35 ± 0.05	0.20 ± 0.04	<0.005
CI Tau	HBC 427	0.6	0.16 ± 0.06	<0.016	<0.130
CoKu Tau 4	V1321 Tau	0	0.13 ± 0.02	<0.006	<0.004
CW Tau	HBC 427	1.5	1.70 ± 0.02	0.35 ± 0.05	0.18 ± 0.07
CY Tau	GL 15a	0.6	0.42 ± 0.06	0.18 ± 0.07	<0.006
DF Tau	V819 Tau	1.6	1.51 ± 0.12	0.15 ± 0.03	<0.004
DG Tau	V819 Tau	1.0	9.83 ± 0.19	0.62 ± 0.04	1.62 ± 0.04
DH Tau	V1321 Tau	0.5	0.75 ± 0.04	0.22 ± 0.02	<0.007
DK Tau	V819 Tau	0.4	1.33 ± 0.09	0.31 ± 0.05	0.10 ± 0.06
DL Tau	HBC 427	1.0	1.11 ± 0.06	<0.018	0.16 ± 0.06
DM Tau	V1321 Tau	0.1	0.56 ± 0.09	<0.017	<0.026
DN Tau	V819 Tau	0	<0.007	<0.007	<0.007
DO Tau	V819 Tau	1.5	5.24 ±0.06	0.49 ± 0.02	0.49 ± 0.04
DR Tau	V819 Tau, No Correction	5.6	0.22 ± 0.05	<0.009	<0.008
DS Tau	V819 Tau	0.6	0.20 ± 0.05	0.11 ± 0.02	<0.005
FM Tau	V1321 Tau, No Correction	3.5	0.70 ± 0.04	0.28 ± 0.04	<0.005
FZ Tau	V1321 Tau	1.6	0.78 ± 0.04	0.12 ± 0.03	0.15 ± 0.02
GH Tau	V1321 Tau	0.1	0.33 ± 0.03	<0.004	<0.004
GI Tau	V819 Tau	0.5	1.30 ± 0.07	0.36 ± 0.07	0.19 ± 0.03
GK Tau	V819 Tau	0.1	0.28 ± 0.02	<0.004	<0.005
GM Aur	HBC 427	0.6	0.35 ± 0.03	<0.009	<0.011
GO Tau	V1321 Tau	0.3	0.16 ± 0.02	0.11 ± 0.04	<0.005
HN Tau	V819 Tau, No Correction	1.3	5.77 ± 0.08	<0.025	1.28 ± 0.30
HQ Tau	HBC 427	0.7	0.37 ± 0.05	<0.007	<0.006
IP Tau	V819 Tau	0.4, 0.3	0.69 ± 0.07, 0.52 ± 0.03	<0.008, <0.005	<0.010, <0.009
IT Tau	HBC 427	0	0.30 ± 0.06	<0.004	<0.004
TW Hya	V819 Tau	0.5	0.50 ± 0.04	0.09 ± 0.02	<0.012
UX Tau A	HR 8832, HBC 427	0.2, 0.2	0.22 ± 0.02, 0.09 ± 0.02	<0.006, <0.006	<0.003, <0.003
VY Tau	V1321 Tau	0	<0.010	<0.008	<0.008
V710 Tau	V1321 Tau	0.1	<0.008	<0.007	<0.011
V773 Tau	HBC 427	0.1	0.54 ± 0.03	<0.003	<0.003
V836 Tau	V819 Tau	0.2	0.58 ± 0.06	0.22 ± 0.09	<0.007

* The 3-σ upper limits were computed assuming an unresolved line of FWHM 6.6 km/s.

are determined from flux calibrated spectra that include the Balmer discontinuity, where the spectrum of the continuum UV-excess can be modeled with accretion shocks (Calvet and Gullbring, 1998; Herczeg and Hillenbrand, 2008). Since our echelle spectra are not flux-calibrated, accretion luminosities can be estimated using well calibrated relationships relating line and accretion luminosities first demonstrated by Muzerolle et al. (1998) and recently summarized in Alcalá et al. (2014). This approach is superior to the older technique of using the emission excess (veiling) at one wavelength in the Paschen continuum, which requires applying an uncertain bolometric correction. Here we will use the calibration on the Hα line luminosity from Alcalá et al. (2014) because it is based on a large sample of low-mass stars and simultaneous UV-excess measurements of the accretion luminosity.

With our echelle spectra, emission line equivalent widths (EW_λ) can be converted into a line luminosity using the following relation:

$$L_{line} = 4\pi\ d^2\ f_\lambda\ (EW_\lambda)(1 + r_\lambda) \tag{4.1}$$

where d is the distance to the science target, f_λ is the photospheric continuum flux density near the line of interest, and the factor (1+ r_λ) converts the observed equivalent width to one that is veiling corrected, i.e. measured in units of the stellar continuum. For this work, we chose Hα for an accretion diagnostic since it is detected in all of our targets. We adopt distances from Herczeg and Hillenbrand (2014), and use their published extinction corrected continuum flux density at 7510 Å, in conjunction with the ratio of the flux densities at 6600 Å and 7510 Å in the Pickles Atlas for stars matched in spectral type to each science target (Pickles, 1998) to determine the stellar flux density near Hα. The veiling r_λ at 6300 Å listed in Table 4.2 is very close to that at Hα and was adopted here. While this approach assumes the stellar continuum has not varied, it does account for any variability in veiling between our observations and that of Herczeg and Hillenbrand (2014) in setting the continuum flux adjacent to the line.

The Hα line luminosities ($L_{H\alpha}$), are then converted to accretion luminosities, L_{acc}, using the relation derived by Alcalá et al. (2014):

$$\log\left(L_{acc}/L_{\odot}\right) = (1.50 \pm 0.26) + (1.12 \pm 0.07) \times \log\left(L_{H\alpha}/L_{\odot}\right) \tag{4.2}$$

The calibration based on $L_{H\alpha}$ can be compromised in sources with large blueshifted and redshifted absorption, masking what otherwise would be a larger emission EW. However, since it is observed in all our targets, we preferred it to other indicators such as He I. Finally, the accretion luminosities are converted into mass accretion rates using the magnetospheric model developed by Gullbring et al. (1998) and the following equation:

$$\dot{M}_{acc} = \frac{L_{acc}\ R_{*}}{GM_{*}(1 - \frac{R_{*}}{R_{in}})} \tag{4.3}$$

where R_* and M_* are the radius and mass of the star, G is Newton's gravitational constant, and R_{in} is the inner truncation radius of the disk. R_{in} is generally unknown, but it is usually assumed to be $\approx 5R_*$, the co-rotation radius (e.g. Gullbring et al. 1998; Shu et al. 1994). For all of the sources, we use the stellar masses and radii from Herczeg and Hillenbrand (2014).

All accretion parameters, including $\mathrm{EW}_{H\alpha}$, $L_{H\alpha}$, L_{acc} and $\dot{M}_{acc}$ are listed in Table 4.3. The table also includes columns for the line luminosity of [O I] 6300 Å, first for the whole line, then for the LVC and then for the NC of the LVC, all with f_λ determined from the Pickles Atlas near 6300 Å. The definition of the latter two will be described in the next section.

We estimate a typical uncertainty for L_{acc} as follows. Sixteen of our targets have multi-epoch R-band photometry measurements (Herbst et al., 1994) where the standard deviation of the photometric points over the mean R-magnitude is at most 0.1, which indicates that variability in the continuum is probably not a major source of uncertainty for most stars. The extinctions derived by Herczeg and Hillenbrand (2014) also have a small uncertainty, only 0.15 dex. Therefore, the major uncertainty in L_{acc} will be the calibration of $L_{H\alpha}$ and L_{acc}. Errors in the slope and y intercept of this relation are included in Equation 2. Adding these uncertainties in quadrature gives a final uncertainty on L_{acc} of ~ 0.3 dex. Variations in TTS Hα EW and veiling, attributed to variations in accretion luminosity, are typically less than a factor of

Table 4.3 Accretion Properties

Source	EW (Hα) [Å]	log $L_{H\alpha}$ [$L_\odot$]	log L_{acc} (Hα) [$L_\odot$]	log $\dot{M}_{acc}$ (Hα) [$M_\odot$/year]	log L_{OI} (total) [$L_\odot$]	log L_{OI} (total LVC) [$L_\odot$]	log L_{OI} (LVC NC) [$L_\odot$]
AA Tau	10.5	-3.48	-2.40	-9.34	-4.74	-4.82	-5.33
BP Tau	97.0	-2.34	-1.12	-8.17	-4.89	-5.00	-5.83
CI Tau	84.5	-2.11	-0.87	-8.03	-4.87	-4.90	—
CoKu Tau 4	1.16	-4.62	-3.67	-10.7	-5.68	-5.72	-5.72
CW Tau	110	-1.91	-0.64	-8.01	-3.74	-3.91	-4.46
CY Tau	114	-2.52	-1.33	-8.20	-5.09	-5.09	—
DF Tau	46.7	-2.22	-0.98	-7.46	-3.94	-4.30	-5.27
DG Tau	63.5	-2.26	-1.03	-8.12	-3.16	-4.05	-4.05
DH Tau	34.5	-3.14	-2.02	-8.93	-4.99	-5.01	-5.50
DK Tau	33.5	-2.67	-1.50	-8.53	-4.17	-4.28	-5.69
DL Tau	92.6	-2.10	-0.85	-8.06	-4.06	-4.64	—
DM Tau	104	-3.14	-2.02	-8.94	-5.65	-5.74	-5.74
DN Tau	13.5	-3.06	-1.93	-8.76	< -5.87	< -5.87	—
DO Tau	136	-2.23	-1.00	-8.21	-3.75	-4.37	—
DR Tau	43.9	-2.10	-0.85	-8.10	-4.45	-4.56	-5.01
DS Tau	49.4	-2.97	-1.82	-9.03	-5.47	-5.47	-6.17
FM Tau	78.3	-3.19	-2.07	-8.66	-5.54	-5.56	-5.92
FZ Tau	176	-1.95	-0.68	-7.77	-4.41	-4.70	-5.22
GH Tau	11.8	-3.28	-2.18	-8.80	-5.02	-5.04	—
GI Tau	22.2	-2.85	-1.69	-8.62	-4.19	-4.38	-4.87
GK Tau	14.9	-2.87	-1.71	-8.58	-4.66	-4.77	-5.15
GM Aur	92.9	-2.19	-0.95	-8.15	-4.66	-4.65	-4.88
GO Tau	45.9	-3.12	-2.00	-8.92	-5.76	-5.73	—
HN Tau	89.2	-2.47	-1.27	-8.69	-3.67	-4.33	—
HQ Tau	2.22	-2.76	-1.60	-8.68	-3.54	-3.71	—
IP Tau	10.4	-3.39	-2.29	-9.30	-4.70	-5.50	—
IT Tau	16.9	-2.83	-1.67	-8.63	-4.63	-4.62	—
TW Hya	230	-2.32	-1.10	-8.34	-5.09	-5.13	-5.13
UX Tau A	10.2	-2.70	-1.52	-8.84	-4.75	-4.70	-4.70
VY Tau	4.24	-3.96	-2.93	-9.81	< -6.13	< -6.13	—
V710 Tau	1.87	-4.49	-3.52	-10.1	< -6.52	< -6.52	—
V773 Tau	3.02	-3.02	-1.88	-8.79	-3.79	-3.86	—
V836 Tau	10.4	-3.58	-2.51	-9.56	-4.94	-4.91	—

Values for IP Tau are from 2006, for UX Tau A from 2012 as described in Section 4.4.1

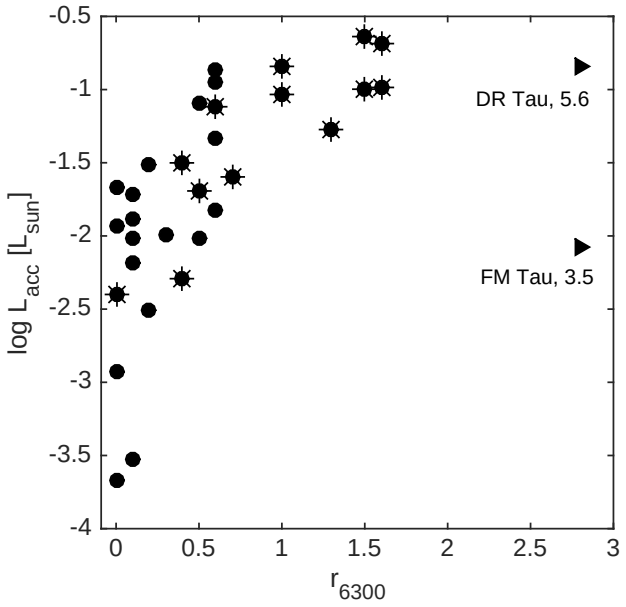

Figure 4.6 There is a general trend of increasing L_{acc} with increasing veiling, defined by a clear lower boundary for L_{acc} at a given veiling with considerable scatter above that boundary. The extreme veiling sources DR Tau and FM Tau, with $r_{6300} = 5.6$ and 3.5, respectively, exceed the plot boundary. Symbols with radial spokes denote sources with a high velocity component at [O I] 6300 Å.

two. Two of our targets, UX Tau A and IP Tau, were observed in both 2006 and 2012 with changes in Hα EW by factors 1.2 and 1.5, respectively, with negligible changes in veiling. This level of variability corresponds to a variation of ~ 0.2 dex in L_{acc}.

The range in Hα EW for our sample runs from a low of 1.2 Å to a high of 230 Å, translating into a span of more than three orders of magnitude in L_{acc} and $\dot{M}_{acc}$, with accretion luminosities from $10^{-3.7}$ to $10^{-0.6}$ $L_{\odot}$, and mass accretion rates from $10^{-10.7}$ to $10^{-7.5}$ $M_{\odot}$/year. Manara et al. (2013) demonstrated that for L_{acc} $< 10^{-3.0} L_{\odot}$ there is a possibility for chromospheric emission to dominate the line luminosity. Since the continuum veiling is a diagnostic of accretion, deriving from excess emission in the accretion shock on the stellar surface, the relation between r_{6300} and L_{acc}, shown graphically in Figure 4.6, offers additional insight on whether a star is accreting. In general these quantities are correlated, in the sense that there

is a well defined lower boundary in L_{acc} at a given veiling with considerable scatter above that boundary.[2] For example, the objects with low veiling (r_{6300} of 0 or 0.1) have inferred accretion luminosities spanning two orders of magnitude. We conclude from this that it is not possible to assign an unambiguous accreting/non-accreting status based on the level of the Hα EW or absence of veiling, sometimes used as thresholds for defining classical (accreting) or weak (non-accreting) TTS. Since all of our targets have disks in various evolutionary states, we will treat them all identically in converting Hα into accretion luminosities. We note that three sources have Hα based accretion luminosities near or below the threshold where accretion cannot be distinguished from chromospheric activity (CoKu Tau 4, VY Tau, and V710 Tau). Two of these three also have no detection of even the strongest forbidden line, [O I] 6300 Å. The third non-detection at [O I] 6300 Å is DN Tau, with Hα EW = 13.5 Å, r_{6300} = 0, and an inferred log L_{acc} of -1.93. As discussed in Section 4.5.1, this appears to the only example of a star that is accreting but does not show forbidden emission.

4.4 Deconstructing Forbidden Line Profiles

The aim of this paper is to better understand the LVC of forbidden line emission in TTS. In this section we describe the fitting technique used to define and separate HVC and LVC emission, and then describe the kinematic properties of the LVC emission.

[2]Note that the two sources with the highest veiling, DG Tau and FM Tau, with r_{6300} = 5.6 and 3.5 respectively, do not fall into the relation between veiling and L_{acc} defined by the other stars. Exceptionally high veilings for these sources were also found by HEG. Either the relation between veiling and accretion luminosity breaks down at high veilings (Gahm et al., 2008) and/or the accretion luminosities based on Hα are severely underestimated due to strong wind absorption features in sources with high disk accretion rates and high veilings.

4.4.1 Gaussian Fitting

The focus of this paper is the behavior of the LVC of the forbidden line profiles. Although in some instances the HVC and LVC are well resolved (e.g. CW Tau, DO Tau) in most cases they are blended (e.g. DK Tau, HN Tau). In the earlier HEG study the separation between HVC and LVC was made simply by assigning emission further than 60 km/s from the stellar velocity to the HVC. With almost a factor of two higher spectral resolution, we attempt to separate blended HVC and LVC using Gaussian fitting. To this end, we fit the profiles interactively using the Data Analysis and Visualization Environment (DAVE) that runs as a Graphical User Interface (GUI) in IDL. This program was developed by the National Institute of Standards and Technology (NIST) Center for Neutron Research (Azuah et al., 2009). In order to find the best fit parameters for each emission feature, we identify the minimum number of Gaussians required to describe each profile, specifying an initial estimate of the centroid velocity (v_c) and full width at half maximum (FWHM) for each component using the Peak ANalysis (PAN) feature of DAVE. PAN then performs many iterations to minimize the reduced chi-squared and outputs the best fit centroid velocities, the FWHM, and the areas under the Gaussian fits. Errors in centroid velocities, measured relative to the stellar photosphere, cannot be less than ± 1 km/s, which is the uncertainty in the stellar radial velocity (see Pascucci et al. 2015 for more details).

The number of Gaussians required to fit each line profile depends on the profile's shape and an RMS estimate of the goodness of fit. The fitted components, individually and summed, are superposed on all 30 detected [O I] 6300 Å profiles in Figures 4.7 and 4.8. Eleven profiles are well fit with a single Gaussian component and another ten with two Gaussians. The remaining nine profiles required 3 components (5 stars), 4 components (3 stars) and in once case, FZ Tau, five components.

The method we adopt to attribute a component to HVC or LVC emission begins with an examination of the distribution of centroid velocities for all individual components across all stars, shown in Figure 4.9. The component centroid veloci-

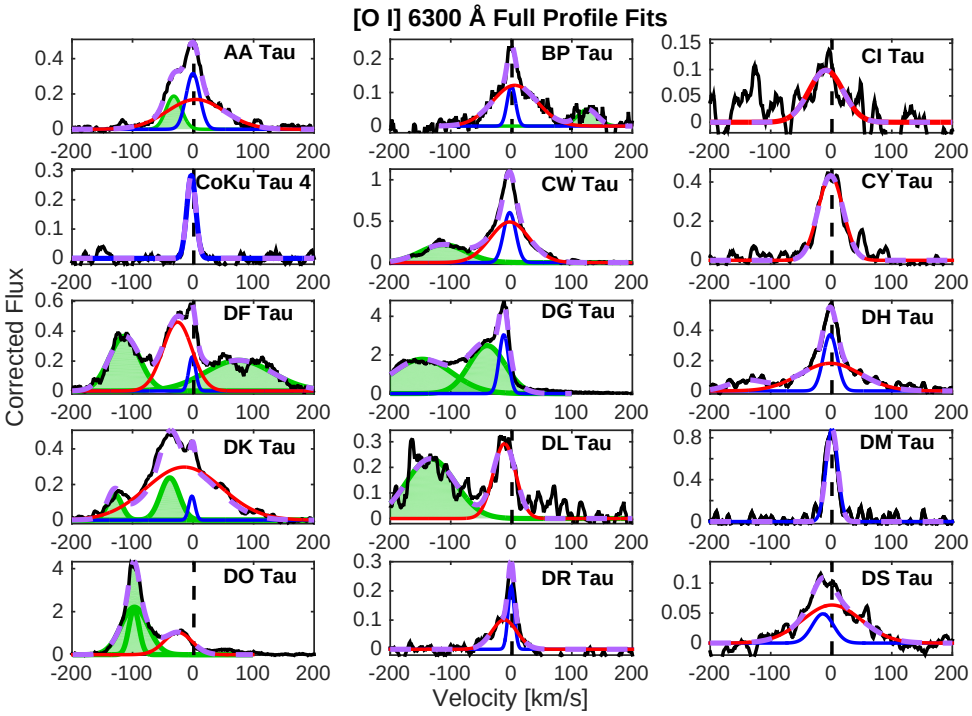

Figure 4.7 Gaussian component fits for half the stars with a detected [O I] 6300 Å line. Areas shaded in green meet the criterion for HVC emission. The LVC fits may be comprised of one or both narrow (blue) or broad (red) components. The sum of all fits is a purple dashed line.

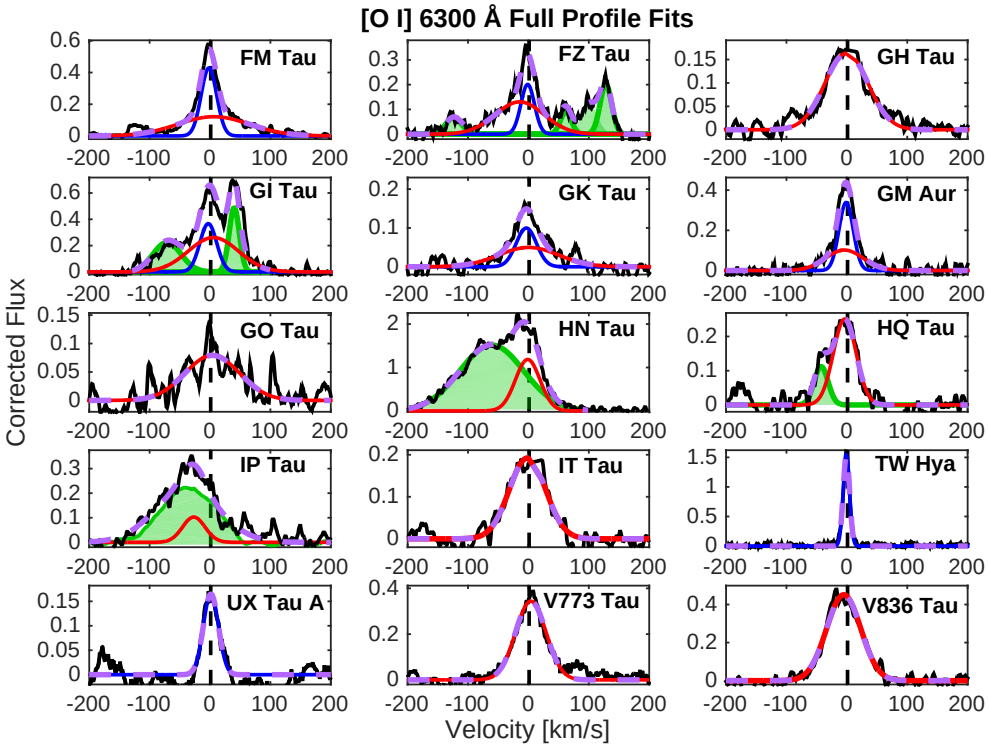

Figure 4.8 Continuation of Figure 4.7. Gaussian component fits for the second half of the stars with a detected [O I] 6300 Å line. Areas shaded in green meet the criterion for HVC emission. The LVC fits may be comprised of one or both narrow (blue) or broad (red) components. The sum of all fits is a purple dashed line.

ties range from -144 km/s (DG Tau) to +130 (FZ Tau), with blueshifts far more common than redshifts and a high concentration at low velocities. Based on this distribution, we adopt a centroid velocity of ± 30 km/s as the threshold between HVC versus LVC emission. With this method, although all detected [O I] lines show LVC emission, HVC emission (highlighted in green in Figures 4.7 and 4.8) is seen in only 13 sources at [O I] 6300 Å and only 3 sources at [O I] 5577 Å. In contrast all 8 [S II] detections show HVC emission but only 2 (CW Tau and HN Tau) show weak LVC emission. The HVC fit parameters of centroid velocity and FWHM are listed in Table 4.4 for all 3 lines, the LVC fit parameters for the two [O I] lines in Table 4.5 and the LVC fit parameters for [S II] in Table 4.6.

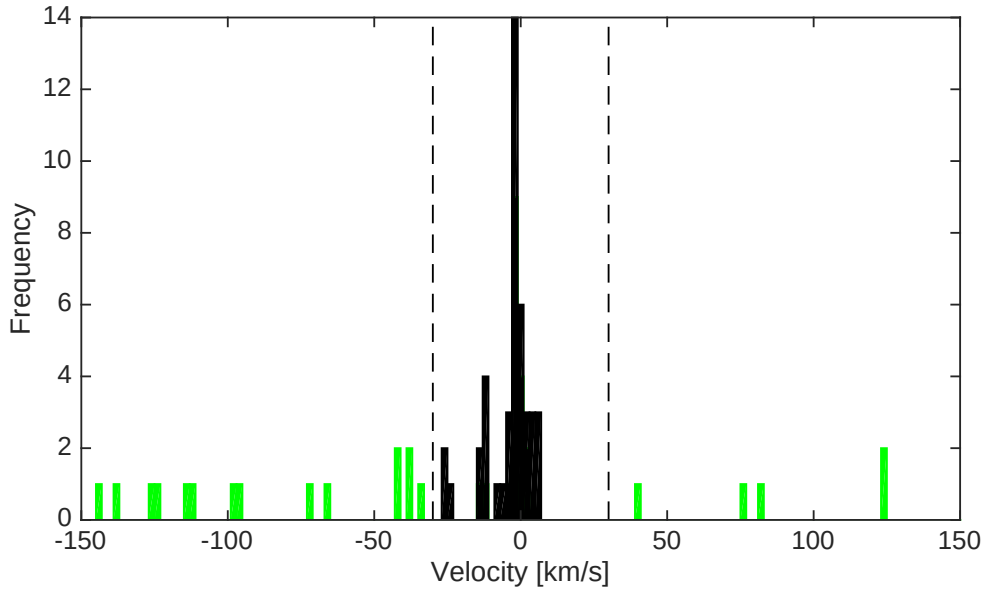

Figure 4.9 Distribution of velocity centroids for Gaussian components used to describe the [O I] 6300 Å profiles. We adopt ± 30 km/s (dashed lines) as the threshold between HVC (green) and LVC (black) emission.

We find this approach to be reinforced when comparing component fits for the cases when both [O I] lines are present. We illustrate four examples in Figure 4.10 including two of the three stars with HVC emission detected at 5577 Å (CW Tau and DO Tau), plus two cases where HVC emission is seen at [O I] 6300 Å but not 5577

Table 4.4 High Velocity Component Fit Parameters

		HVC blue 1		**HVC blue 2**		**HVC red 1**		**HVC red 2**	
Source	Line [Å]	v_c [km/s]	FWHM [km/s]	v_c [km/s]	FWHM [km/s]	v_c [km/s]	FWHM [km/s]	v_c [km/s]	FWHM [km/s]
AA Tau	[O I] λ 6300	-33	25	—	—	—	—	—	—
BP Tau	[O I] λ 6300	—	—	—	—	124	46	—	—
CW Tau	[O I] λ 6300	-112	89	—	—	—	—	—	—
	[O I] λ 5577	-112	89	—	—	—	—	—	—
	[S II] λ 6731	-116	38	—	—	—	—	—	—
DF Tau	[O I] λ 6300	-114	56	—	—	82	102	—	—
DG Tau	[O I] λ 6300	-144	118	-38	68	—	—	—	—
	[O I] λ 5577	-144	118	-38	68	—	—	—	—
	[S II] λ 6731	-103	171	-34	46	—	—	—	—
DK Tau	[O I] λ 6300	-126	37	-42	51	—	—	—	—
	[S II] λ 6731	-56	38	—-	—	—	—	—	—
DL Tau	[O I] λ 6300	-138	115	—	—	—	—	—	—
	[S II] λ 6731	-133	70	—	—	—	—	—	—
DO Tau	[O I] λ 6300	-97	51	-95	19	—	—	—	—
	[O I] λ 5577	-85	74	—	—	—	—	—	—
	[S II] λ 6731	-93	27	—	—	—	—	—	—
FZ Tau	[O I] λ 6300	-124	32	—	—	76	70	125	29
	[S II] λ 6731	—	—	—	—	130	23	—	—
GI Tau	[O I] λ 6300	-71	49	—	—	40	23	—	—
	[S II] λ 6731	-61	31	—	—	39	22	—	—
HN Tau	[O I] λ 6300	-66	130	—	—	—	—	—	—
	[S II] λ 6731	-84	113	—	—	—	—	—	—
HQ Tau	[O I] λ 6300	-41	27	—	—	—	—	—	—
IP Tau	[O I] λ 6300	-38	124	—	—	—	—	—	—

Note. Centroid velocities and FWHMs of Gaussian fits for high velocity components. These have been separated into blue-shifted HVC and red-shifted HVC, both of which there are occasionally two.

Å (AA Tau and DF Tau). In all cases we find that although the HVC components differ between [O I] 6300 Å and 5577 Å, their LVC component(s) are similar. The tendency for the LVC components to be comparable in the two [O I] lines, once the HVC is accounted for, gives us confidence that our method to characterize the LVC emission is generally robust. A close comparison of the LVC in the two [O I] lines will follow in the next section.

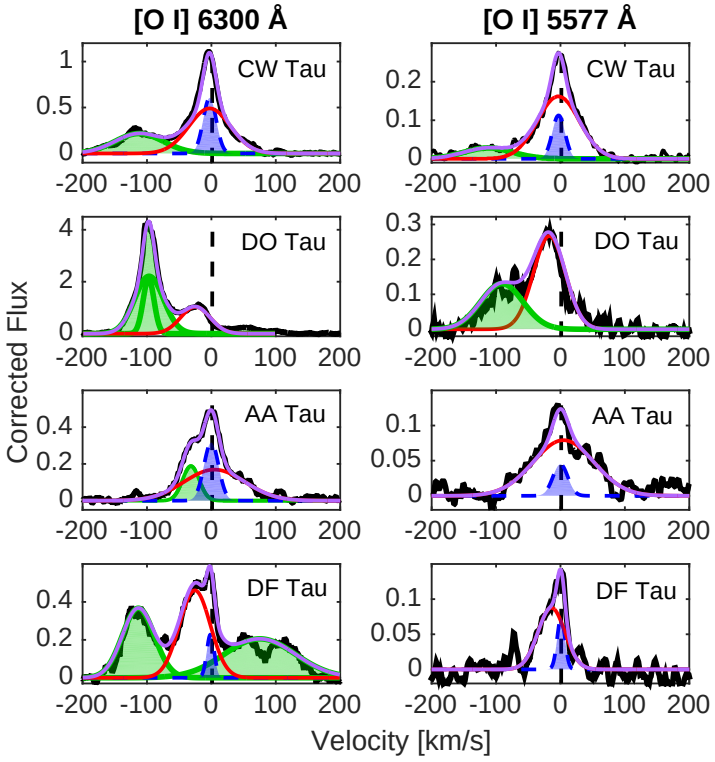

Figure 4.10 Examples showing that when both [O I] lines are present, the LVC components for 6300 Å (left) and 5577 Å (right) are very similar. The narrow component of the LVC is shaded in blue, and the broad component of the LVC is outlined in red. Areas shaded in green meet the criteria for HVC and the purple line shows the sum of all fits.

However, one of the two stars with spectra from both observing epochs, IP Tau, indicates an exception to the finding that LVC emission is always present. We illustrate the change in the morphology of the [O I] 6300 Å profile between the two epochs in Figure 4.11. In 2006 the profile is asymmetric, requiring two Gaussians

Table 4.5 [O I] LVC parameters

	6300 Å						5577 Å					
Source	Narrow Component			Broad Component			Narrow Component			Broad Component		
	FWHM [km/s]	v_c [km/s]	EW [Å]	FWHM [km/s]	v_c [km/s]	EW [Å]	FWHM [km/s]	v_c [km/s]	EW [Å]	FWHM [km/s]	v_c [km/s]	EW [Å]
AA Tau	27	-0.19	0.19	111	4.67	0.42	27	-0.19	0.02	111	4.67	0.18
BP Tau	16	0.11	0.04	87	5.65	0.23	16	0.11	0.01	87	5.65	0.15
CI Tau	—	—	—	66	-8.70	0.15	—	—	—	—	—	—
CoKu Tau 4	18	-2.90	0.12	—	—	—	—	—	—	—	—	—
CW Tau	24	-2.63	0.32	76	-2.70	0.83	23	0.92	0.05	73	1.61	0.25
CY Tau	—	—	—	48	-1.02	0.47	—	—	—	61	-0.98	0.22
DF Tau	14	-1.34	0.07	57	-25.7	0.58	14	0.93	0.03	49	-14.0	0.09
DG Tau	18	-12.3	1.25	—	—	—	19	-10.6	0.26	—	—	—
DH Tau	27	-1.75	0.23	119	-1.31	0.48	27	-1.75	0.08	119	-1.31	0.15
DK Tau	12	-1.90	0.04	137	-11.8	0.98	12	-1.90	0	137	-11.8	0.30
DL Tau	—	—	—	44	-11.3	0.29	—	—	—	—	—	—
DM Tau	23	1.10	0.45	—	—	—	—	—	—	—	—	—
DO Tau	—	—	—	54	-24.9	1.24	—	—	—	58	-17.2	0.31
DR Tau	12	-0.11	0.06	49	-11.6	0.11	—	—	—	—	—	—
DS Tau	39	-13.8	0.04	115	1.10	0.16	39	-13.8	0.02	115	1.10	0.09
FM Tau	30	-1.82	0.29	140	6.15	0.38	30	-1.82	0.12	140	6.15	0.13
FZ Tau	26	-1.28	0.12	95	-14.6	0.28	26	-1.28	0.06	95	-14.6	0.09
GH Tau	—	—	—	84	-0.66	0.31	—	—	—	—	—	—
GI Tau	33	-2.85	0.27	97	5.61	0.57	33	-2.85	0.09	97	5.61	0.23
GK Tau	39	-3.50	0.09	116	0.40	0.13	—	—	—	—	—	—
GM Aur	28	-1.26	0.21	73	-4.11	0.15	—	—	—	—	—	—
GO Tau	—	—	—	106	3.84	0.17	—	—	—	106	3.84	0.11
HN Tau	—	—	—	48	-1.18	1.27	—	—	—	—	—	—
HQ Tau	—	—	—	44	-3.47	0.25	—	—	—	—	—	—
IP Tau	—	—	—	44	-26.9	0.11	—	—	—	—	—	—
IT Tau	—	—	—	71	-1.54	0.31	—	—	—	—	—	—
TW Hya	12	-0.78	0.46	—	—	—	11	0.37	0.07	—	—	—
UX Tau A	29	1.50	0.10	—	—	—	—	—	—	—	—	—
V773 Tau	—	—	—	59	3.91	0.46	—	—	—	—	—	—
V836 Tau	—	—	—	67	-5.23	0.63	—	—	—	67	-5.23	0.12

to describe it, but in 2012 it is symmetric and fit by one component. Using our definition of HVC and LVC, the single component seen in 2012 is classified as HVC emission, and it is identical in velocity centroid and FWHM to one of the two components describing the 2006 profile. In contrast the second component in 2006 meets the criteria of LVC emission. Throughout this work we will use the 2006 spectrum for IP Tau so its LVC profile can be compared with the other stars. We note that the issue of variability of the LVC will be addressed further in Section 5.1, where we find that the LVC is typically constant when compared to profiles found in the literature. Thus cases like IP Tau would be interesting to monitor for further variability.

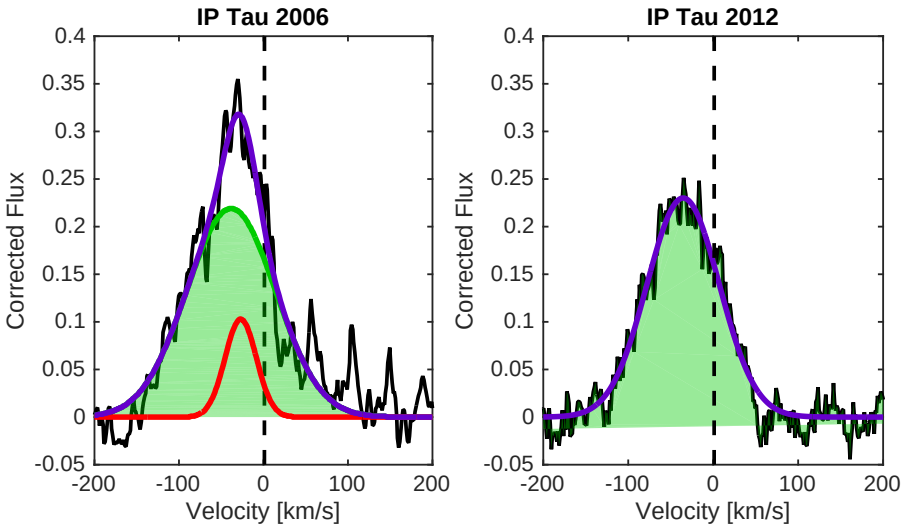

Figure 4.11 [O I] 6300 Å profiles for two observing epochs for IP Tau. In 2006 two gaussian components describe the profile, but in 2012 only one is required. The area shaded in green is the HVC, identical in both epochs. The red line denotes a broad LVC, seen only in 2006.

4.4.2 The Low Velocity Component

In this section we subdivide the LVC into two components, one broad (BC) and one narrow (NC), based on examination of residual LVC profiles generated by subtracting the HVC component fits from the observed profile. The motivation for this

Table 4.6 [S II] 6731 Å LVC Parameters

	FWHM [km/s]	v_c [km/s]	EW [Å]
CW Tau	24	-5.51	0.10
HN Tau	55	-9.43	0.45

further subdivision is that although [O I] LVC residual profiles from 17 stars are described by one gaussian component, 13 have LVC profiles that require a composite of two gaussians, with one component significantly broader than the other. The residual LVC [O I] 6300 Å profiles, with component fits superposed, are presented in two figures, in Figure 4.12 for the 17 single component fits and in Figure 4.13 for the 13 two component fits.

The combination of a broad and narrow component in the 13 composite LVC profiles is shown quantitatively by the distribution of their FWHM, presented in the upper panel of Figure 4.14. In the figure, the LVC with two-component fits are highlighted with a darker shading than those with one-component fits. Among the components with the composite profiles, the narrower component, with FWHM from 12 to 39 km/s, a median of 27 km/s and a standard deviation 9 km/s, can be contrasted with the broader component, with FWHM from 49 to 140 km/s, a median of 97 km/s and a standard deviation of 29 km/s. Based on this FWHM separation between the two components, we designate NC LVC as those with FWHM $\leq$ 40 km/s, and BC LVC as those with FWHM $>$ 40 km/s, and color-code them in the figure with red for BC and blue for NC. With this subdivision, we can further classify the single-component LVC fits (lighter shading in Figure 4.14), into 12 BC LVC and 5 NC LVC. In sum, of the 30 TTS with [O I] 6300 Å LVC emission, 18 have NC and 25 have BC, with 13 stars showing both components.

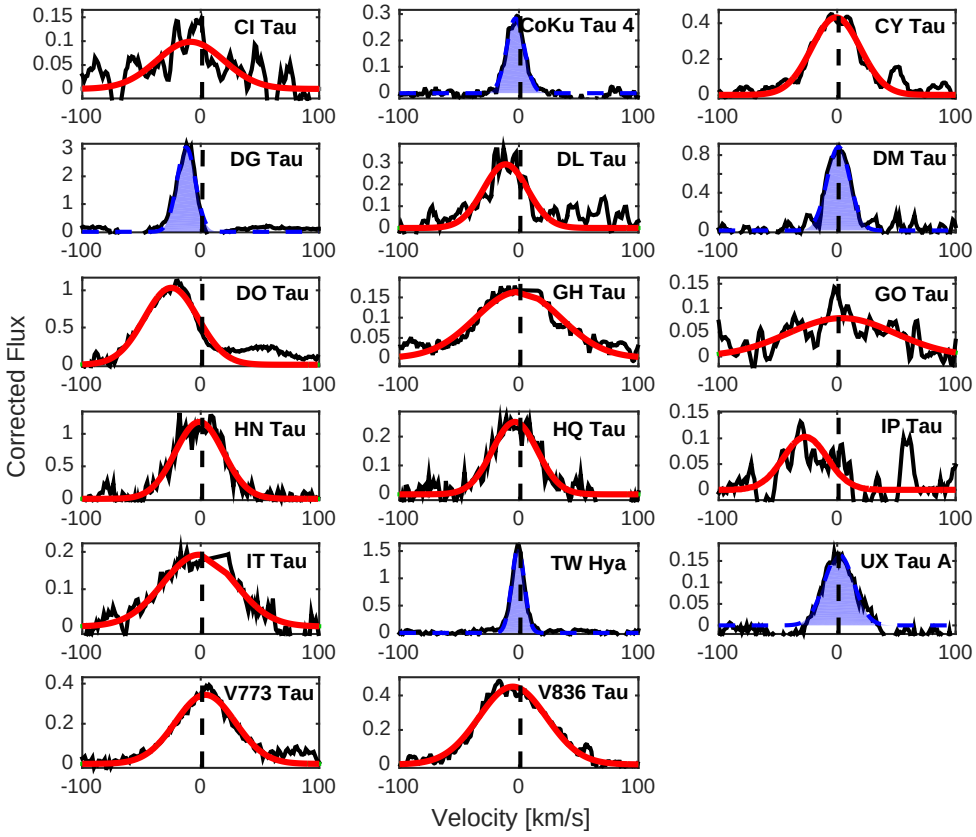

Figure 4.12 Residual [O I] 6300 Å LVC profiles, after the HVC has been removed, for sources that can be fit with one gaussian. Areas shaded in blue represent the narrow component of the LVC, whereas red lines represent the broad component of the LVC as explained in Section 4.4.2.

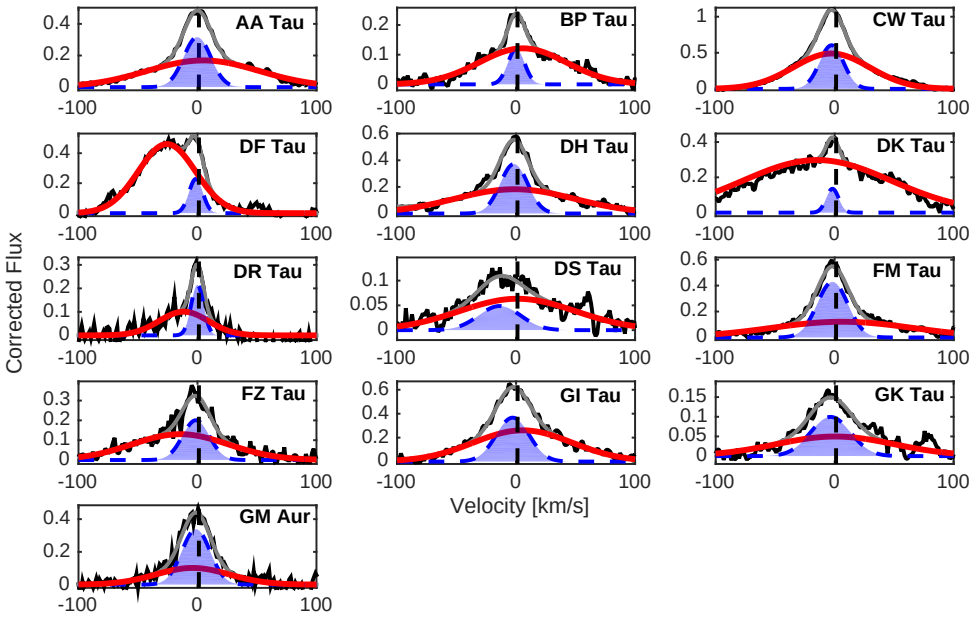

Figure 4.13 Residual [O I] 6300 Å LVC profiles, after the HVC has been removed, for sources that are fit with two gaussians. Areas shaded in blue represent the narrow component of the LVC, whereas red lines represent the broad component of the LVC as explained in Section 4.4.2. Gray lines show the total (narrow+broad component) fits.

The lower panel of Figure 4.14 presents the distribution of centroid velocities (all by definition less than 30 km/s) of the NC and BC LVC. Their centroid velocities overlap, together spanning a range from -27 km/s to +6 km/s with both groups peaking at blueshifts of a few km/s. A K-S test between the NC and the BC centroid velocities gives a $\sim 9\%$ probability that they are drawn from the same parent population, in the sense that the NC and BC velocity distributions are statistically indistinguishable. However, there are a few considerations that suggest otherwise. Although they have similar average centroid velocities, -2.5 km/s for the NC and -3.7 km/s for the BC, the standard deviation for the NC is almost a factor of three smaller than for the BC, 3.6 km/s versus 9.7 km/s. We will explore possible differences in the centroid velocities of the NC and BC in the next section.

A comparison of the residual LVC profiles between the two [O I] lines can made for the 16 stars with [O I] 5577 Å, where only 3 stars (CW Tau, DG Tau, DO Tau) had HVC that needed to be subtracted. This is illustrated in Figure 4.15 where both residual LVC are normalized to their respective peaks so the profile structure can be compared. We see that for most stars the LVC structure is very similar between the two lines. This similarity is strengthened when their LVC fit parameters, listed in Table 4.5, are compared. For example in AA Tau and BP Tau the centroids and FWHM of both the BC and NC between the two lines is identical and the difference in the superposed profiles is due to a different ratio of BC to NC. This similarity again suggests that the process of subdividing the LVC into BC and NC is robust.

There are 3 cases where there are differences in the LVC components between the two [O I] lines. The most extreme case is DF Tau, where the [O I] 6300 Å BC LVC extends further to the blue than 5577 Å, with centroids of -26 km/s and -14 km/s, respectively. For this star it is possible that there is uncorrected HVC emission at 6300 Å that is blended with the LVC (see Figure 4.10). Reassuringly, this is the only case with such an extreme difference. For the other two cases, CW Tau and DO Tau, the LVC centroid velocities are again more blueshifted at 6300 Å compared to 5577 Å but by only a few km/s. We will discuss these differences further in the next section. However we reiterate that for the majority of the stars

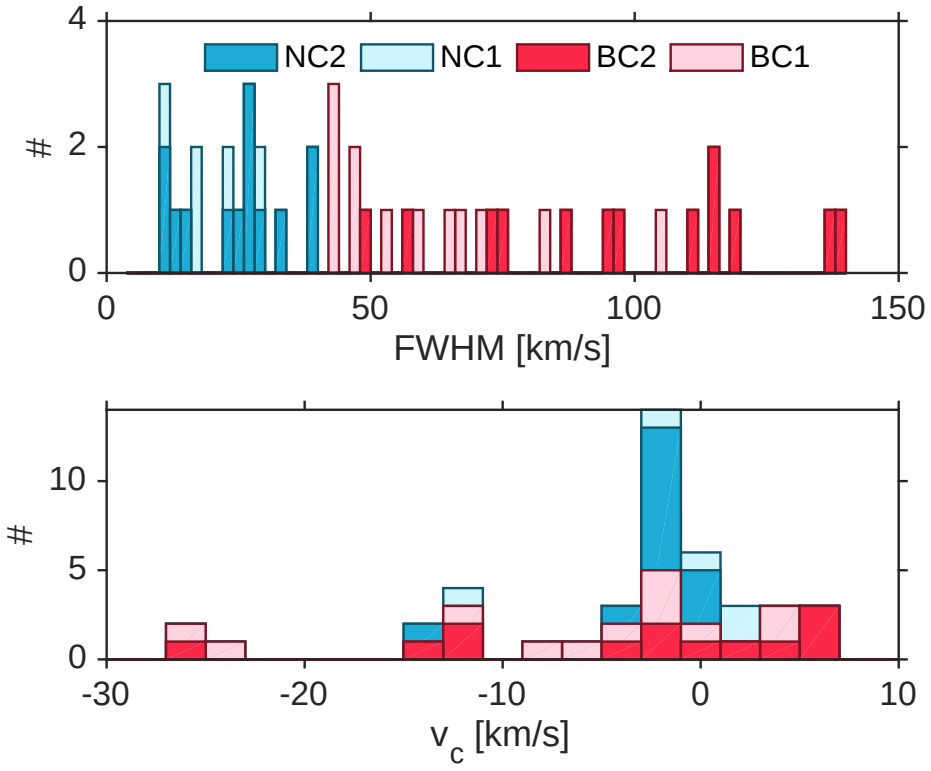

Figure 4.14 **Upper**: Histogram of FWHM for the components found in the [O I] 6300 Å LVC. The darker shading highlights sources with 2-component fits, with narrower FWHM (blue) clearly separated from broader FWHM (red) components. This leads to the adoption of 40 km/s as the boundary between NC and BC LVC emission. Lighter shading with the same color scheme shows the distribution of the sources with a single kinematic component. **Lower**: Histogram of the peak centroid values for [O I] 6300 Å for the components found in the [O I] 6300 Å LVC. Again, darker shading is for sources with 2-component fits. Bin sizes are 2 km/s.

the centroids and FWHM of the LVC components are essentially identical, within the errors, for both [O I] lines, suggesting that this approach is robust.

4.4.3 Velocity Shifts Among LVC

Although most stars with both [O I] lines show similar LVC kinematic properties, 4 sources, all with significant HVC emission, show LVC velocity centroids with velocity shifts among different lines, in the sense that the [O I] 5577 Å is less blueshifted than the [O I] 6300 Å, which in turn is less blueshifted than the [S II] 6731 Å. These small velocity offsets are illustrated in Figure 4.16, where the forbidden line LVC are superposed and plotted on an expanded velocity scale.

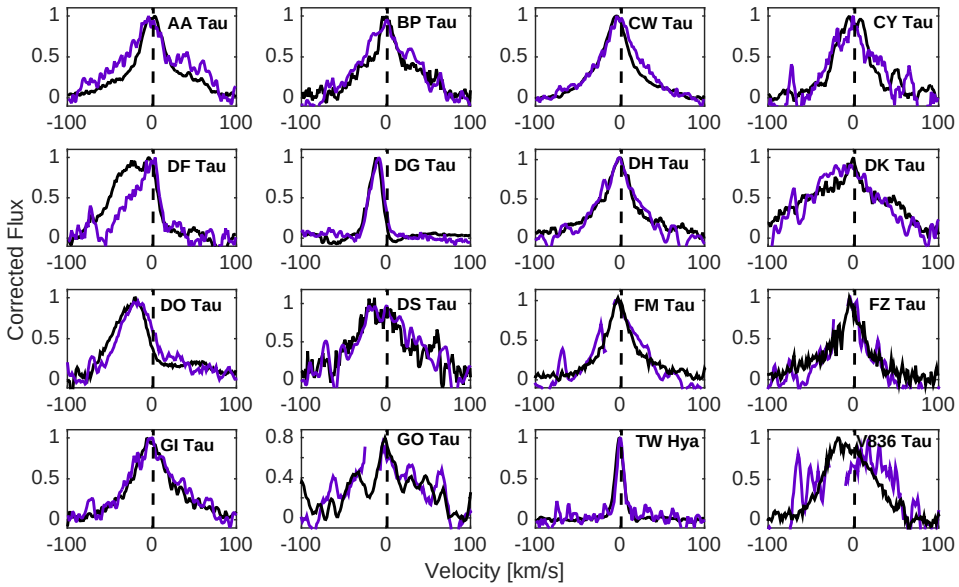

Figure 4.15 [O I] residual LVC profiles for 6300 Å (black) and 5577 Å (purple) scaled to a peak of 1 for the 16 sources where both lines are detected.

In the case of CW Tau and DF Tau, the velocity differences are seen in the NC of the LVC and in DO and HN Tau the velocity shifts are seen in the BC of the LVC. To best illustrate the NC shifts for CW Tau and DF Tau, where both [O I] lines require a two-component fit to their LVC, in Figure 4.16 the BC of the LVC has been subtracted, so only the NC are shown. The velocity centroids for the 3 NC

LVC for CW Tau are -5.5 km/s for the [S II], -2.63 km/s for the [O I] 6300 Å, and 0.92 km/s for the [O I] 5577 Å. For DF Tau they are -1.3 km/s and 0.9 km/s for the 6300 Å and the 5577 Å lines, respectively.

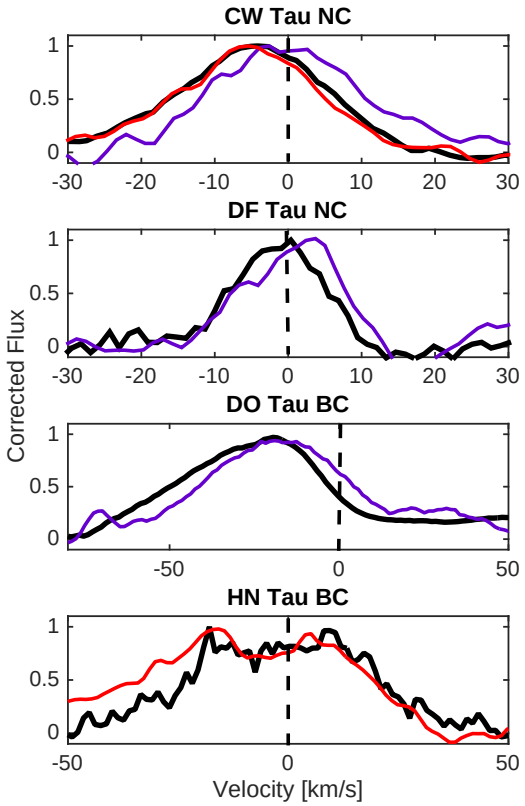

Figure 4.16 Superposed residual LVC profiles, after removal of the HVC, for [O I] 6300 (black), [O I] 5577 (purple) and [S II] 6731 (red) for the 4 sources that show different velocity centroids in the LVC components (see Section 4.4.3). In the cases of CW and DF Tau (top two) the [O I] LVC had both a BC and a NC, but in this figure the BC is removed. When detected the [S II] emission is more blueshifted than the [O I] 6300 Å which, in turn, is more blueshifted than the [O I] 5577 Å.

For the two stars with shifts in the BC, there are no NC contributions to the LVC. For DO Tau, the centroid velocity for [O I] 6300 Å is -25 km/s compared to -17 km/s at 5577 Å. Again, for HN Tau, the centroid for [S II] is -9.4 km/s and -1.2 km for [O I] 6300 Å, although in this source the major differences in the two

lines is a more extended blue wing at [S II]. A similar effect of more blueshifted LVC in lines of lower critical density was also found by HEG, suggesting that the lower critical density lines reflect acceleration in a slow wind in a few stars (see also Section 4.5.7).

4.5 Results for the Low Velocity Component

As shown in the previous section, LVC emission, seen in all 30 TTS with detected forbidden lines, can be further subdivided into NC and BC kinematic features. We do not find any commonality in the line profiles of the 10 multiple systems in our sample and see no trend with the companion separation (see Tables 3 and 4 in Pascucci et al. 2015 for stellar separations). As such we will not discuss the possible effect of binaries on the LVC. Instead, we will examine how the emission relates to accretion luminosities, assess the role of disk inclination in determining their FWHM, explore disk surface brightness distributions that can account for the observed profiles, and look at line ratios among the different forbidden lines. We begin by comparing relevant aspects of our results to the previous results.

4.5.1 Comparison to HEG

Since both this study and that of HEG focus on TTS in Taurus, there are 20 objects in common whose forbidden line properties can be examined for variability. In Figure 4.17, we overlay the [O I] 6300 Å profiles for these 20 sources, with the older profiles rescaled in peak intensity to match the current spectra, providing a comparison of the kinematic structure of the profiles over several decades. Recalling that there is almost a factor of 2 higher spectral resolution in the HIRES spectra (6.6 km/s versus 12 km/s), two things are apparent. *(1) The structure of the LVC is identical in most instances.* One dramatic exception is DN Tau, where the LVC has disappeared between 1995 and 2006. The DG Tau LVC profile is also different, where in 2006 there is a NC peak at -12 km/sec that is not seen in HEG. In the earlier spectrum the lowest velocity peak is at -50 km/s and does not qualify as

"Low Velocity" emission. However the red side of the profiles in both epochs are very similar, suggesting the more recent LVC peak may have been present, but much weaker, a few decades ago. (2) *The HVC is quite different in 4 sources* (CW Tau, DF Tau, DG Tau, and DR Tau), and in the case of DR Tau it has vanished between 1995 and 2006. Since the HVC arises in spatially extended microjets that form time variable knots of shocked gas, such changes are not surprising, especially as differences in slit length and orientation coupled with differences in the width of the stellar point spread functions (PSF) between the two studies can also yield different profiles for extended emission. However, we conclude that the velocity structure of the LVC is generally stable over a timescale of decades in most stars.

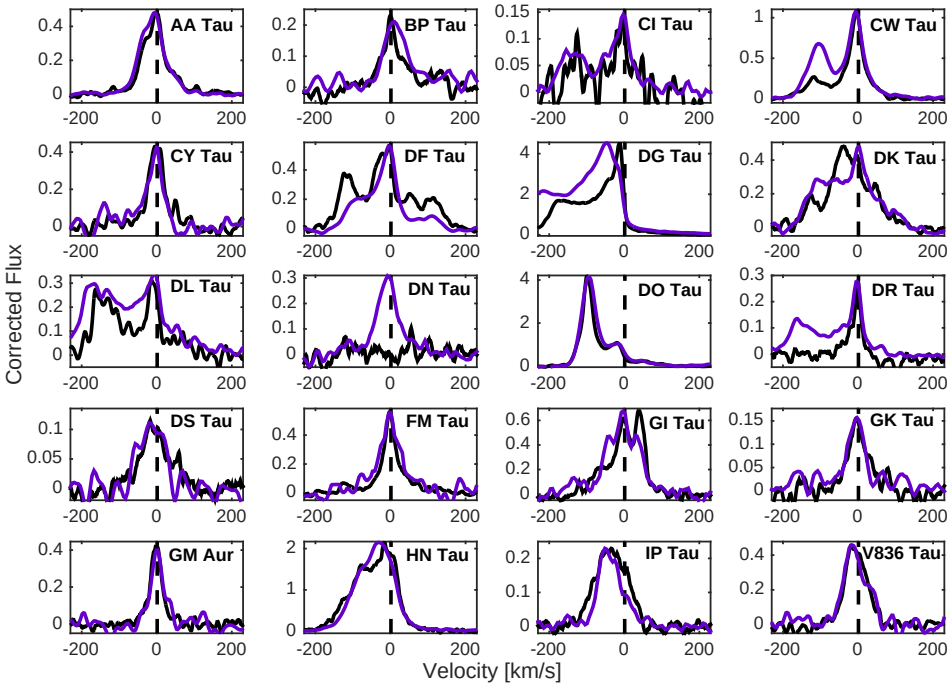

Figure 4.17 Comparison of 20 [O I] 6300 Å profiles in common with this work (black) and HEG (purple), scaled to the peak intensities of our spectra.

We can also examine whether the strength of the LVC emission is comparable between the 2 studies. We do this in Figure 4.18 by comparing the LVC equivalent

widths normalized to the photospheric continuum, (EW $\times$ (1+r_λ)), with the caveats that the HEG definition of the LVC was any emission within 60 km/s of the stellar velocity, in contrast to our approach of isolating kinematic components by Gaussian fitting, and the difference in wavelength for which the veiling is reported, r_{5700} in HEG versus r_{6300} here. This comparison of veiling corrected EW shows comparable emission strength of the LVC for most sources, with the exception of DN Tau, which, as seen in Figure 4.17, has disappeared since 1995. In the other sources, the differences in the veiling corrected equivalent width between the two epochs could be attributed to differences in the definition of the LVC, variation in the stellar continuum and/or variability in the line luminosity itself, or possibly to extended emission in some LVC observed with different stellar PSF or slit orientations, as hinted at in Hirth et al. (1997).

The complete disappearance of [O I] 6300 Å emission in DN Tau is surprising, making it the only source known to date that is accreting but has no [O I] 6300 Å emission. The [O I] 6300 Å equivalent width found by HEG is 0.43 Å while our upper limit $\sim$ 0.007 Å, about two orders of magnitude lower than in 1995. The corresponding decrease in the Hα equivalent width is only $\sim$ 30% (see Beristain et al. 2001), and differences in veiling ($r_{5700} = 0.1$ versus $r_{6300} = 0$) are small, consistent with the estimated uncertainty. We checked for variability in the continuum with the Herbst et al. (1994) catalogue. It was rather stable at R mag $\sim$ 11.5 between 1980 and 1986, and brightened by $\sim$ 0.5 mag through 1995, the last year of recorded data. The profile for DN Tau seen in HEG qualifies as solely LVC, which combined with our current two epochs for IP Tau (see Figure 4.11), gives two examples where the LVC has vanished, although in most stars it appears stable over timescales of decades. Additional observations of both DN Tau and IP Tau would be of interest to see if their LVC returns.

Another interesting comparison is the implication for the velocity of the LVC, noted to be typically blueshifted by $\sim$ 5 km/s by HEG. Although the kinematic structure in the LVC is unchanged in the two studies (Figure 4.17), in the present study of LVC emission we find that only 12/25 of the BC and 9/18 of the NC are

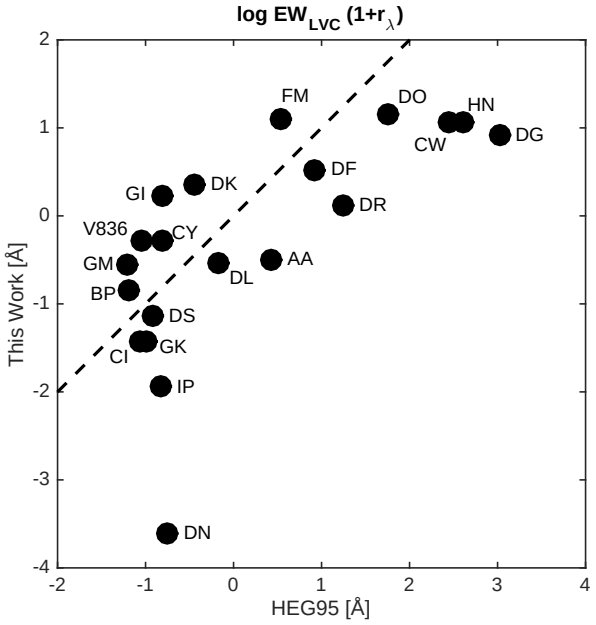

Figure 4.18 Comparison of veiling corrected EW of the [O I] 6300 Å LVC in common with this work and HEG. The definition of the LVC is different in the two studies, where HEG includes any HVC emission within 60 km/s of the stellar velocity. The dashed line is for a one-to-one correspondence.

blueshifted relative to the stellar photosphere (Table 4.5). The process of defining and separating full profiles into HVC, NC, and BC and then subtracting a HVC that is blended with a LVC (e.g. AA Tau) and/or separating a blueshifted BC LVC from a NC LVC (e.g. FZ Tau), means the resultant BC or NC may no longer be identified as blueshifted, although in the full profile the LVC looks to be predominantly blueward of the stellar velocity. However, we find roughly half the LVC components are blueshifted, and as seen in HEG and discussed here in Section 4.4.3, in four stars these blueshifts show velocity gradients among different forbidden lines, with higher blueshifts for lines of lower critical density. We note that these four stars, CW Tau, DF Tau, DO Tau and HN Tau, have some of the highest veiling corrected [O I] 6300 Å LVC equivalent widths, as shown in Figure 4.18.

4.5.2 Comparison to Recent Studies of Luminosity Relations

The two recent studies of forbidden LVC emission, R13 and N14, found correlations between the accretion luminosity with both the luminosity of the [O I] 6300 Å LVC and the stellar luminosity, but not with the X-ray luminosity, for samples primarily from Taurus and Lupus. Additionally, a relation between L_{acc} and L_* was found by Mendigutía et al. (2015) for a large sample of objects in various star forming regions.

Although the correlation in R13 was based mostly on the HEG sample, with which we strongly overlap, we look here at these relations for our data, since R13 used the original 1995 assessment of the LVC luminosity in contrast to our component fitting and here we have a more consistent and reliable conversion of EW of both Hα and [O I] to line luminosities. We use the Astronomy SURVival package (ASURV) developed by Lavalley et al. (1992) because it includes upper limits in the linear regression and correlation tests.

In the lower panel of Figure 4.19, we compare L_{OI} for both the complete LVC and only for the NC of the LVC to L_{acc}. For the former, the Kendall τ test lends to a strong correlation, with a probability of 0.07% that the variables are uncorrelated.[3]

[3]This test includes three non-detections in L_{OI} (DN Tau, V710 Tau, and VY Tau).

The best fit linear regression is:

$$logL_{[OI]\ LVC} = 0.65(\pm 0.13) \times logL_{acc} - 3.84(\pm 0.23) \tag{4.4}$$

when both luminosities are measured in $L_{\odot}$. This fit is the same as that in R13 and N14. The reason we have a larger uncertainty on the slope and intercept of our linear regression is because our targets cover a narrower range of L_{acc} ($logL_{acc}$ between -3.7 and -0.6) than the samples of R13 ($logL_{acc}$ between -3.2 and 1.8) and N14 ($logL_{acc}$ from -4.8 to -0.3).

The lower panel of Figure 4.19 also shows the relation between L_{OI} for the NC of the LVC and L_{acc}. Again, for the 18/33 sources for which NC LVC is detected there is only a $\sim$ 2% probability that the NC LVC and accretion luminosity are uncorrelated. Of note in this figure is the fact that the NC of the LVC is found over the full range of L_{acc}, and when present, increases proportionately with the accretion luminosity. In contrast to the correlation with L_{OI}, L_{acc} shows no correlation with L_*. Although such a correlation has been found in other samples, its absence here is probably because our sample covers a factor of $\sim$100 in L_* while that of Mendigutía et al. (2015) which includes brown dwarfs, spans 8 orders of magnitude.

For the comparison with the X-ray luminosity, 22 of our sources have L_X values as reported in Table 4.1. As in the earlier studies, we find no correlation with L_{OI} of the LVC, with a Kendall τ probability not low enough (10.8%) to indicate that the L_X and L_{OI} LVC are correlated.[4]

4.5.3 Fractional Contributions of the BC and NC to the LVC

Thirteen out of 30 sources with [O I] 6300 Å emission have LVC comprised of a combination of BC and NC emission. The remaining sources show LVC that are either entirely BC (12/30) or entirely NC (5/30). The proportion of the LVC that is BC (or NC) emission is not strongly dependent on the accretion luminosity, as

[4]This test includes three non-detections in L_{OI} (DN Tau, V710 Tau, and VY Tau).

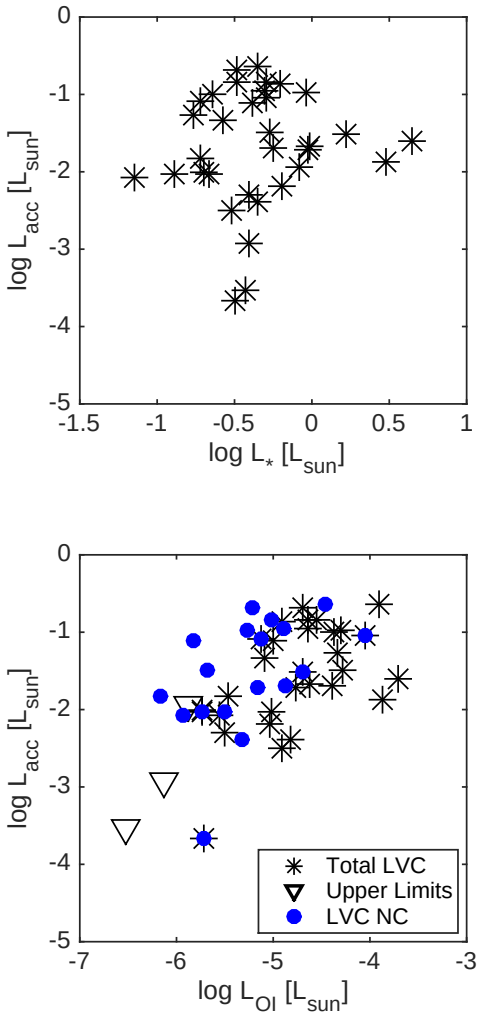

Figure 4.19 **Upper:** There is no correlation between the accretion luminosity and the stellar luminosity. **Lower:** The accretion luminosity is correlated with the luminosity of [O I] 6300 Å, both for the full LVC (asterisks) and for the NC of the LVC (blue circles), when detected.

shown in Figure 4.20. For example, the 12/30 sources that show only BC emission cover a wide range of disk accretion rates. The same is true for the 5/30 sources that show only NC emission. However, this figure also shows distinctive behavior for transition disk sources, all 5 of which have LVC emission dominated by the NC, and 4 of those 5 have no BC emission.

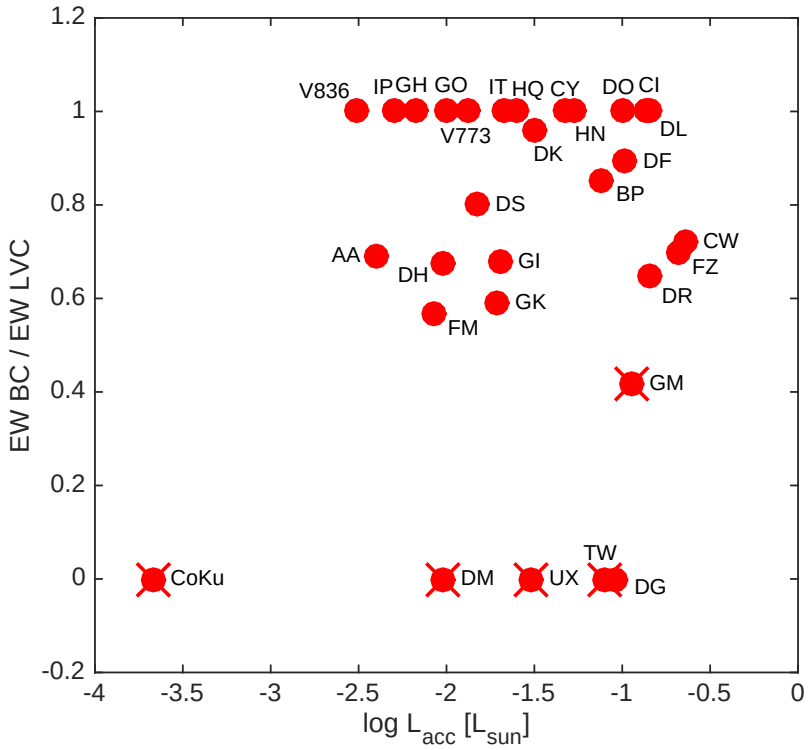

Figure 4.20 Proportion of LVC with BC emission plotted as a function of the accretion luminosity. Transition disk sources are marked with X's.

Combining the relations in Figure 4.19 and Figure 4.20 we find that while NC and BC emission are seen over a wide range of accretion luminosities, the luminosity of each component correlates with the accretion, but not the stellar, luminosity.

4.5.4 Velocity Centroids of the BC and NC of the LVC

The histogram of the velocity centroids for the two components of the [O I] 6300 LVC shows considerable overlap in velocity distributions (see Figure 4.14). Here we

add another dimension in the comparison of the centroid velocities, with Figure 4.21 showing the relationship between L_{acc} and v_c for the BC and NC. We conservatively use a $\pm$1.5 km/s from the stellar velocity as the area (depicted in gray in Figure 4.21) within which velocities cannot be distinguished from being at rest with respect to the star.

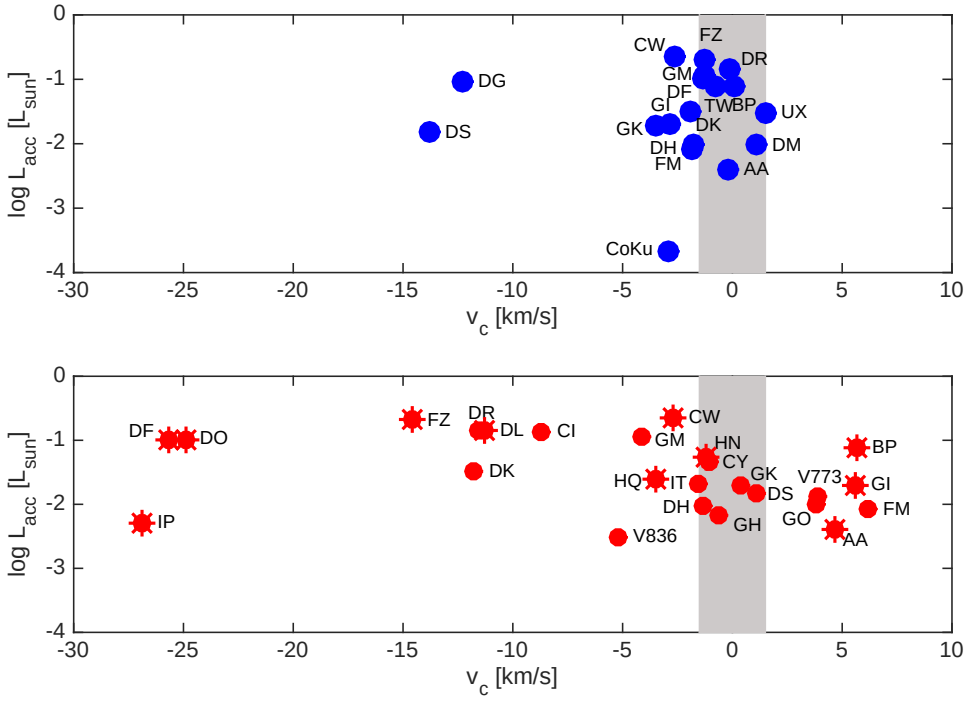

Figure 4.21 Relationship between L_{acc} and v_c for the 6300 Å NC of the LVC (upper) and BC of the LVC (lower). Sources with HVC removed are marked with spokes. The gray area around the stellar velocity, $\pm$ 1.5 km/sec, marks the uncertainty in centering the profiles.

For the BC centroids there is a tendency for the stars with higher accretion rates to have blueshifted v_c. Specifically, 7/12 stars with log $L_{acc}/L_{\odot} \geq$ -1.5 have v_c blueshifted from -9 to -26 km/s, while with one exception (IP Tau) all the stars with lower accretion rates have v_c within 6 km/s of the stellar velocity. A Kendall τ test gives a probability of only 2% that the BC centroids and L_{acc} are uncorrelated. Interestingly, 6 sources have BC that are redshifted between +3.8 to +6.2 km/s (AA

Tau, BP Tau, FM Tau, GI Tau, GO Tau, V773 Tau). While blueshifted centroids are readily associated with winds (12 sources), and unshifted centroids with bound disk gas (7 sources), the small redshifts seen in 6 sources can also be consistent with a wind with certain disk geometries. For moderate disk inclinations or strong flaring of the surface, the extended disk height at large radii may obscure (from the observer's perspective) the approaching part of a wind with a wide opening angle from the inner disk while the receding gas from the far side of the disk remains unobstructed (Gorti et al. in preparation).

Among the 18 NC detections, there is no trend between v_c and accretion luminosity and the centroid velocities either have small blueshifts or are consistent with the stellar velocity. A Kendall τ test lends to a 65% chance that the NC centroids and L_{acc} are uncorrelated. Blueshifted NC centroids (v_c from -1.75 to -13.8 km/s) indicative of slow winds are seen in 9 sources (CoKu Tau 4, CW Tau, DG Tau, DH Tau, DK Tau, DS Tau, FM Tau, GI Tau, GK Tau) while the remaining 9 are consistent with bound gas (AA Tau, BP Tau, DF Tau, DM Tau, DR Tau, FZ Tau, GM Aur, UX Tau A and TW Hya). There are no redshifted NC.

From these comparisons, although the K-S test comparing the distribution of NC and BC centroids indicated a 9% chance they were drawn from the same parent population (Section 4.4.2), we conclude that there are significant differences in the behavior of the v_c in these two components.

4.5.5 FWHM of BC and NC of the LVC: Dependence on Disk Inclination

The two-component nature of the LVC forbidden line emission in TTS is reminiscent of kinematic behavior found in a series of papers looking at high resolution VLT-CRIRES spectra of the 4.6 μm CO ro-vibrational fundamental lines in Class I and II sources (Bast et al. 2011; Pontoppidan et al. 2011; Brown et al. 2013; Banzatti and Pontoppidan 2015). The CO ν =1-0 line sometimes shows a NC/BC structure, while the ν =2-1 transition predominantly traces the BC, which allows it to be isolated when both transitions are observed. The finding that the FWHM of the broad and narrow CO features may derive from the system inclination leads us to

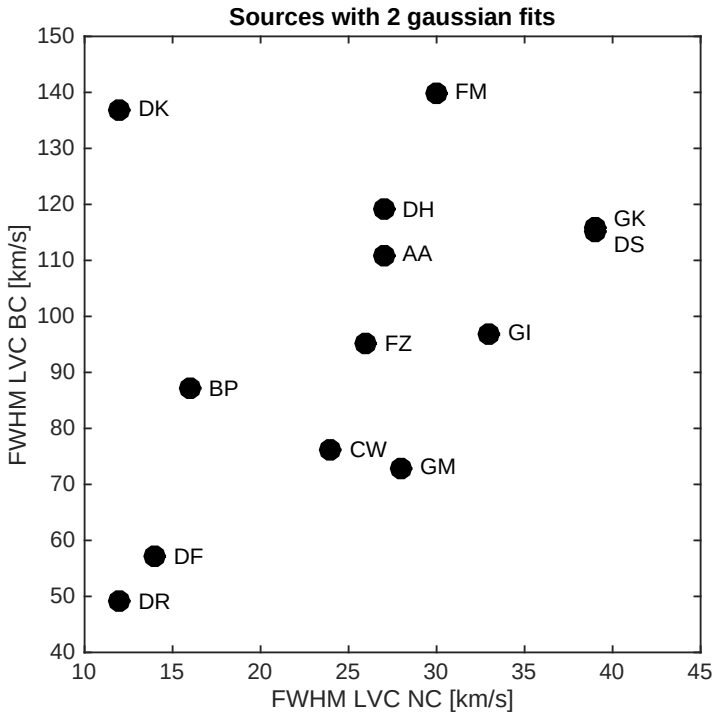

Figure 4.22 Relation between the FWHM for the NC and BC of the [O I] 6300 LVC in the 13 sources where both are present.

explore this possibility for the FWHM of the two components of the [O I] 6300 Å LVC.

First, we look at the relation between the FWHM of the NC and BC in those 13 sources where both components are seen at [O I] 6300 Å LVC. Each of these components shows a range in line widths (Figure 4.14), and if both were rotationally broadened we would expect to see a correlation between them in sources where both are present. We show this relation in Figure 4.22, where the FWHM of the NC, ranging from 12 to 39 km/sec, is reasonably well correlated with the FWHM of the BC, ranging from 44 to 140 km/sec, in all but one source (DK Tau). The Kendall τ probability that the two quantities are uncorrelated is indeed only 0.9% if we exclude DK Tau, but it increases to 7.5% when DK Tau is included.

We next explore the relationship between the width of the [O I] 6300 Å LVC

NC and BC with the published values for disk inclination in 22 sources. To directly compare our results with those already published for the CO ro-vibrational line, we follow Banzatti and Pontoppidan (2015) and plot the FWHM divided by the square root of the stellar mass versus the inclination from spatially resolved disks, rather than the FWHM vs the sine of disk inclination, which would be a better description of the relation expected for Keplerian broadening (left panel of Figure 4.23). The figure shows that the two quantities are positively correlated, both for the BC and the NC components. There are two outliers in the BC relation, DK Tau and FM Tau. DK Tau is the source that did not show the expected behavior between NC and BC FWHM in Figure 4.22 and here we see that the NC is in line with other sources at similar inclinations. The very low mass source FM Tau (0.1 $M_{\odot}$) lies off the scale of the plot, but as we will show in Section 4.5.6, this can be explained if the emitting region is closer in than for stars of higher mass.

Again, following Banzatti and Pontoppidan (2015) we will use the positive linear correlation to infer disk inclinations for the remaining sources. In order to include uncertainties in this process we assume an uncertainty of $\sim$ 10% in the disk inclination, as reported in the references in Table 4.1. For the FWHM, we adopt a Monte Carlo approach similar to that discussed in Section 4.2.4 in relation to the uncertainties on the measured EWs. Using the 17 single component LVC sources, we find an average uncertainty that is $\sim$ 13% of the measured FWHMs. As for the uncertainties on stellar masses, we assume 10% for stars with masses $\geq$ 1 $M_{\odot}$ and 30% for stars with masses $<$ 1 $M_{\odot}$ (see Stassun et al. 2014). Finally, in order to calculate the total uncertainty on the y-axis, we propagate the error on the stellar mass and FWHM, assuming they are independent.

Adopting these uncertainties and using a linear relationship between FWHM / $\sqrt{M_*}$ and disk inclination, we find the following best fits from the 22 sources with measured inclinations:

$$FWHM_{NC}/\sqrt{M_*} = 0.36(\pm 0.07) \times i + 7.87(\pm 3.72) \tag{4.5}$$

$$FWHM_{BC}/\sqrt{M_*} = 1.75(\pm 0.41) \times i + 0.09(\pm 21.8) \quad (4.6)$$

where FWHM is measured in km/s, M_* is measured in $M_\odot$ and inclination is measured in degrees. These fits demonstrate that although the NC and BC both correlate with disk inclination, they have different slopes, suggesting that they trace different regions. Assuming that the broadening is due solely to Keplerian rotation, we compute the [O I] disk radii from the velocity at the HWHM. The black solid lines in Figure 4.23 show that the NC probes disk radii between 0.5 and 5 AU while the BC traces gas much closer in, between 0.05 and 0.5 AU.[5]

We can compare these results to those of Banzatti and Pontoppidan (2015) for CO, where our linear fits are shown as red lines in Figure 4.23 and those for CO are shown in green. We find similar slopes for the BC of both CO and [O I] but slightly more extended disk radii for the [O I] than for the CO (the BC CO disk radii range from 0.04 to 0.3 AU). The slopes for the NC of CO and [O I] are not in agreement, and the inferred formation region for [O I], from 0.5 to 5 AU, is again slightly further from the star than that inferred for the NC of CO (0.2-3 AU).

We can then use the linear fits presented above to derive disk inclinations for the sources with no disk-based inclination values in the literature (right panel of Figure 4.23). For the sources where the LVC has only one component, we calculate the inclination using equations 5 or 6 depending on whether it is classified as NC or BC. For the sources where the LVC has both a broad and a narrow component, we calculate the inclination of each component individually (both are shown in Figure 4.23) and take a weighted mean to derive the source inclination. Inclinations derived from these fits to the BC and NC relations are reported in Table 4.1 and are marked with a dagger.

[5]Note that the dashed lines in Figure 3 of Banzatti and Pontoppidan (2015) provide the CO inner disk radius computed from the FWHM. However, the CO disk radii used through their paper are calculated from the velocity at the HWHM.

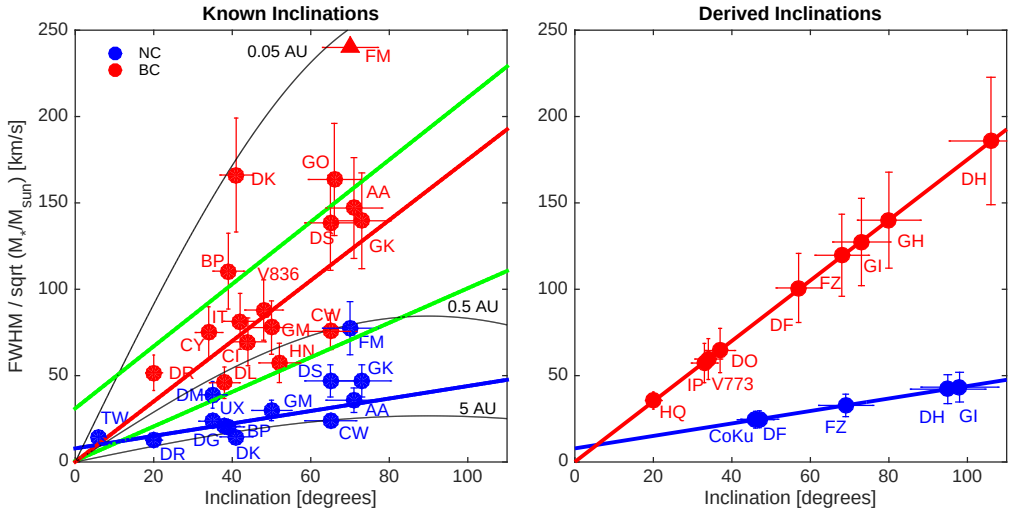

Figure 4.23 **Left**: Relation between the FWHM normalized by the stellar mass and known inclinations, for both NC and BC LVC. Derived linear fits are shown in red (BC) and blue (NC), those found by Banzatti and Pontoppidan (2015) from CO are shown in green. Black lines show line widths as a function of inclination at disk radii of 0.05, 0.5, and 5 AU. **Right**: Inclinations derived from the observed FWHM for NC and BC observations for sources with unknown inclinations, using the fits from the left panel.

4.5.6 Radial Surface Brightness of the Narrow LVC

In the previous section, we found that the NC of the LVC has a line width consistent with Keplerian broadening at a distance between 0.5 and 5 AU from the star. Here we will explore the range of radii in the disk required to account for the observed NC profile assuming a simple power law surface brightness fall off. Of the 18 sources with NC in their LVC, 9 have velocity centroids consistent with bound gas meaning that their profiles can be modeled with a simple Keplerian disk. Of these 9 sources 4 are transition disks (TDs), so we can also test whether the distribution of the gas in disks with dust cavities extending from a few to tens of AU (Espaillat et al., 2014),

Table 4.7 Results from Modeling the 9 Sources with Bound LVC NC

Source	M_* [$M_\odot$]	R_{in} [AU]	R_{out} [AU]	$R_{80\%}$ [AU]	α
Transition Disks					
UX Tau A	1.51	0.50	18.0	1.83	2.22
GM Aur	0.88	0.07	10.9	0.40	1.89
TW Hya	0.69	0.05	11.1	0.18	2.23
DM Tau	0.35	0.02	3.00	0.35	1.47
Full Disks					
DR Tau	0.90	0.46	18.2	3.39	1.65
BP Tau	0.62	0.08	9.20	3.90	0.94
FZ Tau	0.63	0.17	19.7	1.50	1.66
AA Tau	0.57	0.22	11.4	2.04	1.56
DF Tau	0.32	0.20	8.61	6.92	0.00

is different from the NC of Class II sources.

Our modeling uses a power law distribution for the line surface brightness of the form $I_{OI}(r) \propto r^{-\alpha}$, where r is the radial distance from the star and α is varied between 0 and 2.5 (see e.g. Fedele et al. 2011). The radial profile is converted into a velocity profile assuming Keplerian rotation, with the stellar mass and disk inclination in Table 4.1 as additional input parameters. The model line is convolved with a velocity width $v = \sqrt{v_{\rm in}^2 + v_{\rm th}^2}$ where $v_{\rm in}$ is the instrumental broadening (6.6 km/s) and $v_{\rm th}$ is the thermal broadening. We assume a temperature of 5,000 K to compute $v_{\rm th}$ because the [O I] emission might trace hot collisionally excited gas (Ercolano and Owen 2010, 2016). We then use the *mpfitfun* IDL routine[6] to find the best fit to the observed line profiles where an uncertainty equal to the RMS on the

[6]http://cow.physics.wisc.edu/∼craigm/idl/idl.html

continuum is adopted for each flux measurement. The parameters that are varied in the fitting procedure are the inner and outer radii of the emitting gas and α.

Our best fits to the NC [O I] 6300 Å profiles of three representative sources with very similar inclinations ($i \sim 35 - 40^o$) but different disk types and mass accretion rates are shown in Figure 4.24. Our simple model does a good job in reproducing the observed NC profiles and shows that the radial extent of the gas emitting the NC LVC is from within 1 AU, to explain the relatively large FWHMs, out to ∼10 AU, to explain the lack of double peaks in the profiles (see Table 4.7 for a summary of inferred parameters). We see a trend between the inner and outer radii and the stellar mass, with the smallest [O I] emitting region located around the lowest mass star DM Tau and the largest around the most massive $\sim 1\,M_{\odot}$ stars in our sample DR Tau and UX Tau A. The power law index of the surface brightness ranges from flat α= 0 (for DF Tau) to α= 2.2 (for UX Tau A and TW Hya). Using the best fit surface brightness we also compute the radius within which 80% of the NC LVC emission arises ($R_{80\%}$ in Figure 4.24 and Table 4.7) and find it to be within $\sim$ 5 AU, in agreement with the [O I] disk radii estimated from the NC HWHM (see Figure 4.23). Our steepest power law indexes of ∼2.2 are very similar to those inferred for CW Tau and DQ Tau by HEG after re-centering their blueshifted [O I] profiles in the stellocentric frame and assuming that the entire line broadening is due to Keplerian rotation. The extent of the [O I] emitting region for these two sources is inferred to be between 0.1 out 20 AU, similar to the ranges we find. This hints that Keplerian broadening may also dominate the profile of wind sources. We plan to model wind profiles in a future paper by adding an unbound component with a prescribed velocity field to the bound Keplerian disk.

In summary, our modeling of LVC NC profiles consistent with bound gas shows no difference in the radial distribution of the gas for TDs and Class II sources. Given that the sub-mm dust cavity of UX Tau A and DM Tau are $\sim$ 25 AU (Andrews et al. 2011; Kraus et al. 2011; Ingleby et al. 2013; Alcalá et al. 2014) and $\sim$ 19 AU (Andrews et al. 2011; Kraus et al. 2011; Ingleby et al. 2013) respectively, our results also imply that the [O I] 6300 Å NC traces gas inside the dust cavity. We find

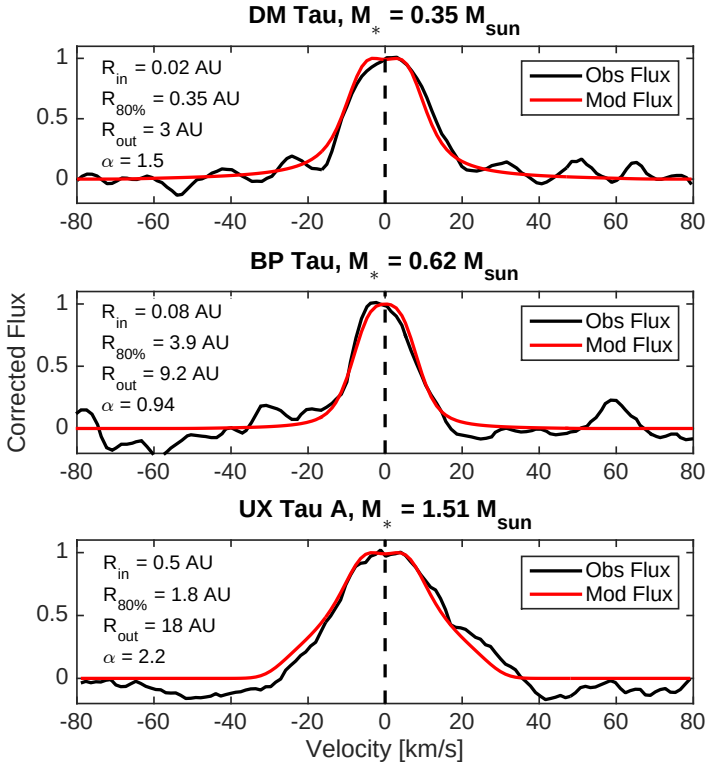

Figure 4.24 Comparison of computed profiles in bound disk gas to unshifted NC [O I] 6300 Å profiles in 3 sources with the same inclination. Two (DM Tau and UX Tau A) are transition disks and one (BP Tau) is a Class II source. Values for the inner and outer disk radii, the radius within which 80% of the emission arises, and the surface brightness power law are indicated.

similar results for the other 2 transition disks with NC centroids consistent with bound gas[7], see Table 4.7. Thus, we conclude that the [O I] 6300 Å NC profiles of TDs can be explained by radially extended [O I] emission, most of which is confined within their dust cavities (see Espaillat et al. 2014, pp. 297-520 for the dust cavities of TDs).

4.5.7 Line Ratios

Ratios of forbidden line equivalent widths can provide insight into the temperature and density of the LVC emitting line region. For example, the ratio of [O I] 5577/6300 for one of our sources, the transition disk TW Hya, with a value of ∼1/7 (Pascucci et al., 2011), has been interpreted by Gorti et al. (2011) as tracing the warm (∼1,000 K) and bound molecular layer where OH molecules are photodissociated by FUV photons. The LVC [O I] 5577/6300 ratio for the HEG stars was examined by R13 who found values between ∼1 and 1/8 for all sources except two with microjets that display smaller ratios (∼0.07). R13 attributed the larger ratios of 1 to 1/8 also to FUV photodissociation of OH molecules while N14 prefer the alternative possibility of thermal emission from a very hot (∼5,000 - 10,000 K) and dense ($n_H > 10^8\,cm^{-3}$) gas to explain similar ratios in a different sample of stars with disks.

The mean EW [O I] 5577/6300 ratio for the full LVC for our sample stars is 0.25, similar to those found previously. However, with the decomposition of our high resolution spectra into BC and NC contributions to the LVC we can look to see if these two LVC components have the same ratio. There are only 4 stars where we have sufficient signal to noise in both of these lines to evaluate the [O I] 5577/6300 for each component: AA Tau, BP Tau, CW Tau, GI Tau. In each case the BC ratio is a factor of a few higher than the NC ratio of [O I] 5577/6300.

Figure 4.25 compares the observed [O I] 5577/6300 values for these 4 stars (BC in red and NC in blue) with those predicted by a homogeneous and isothermal gas where the excitation is due solely to electron collisions, see Appendix E for details.

[7]We did not model the fifth TD, CoKu Tau 4, since its NC is blueshifted by 3 km/s

This figure shows that the BC emitting region is about a factor of 3 denser than the NC region if these two components arise from gas at the same temperature. Alternatively, if they trace similarly dense ($n_e \geq 10^7\,\mathrm{cm}^{-3}$) gas, the BC gas is ∼25% hotter than the NC gas. In either scenario, gas needs to be hot (≥5,000 K) to explain the observed ratios if the lines are thermally excited. For gas at 8,000 K the observed ratios can be explained by n_e ranging from $\sim 5 \times 10^6$ to $5 \times 10^7\,\mathrm{cm}^{-3}$ implying gas densities of a few $10^7 - 10^8\,\mathrm{cm}^{-3}$ for an ionization fraction of 0.33, close to the value expected in the [O I] emitting region in some photoevaporative wind models (see Figure 2 in Owen et al. 2011). By 5,000 K electron densities become very high ($\geq 10^8\,\mathrm{cm}^{-3}$) and, as discussed in the context of TW Hya (Gorti et al., 2011), are unlikely to be present in the hot surface of protoplanetary disks. An alternative interpretation for those sources with no definite blueshift is that the [O I] emission is not thermal but results from the photodissociation of OH molecules in a cooler (∼1,000 K), bound, and mostly neutral layer of the disk (Gorti et al., 2011).

Although the higher ionization [O II] 7330 line is not detected in any of our sources, we can use the upper limits to further constrain the gas temperature and density discussed above. Figure 4.26 shows the predicted [O II] 7330/ [O I] 6300 ratios versus the [O I] 5577/6300 ratios for the full LVC. As expected, since the critical electron densities for both the [O II] and [O I] lines are similar ($\sim 2 \times 10^6$ cm^{-3}), the [O II]/[O I] ratio is most sensitive to the gas temperature, given an ionization fraction which again we take to be 0.33. Models with the same electron density (green lines), but different temperatures, run diagonally in Figure 4.26. This figure shows that the gas temperature must be lower than 6,500 K if a single temperature is to explain all of our [O II] 7330/ [O I] 6300 upper limits, which would imply high electron densities ($\geq 10^{7.5}\,\mathrm{cm}^{-3}$) based on the [O I] 5577/6300 ratios. Higher temperatures are possible only in combination with an ionization fraction lower than 0.33.

As discussed earlier, it is also possible that the [O I] emission is not thermal but results from the dissociation of OH molecules (Gorti et al., 2011). A way to discriminate between thermal vs non-thermal emission would be to obtain high

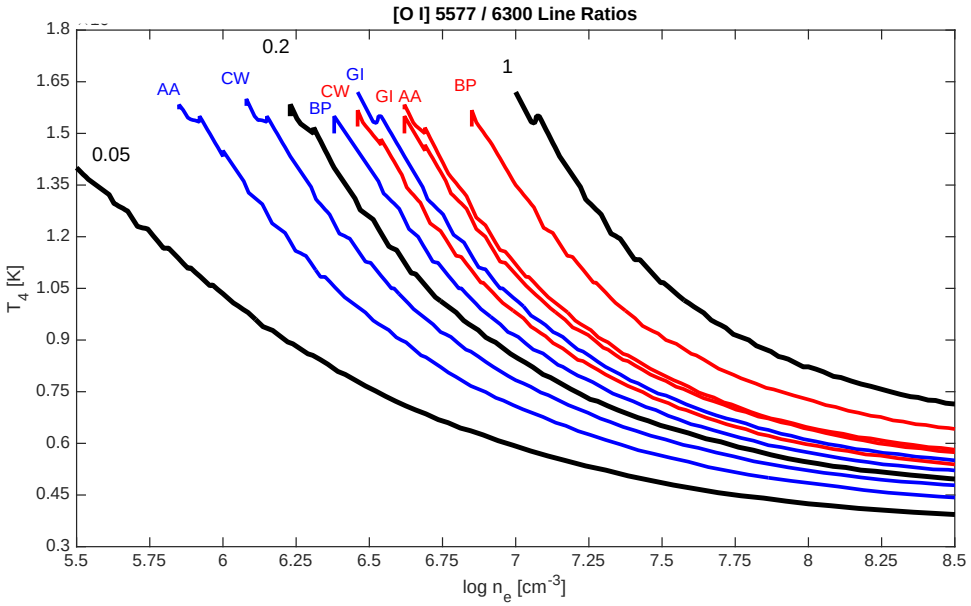

Figure 4.25 Contours of the thermal ratio of [O I] 5577/6300 Å as a function of gas temperature (divided by 10,000 K) and electron density. The line ratios for the four TTS with two kinematic components and high signal-to-noise profiles are shown in red (BC) and blue (NC). The BC has higher ratios than the NC implying a higher electron density for gas at the same temperature. Regardless of the kinematic component, if the lines are thermally excited, gas needs to be hot ($\geq$5,000 K) and dense to explain the observations.

spectral resolution observations of the [S II] line at 4068.6 Å because this line has a critical density of $2.6 \times 10^6\,\mathrm{cm}^{-3}$, very similar to that of the [O I] line at 6300 Å (see e.g. Natta et al. 2014). Similar line profiles for the [S II] and [O I] lines would clearly point to thermal emission in a hot dense gas.

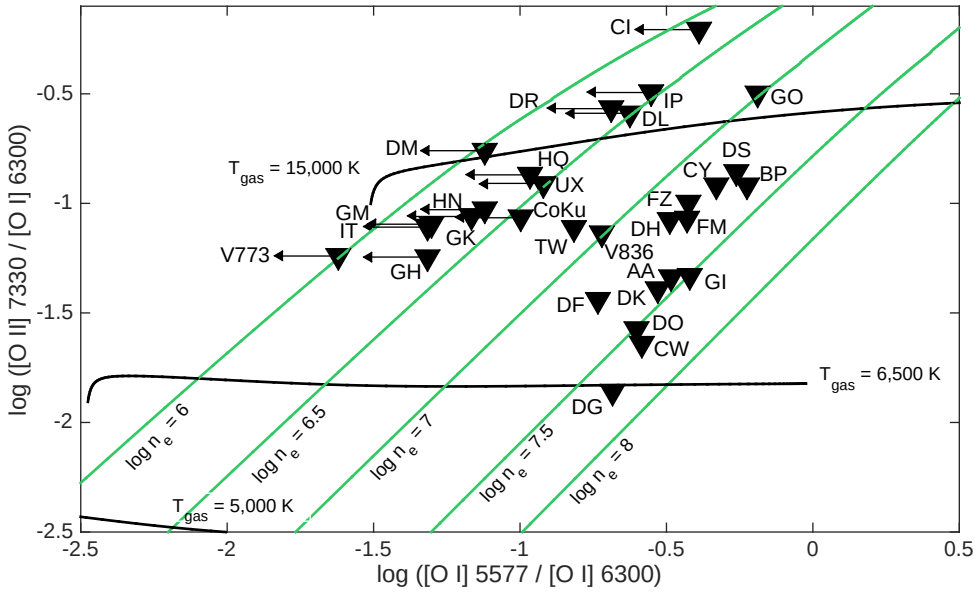

Figure 4.26 Oxygen line ratios are compared to predicted values assuming collisional excitation by electrons and an ionization fraction of 0.33. The [O II] 7330 Å transition is never detected so downward pointing triangles denote upper limits. Sources with no detection at [O I] 6300 show left pointing arrows for upper limits. Solid black lines denote ratios for gas at constant temperatures while diagonal green lines for gas at the same electron density. Temperatures lower than 6,500 K are consistent with all [O II]/[O I] upper limits, the most stringent one coming from DG Tau. Higher temperatures are possible only if the ionization fraction is lower than 0.33.

4.6 Discussion

The major contribution of this work is demonstrating that the low velocity forbidden emission in TTS has kinematic properties that can be described as coming from a combination of a broad and a narrow line formation region. Most of our analysis

is based on characterizing the behavior of the BC and NC as though they are two physically distinct emission regions. However, based on the current data we cannot assess whether they both arise from the same phenomenon from different radial ranges in the disk or whether they arise in two different formation scenarios. The most likely formation scenarios for the LVC are mass loss in the outer part of a centrifugally driven disk wind, mass loss in a photoevaporative flow, and bound gas in the disk. We first review the highlights of our findings here and then look at the merits of attributing the LVC to these scenarios.

The BC of the LVC is very common, seen in 25/30 stars spanning the full range of disk accretion rates. In contrast, the NC of the LVC is somewhat less common, detected in only 18/30 stars, but again is found over the full range of disk accretion rates. Of the 5 stars which show only NC emission, 4 are transition disks and the 5th transition disk (GM Aur), has the highest percentage of NC emission in the LVC among the sources with BC emission. If the BC comes primarily from within 0.05 to 0.5 AU, as suggested by the relation between its FHWM and disk inclination, then its absence in transition disks is likely due to a paucity of significant disk gas in this region. This conclusion is in line with what has been proposed for TW Hya from detailed modeling of emission lines covering a large range of radial distances (Gorti et al., 2011).[8] Four of our sources (BP Tau, DF Tau, FZ Tau, and GI Tau) have a redshifted HVC that might also hint to depletion in the inner disk, in this case of the dust component, which is the main source of opacity. However, their infrared indices, as reported in Furlan et al. (2011), place them in the full disk portion. Also their LVC are not reduced with respect to sources with no redshifted HVC (compare BP Tau to AA Tau), thus viewing through a disk hole cannot explain the redshifted HVC emission.

[8]We note that DG Tau, a high accretion rate object which appears to have a full disk and strong HVC emission from a micro jet, is the fifth object with no BC emission. It is possible that our method cannot isolate the LVC BC given the intensity and large velocity range covered by the HVC and/or we are not directly seeing this region because DG Tau is embedded in significant nebulosity as inferred from dust scattering.

While the range of observed FWHM for the BC and the NC can be explained as a result of Keplerian broadening from different radii in the disk (between 0.05 to 0.5 AU for the BC and 0.5 to 5 AU for the NC), the different behaviors of their centroid velocities are the most useful in trying to understand their connection to disk winds.

4.6.1 Role of Winds in the Low Velocity Component

A basic expectation of any wind model is that not only the FWHM but also the centroid v_c of a line formed in the wind will correlate (oppositely) with disk inclination. In a close to face-on configuration Keplerian broadening is minimal and the vertical component of the wind dominates, giving rise to an asymmetric blueshifted profile. On the opposite extreme, for a close to edge-on configuration, Keplerian broadening dominates and because the wind is emerging in the plane of the sky, the resulting profile is symmetric and centered at the stellar velocity (see e.g. Alexander 2008). We see the expected relations with FWHM and inclination for both the BC and NC LVC but the situation is not so clear when their centroid velocities are also considered. We illustrate the relation between all 3 quantities in Figure 4.27, plotting the observed [O I] 6300Å FWHM vs v_c for the LVC BC (upper panel) and NC (lower panel) with datapoints color-coded by disk inclination (see Section 4.5.5).

In the case of the BC, we see larger FWHM associated with larger disk inclination (vertical color gradient) coupled with, for most of the sources, larger blueshifts for narrower lines and lower disk inclination (horizontal color gradient). These are the expected behaviors for a wind. A Kendall τ test gives a probability of only $\sim 1\%$ that the BC FWHM and v_c are uncorrelated. Moreover, the sources with small BC redshifts are mostly in disks seen at high inclination, where, as described in Section 5.4, an extended disk height at large radii may obscure part of the wind from the inner disk while the receding gas (from the observer's perspective) remains unobstructed (Gorti et al. in preparation). As the BC has the general characteristics expected for a simple wind and seems to arise in the innermost disk with maximum velocities of 10 to 27 km/s, we find it likely that the BC is the base of an MHD disk

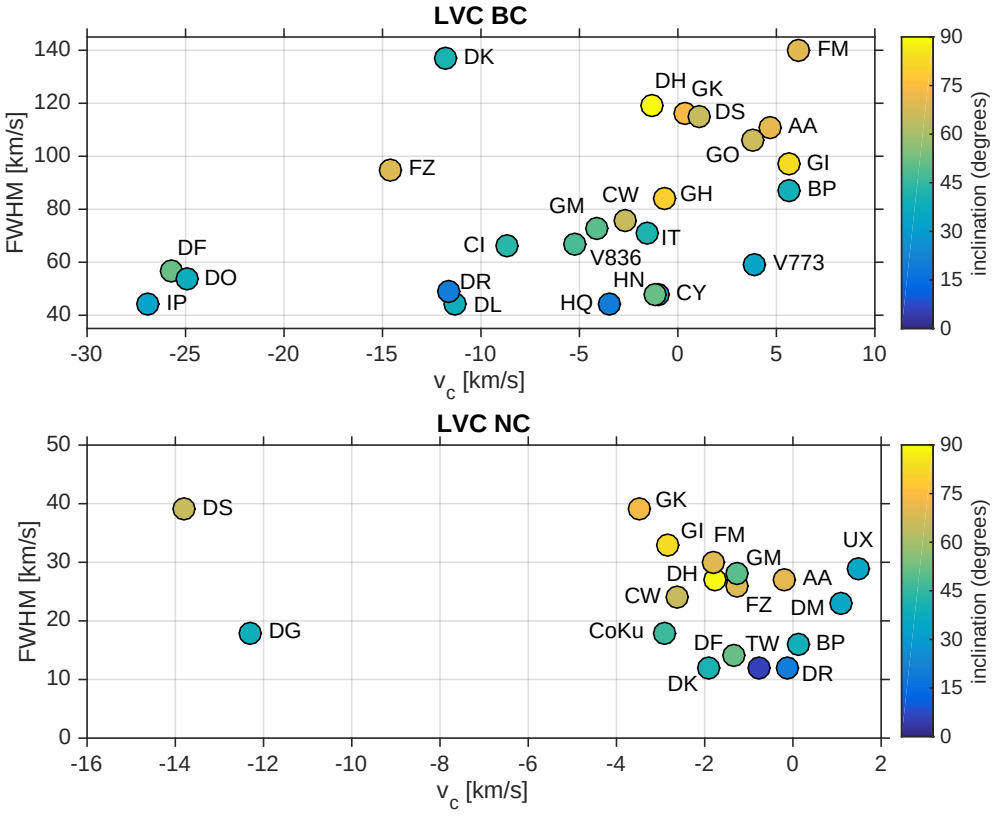

Figure 4.27 Observed FWHM versus v_c for the LVC BC (upper panel) and NC (lower panel). Colors indicate the observed inclination or, if not observed, the one derived in Section 4.5.5. Both BC and NC show a tendency for increasing FWHM with increasing inclination but only the BC has decreasing v_c with increasing inclination as expected in wind models.

wind, since thermal speeds cannot reach the necessary escape speeds this deep in the stellar gravitational potential field and photoevaporation cannot occur.

In the case of the NC, plotted over a smaller range of FWHM and v_c than the BC, again we see FWHM associated with larger disk inclination (vertical color gradient), however there is no relation between the v_c and either the FWHM or the inclination. A Kendall τ test lends to a probability of $\sim 21\%$ that FWHM and v_c are uncorrelated, consistent with no correlation. Two sources (DS Tau and DG Tau) stand out with much higher blueshifts than the rest of the NC, but one is close to face on and the other close to edge on. Thus, although half of the NC have blueshifted v_c, they do not behave in the manner expected for a simple wind.

Although Figures 4.23 and Figure 4.27 show a relation between FWHM and inclination in the BC and NC there is considerable scatter and a few outliers. However, we have not taken into account the fact that there will be an additional source of broadening in both the BC and NC if they are formed in outflowing gas. In the Class II sources, comprising most of our sample, a dusty disk is assumed to occult the receding flow, and the observed FWHM would come both from Keplerian rotation and expanding wind streamlines, producing anomalously high line widths for certain wind geometries (e.g. BC of DK Tau and FZ Tau). In the case of the transition disks, dominated by NC LVC emission, the large dust-free cavities appear to have bound gas, although the gas is not as close in to the star to produce BC emission (Section 5). However, as there would presumably be no opacity source to occult a receding flow, the NC could include a contribution from flowing gas but still be centered on the stellar velocity and the line width would be enhanced by both approaching and receding gas (see the case of TW Hya discussed in Pascucci et al. 2011, and modeling by Ercolano and Owen 2010).

4.6.2 Comparison with Wind Models

The past decade has seen significant advancements in the theory of thermal photoevaporative flows and sophisticated models, accounting for heating by stellar X-rays, EUV, and FUV photons, are now available (e.g. Alexander et al. 2014 for a re-

view). We anticipate that these models will be soon providing more rigorous tests of whether the LVC might arise in thermal winds. Theoretical models for magnetically driven centrifugal disk winds have also grown increasingly sophisticated and recently the relevance of MRI-driven accretion over much of the disk has been challenged (e.g. Turner et al. 2014) putting MHD disk winds back in the spotlight for extracting disk angular momentum to enable accretion onto the star (e.g. Bai et al. 2016). Global simulations of these winds have been recently presented by Gressel et al. (2015) and thermal-chemical models have been investigated by Panoglou et al. (2012), but predictables that can be directly compared with observations of TTS forbidden lines are still lacking.

We began this study to investigate the possibility that the LVC in TTS might arise in photoevaporative flows. It seems unlikely this could be the case for the BC of the LVC, which we attribute to the base of an MHD disk wind. However, despite the lack of a convincing trend between centroid velocity and FWHM/disk inclination for the NC of the LVC we note that the *range* of FWHM and v_c for the NC are consistent with those predicted for photoevaporative flows by Ercolano and Owen 2010, 2016. Using the radiation-hydrodynamic code of Owen et al. (2011), which includes X-ray and EUV irradiation, Ercolano and Owen (2016) find that the [O I] 6300 Å line is produced by collisional excitation and extends to $\sim$35 AU above the disk, where EUV photons and soft X-rays are absorbed and the gas is hot. Predicted FWHM range from 8 to 32 km/s while peak centroids go from 0 to -7 km/s, with the largest blueshifts occurring for intermediate disk inclinations ($i \sim 40 - 60^{o}$), contrary to a simple wind geometry. We do not see this trend either.

Although hydrodynamical models that can predict line profiles of flows driven by FUV photons have not been developed, the expectation is that these flows, being cooler ($\sim$1,000 K) and mostly neutral, will have smaller velocities than those driven by X-rays. The sound speed for such cool flows is only $\sim$2 km/s and the critical radius beyond which the gas would be unbound is $\sim$10 AU around a solar-mass star. In this scenario, the [O I] emission will not be thermal and will arise from the dissociation of OH molecules in mostly bound gas inside of 10 AU (Gorti et al.,

2011), which could explain the very small or absent blueshifts we see in many NC lines. In summary, at the present time the connection of the forbidden line NC of the LVC in TTS to photoevaporative flows remains ambiguous, and we cannot exclude that the NC is also part of a MHD disk wind.

4.7 Conclusions

We have analyzed optical high-resolution ($\sim$7 km/s) spectra from a sample of 33 TTS whose disks span a range of evolutionary stages to clarify the origin of the LVC from oxygen and sulfur forbidden emission lines. We detect the [O I] 6300 Å line in 30/33 TTS, the [O I] 5577 Å line in 16/33, and the [S II] 6730 Å in only 8/33 TTS. After isolating the forbidden LVC emission by removing any HVC contributions, if present, we draw the following conclusions about the residual LVC component:

- All TTS with [O I] detections show LVC emission. Thirteen out of 30 sources with [O I] 6300 Å emission have LVC emission that can be described as the combination of a broad (BC) and a narrow (NC) line emitting region. The remaining sources show LVC emission that is either only BC (12/30) or only NC (5/30).

- The BC of the LVC is very common, seen in 25/30 TTS. The NC of the LVC is less common, seen in 18/25 TTS. Both components are found over the full range of accretion luminosities/disk accretion rates and their luminosities, combined or individually, correlate with the accretion luminosity. LVC that are solely or predominantly NC are usually transition disk sources.

- Comparison with spectra from HEG shows that in most stars the LVC is stable over timescales of decades. However, we do find evidence for variations, with the LVC disappearing entirely in one star and only the NC of the LVC disappearing in another star.

- The BC shows a relation between the FWHM and either observed or derived disk inclination suggesting it is broadened by Keplerian rotation at disk radii

between 0.05 to 0.5 AU. Also, a significant number of BC have blueshifts in excess of 5 km/s. These larger blueshifts are associated with narrower lines and lower disk inclinations, as expected if the BC includes emission from a wind, in addition to Keplerian broadening. The BC with larger blueshifts also tend to be found in sources with higher accretion luminosity and HVC emission from microjets. Since the emission likely arises from 0.05 to 0.5 AU, where the gravity of the star and the disk is strong, it is unlikely to trace a photoevaporative flow but rather the slower moving portion of an MHD disk wind.

- The NC also shows a relation between the FWHM and either observed or derived disk inclination suggesting it is broadened by Keplerian rotation at disk radii between 0.5 to 5 AU. Half of the NC features are blueshifted between -2 to -5 km/s and the other half have centroids consistent with the stellar velocity. Although the expected relation for a simple wind between disk inclination and centroid velocity is not found, we cannot exclude the possibility that the NC of the LVC arises in photoevaporative flows.

- Regardless of the disk evolutionary stage, NC profiles consistent with bound gas can be reproduced by gas in Keplerian motion with a surface brightness decreasing as a power law between 0.1 AU and ∼10 AU, but with 80% of the emission arising within 5 AU. The implication for transition disks is that the NC arises from gas inside the dust cavity.

- If forbidden emission lines are produced by collisional excitation with electrons, the [O I] 5577/6300 ratios suggest high temperatures (>5,000 K) and large electron densities ($> 10^6$ cm^{-3}). Without the additional constraints on density and temperature that would be provided by high resolution spectra of the [S II] 4069 Å line, the possibility remains that the excitation of [O I] is not thermal. Dissociation of OH molecules in a cool (∼1,000 K), bound, mostly neutral disk layer could be the source of the [O I] emission in objects with very small and absent shifts in the NC LVC.

Disk winds, both MHD and photoevaporative, deplete material from several scale heights above the midplane. As dust grains grow they settle toward the midplane. The implication is that disk winds mostly deplete the protoplanetary disk of gas, which consequently increases the dust-to-gas ratio with time (Gorti et al., 2015; Bai et al., 2016). This increase can directly impact the formation of planetesimals, terrestrial planets, and the cores of giant planets. Since disk winds play a significant role in disk dispersal and planet formation, both models and expanded observational data sets need to pursue the origin of the LVC NC, and constrain the rate at which material is lost via disk winds.

5.0 CONCLUSIONS AND FUTURE WORK

5.1 Part I: Summary of Significant Results

Part I of this dissertation had two goals: 1) to determine the conceptual and reasoning difficulties prevalent among general education astronomy students on the topic of planet formation prior to instruction; 2) to validate an instrument designed to assess change in students' understanding of planet formation over time. In Chapter 2, we described a study in which we provided over 1,000 introductory astronomy and planetary science students with open-ended survey questions covering a range of topics relevant to planet formation. We found that, pre-instruction, students lacked the foundational knowledge necessary to explain the physical processes that contribute to a real understanding of planet formation (e.g. the role of gravity, accretion, condensation temperature etc...). Common naive ideas from our dataset included but were not limited to:

- the belief that our Solar System formed at the same time as/as a direct result of the Big Bang
- the inability to distinguish between mass and density which ultimately led to an incorrect understanding of the role of gravity (and the gravity equation)
- the inability to define basic concepts (e.g. a planet, a solar system, an exoplanet versus a dwarf planet)
- the belief that a planet's distance from the central star, and subsequently how much heat it receives, is predominantly responsible for the compositional differences we observe amongst planets

These reasoning difficulties ideas, among others, ultimately served as the distractors for each of the PFCI's content items. The study detailed in Chapter 2 of this dissertation laid the groundwork for the development of the PFCI.

Chapter 3 described the iterative design process we used to develop the final and most robust version of the PFCI. Version 3 of the PFCI was administered to seven introductory astronomy and planetary science courses at the beginning of the Fall 2018 semester before any applicable material was taught (pre-test), and again to six of those classes at the end of the semester (post-test). Utilizing classical test theory (CTT), we calculated the instrument's reliability, assessed its validity, and conducted a preliminary statistical analysis of each of the PFCI's 20 content items. An exploration into student learning gains revealed that the range of individual gain scores was much greater than the range of average gain scores we observed for the six classes, with 76% of students performing better on the PFCI after instruction. Most importantly, we demonstrated through our statistical analysis that Version 3 of the PFCI met the criteria required of a valid and reliable instrument for assessing undergraduate students' learning on the topic of planet formation over time.

5.2 Future Work

As mentioned in Chapter 3 Section 3.5, the next step is to test the PFCI nationally. The scale would allow us to investigate the PFCI's reliability and validity with a much larger sample size, and with a larger sample of course instructors. With the sample of courses surveyed in Chapter 3, the PFCI Version 3 was unable to distinguish between classes there were deemed interactive and those that were not. A larger sample of classes would potentially allow us to postulate whether that finding was unique to our sample size, or reflective of how the topic of planet formation is taught nationwide. The PFCI Version 3 was, however, able to differentiate science majors from non-science majors and experts from novices. It would be interesting to investigate whether any other demographic trait is a predictor of success with a more generalizable sample of students.

Once the national study has been conducted, the next step is to corroborate our CTT findings utilizing item response theory (IRT). IRT is a statistical analysis method that creates a probability model for each individual student in the larger dataset. This probability model analyzes the patterns of answers to each test item, and outputs a predictor of students' ability to answer questions correctly on a certain topic (see e.g. Wallace et al. 2018 for an example of IRT applied to a concept inventory in astronomy). IRT is more sensitive than CTT to individual test items, and is able to determine which of an item's distractors is "more wrong" than the others. We plan to use both CTT and IRT to analyze the data from the PFCI's national administration.

Finally, looking at post-test results from a robust national study would allow us to identify the conceptual and reasoning difficulties that do not improve with instruction. These naive ideas would serve as a framework for interactive pieces of curriculum developed to teach the topic of planet formation more effectively (e.g. lecture tutorials, Think-Pair-Share questions, ranking tasks). Once interactive curriculum is developed that specifically targets the topics covered on the PFCI, instructors will be able to tailer their ASTRO 101 curriculum accordingly. The emergence, and subsequent implementation of such curricular activities has the ability to positively transform the way students learn about our place in the Universe.

5.3 Part II: Summary of Significant Results

In Chapter 4, we analyzed a sample of 33 T-Tauri stars with disks covering a range of evolutionary stages and a spectral resolution of 6.6 km/s. Our work focused predominantly on the LVC of the [O I] forbidden line at 6300 Å to better elucidate its origin. Confirming the finding of Rigliaco et al. (2013), we were able to break the LVC into two distinct components: a broad component (FWHM $>$ 40 km/s) and a narrow component (FWHM $<$ 40 km/s). Both of these components were observed over a substantial range of disk accretion rates, and their line luminosities correlated with the accretion luminosity. Furthermore, we found that the FWHM of both

components correlated with disk inclination, consistent with Keplerian broadening from radii of 0.05 to 0.5 AU for the BC and 0.5 to 5 AU for the NC. A majority of the BCs had blueshifts > 5 km/s, and larger blueshifts were associated with narrower lines and closer to face-on disks; consistent with the predicted behavior of a wind. Since the BC emission arose inward of 0.5 AU where the gravity of the star/disk system is strong, we eliminated the possibility that the BC traced a photoevaporative wind and instead suggested that the BC of the LVC arose in a MHD disk wind. For the NC, however, the origin remained more elusive. Half of the NC features we observed had centroid velocities consistent with the stellar velocity, and the other half had blueshifts between -2 and -5 km/s. We did not observe the relationship between centroid velocity and disk inclination typical of a wind, but we could not exclude the possibility that the NC traced a photoevaporative flow.

5.3.1 Implications for Planet Formation

The dispersal of material during the planet-forming era via disk winds has direct implications for the final architecture of planetary systems. Disk winds have the ability to remove predominantly gas from several scale heights above the midplane (Bai et al., 2016). Due to the relatively laminar nature of the disk in this region, a majority of the dust grains subsequently settle towards the midplane. As a result, disk winds are only able to deplete the disk of a negligible amount of dust, which increases the dust-to-gas mass ratio as the disk evolves (Gorti et al., 2015). This increase in the amount of solids can trigger planetesimal formation, leading to the eventual formation of terrestrial planets and giant planet cores.

Planet formation via the core accretion theory suggests that giant planets form from rocky cores that grow large enough to attract surrounding gas, resulting in either gas-rich (e.g. Jupiter) or gas-poor (e.g. Neptune) giant planets (Gorti et al., 2015). Since winds have the ability to quickly and efficiently deplete the disk of gas, the final mass of giant planets depends strongly on disk dispersal timescales (Rogers et al., 2011). Planet formation models including photoevaporative (but not MHD) winds suggest that once the gas-to-dust ratio decreases by a factor of 2,

there is approximately 2-10 M_J of gas remaining in the disk. This number decreases dramatically to 1-2 M_J if the gas-to-dust ratio is depleted by a factor of 10 (Gorti et al., 2015). As a result, these models suggest that even if giant planet cores could form on relatively short timescales (on the order of 0.5 Myr), there may not be enough gas available in the disk to habitually form Jupiter-sized planets. This has direct implications for the types of planets typically found in exoplanetary systems, and why gas-poor giants may be more prevalent than gas-rich giants (Gorti et al., 2015). This same quick and effective gas dispersal can also halt the inward migration of giant planets, for which the final locations affect the delivery of volatiles (including water) to planets located in the inner solar system. Although disk winds have the ability to influence the final mass and semi-major axes of giant planets, the extent of their influence depends strongly on the efficiency (mass-loss rate) and location of the outflow within the disk (Ercolano and Pascucci 2017; Alexander et al. 2014).

Additionally, winds have the ability to deplete the disk of lighter elements (e.g. Hydrogen and Helium), while heavier elements (like the noble gases) have a smaller disk escape rate (Alexander et al. 2014). The preferential removal of volatile elements that remain in the gas phase (due to much lower condensation temperatures) may contribute to a midplane enriched in refractory elements as the disk evolves (Alexander et al. 2014; Ercolano and Pascucci 2017). This process could help explain the abundance of Argon (Ar), Krypton (Kr), and Xenon (Xe) measured in Jupiter's atmosphere by the Galileo probe (Owen et al., 1999). Ultimately, this finding illustrates that disk winds have the potential to play a significant role in altering the chemistry of the disk, which has direct implications for the planets that could form there.

Due to these aforementioned implications for planet formation, it is essential that we identify the type of winds dominating the dispersal of protoplanetary material at various stages in the disk's lifetime. We need to better understand the role of both MHD and photoevaporative winds before we can make quantitative estimates regarding how efficiently they remove material from the disk/star system.

5.4 Future Work

The work conducted in Chapter 4 of this dissertation has inspired continued exploration into the empirical properties of optical forbidden lines. Banzatti et al. (2019) expanded upon our analysis by focusing on the kinematic links between individual components of the [O I] line at 6300 Å. Of the 65 objects in their sample, 61 had detections of the [O I] 6300 Å, and 23 of their sources had two LVC components (a BC and a NC as defined by the methods described in Chapter 4 Section 4.4.2). A direct comparison of the BC and NC kinematic properties found strong correlations between the centroid velocities, FWHMs, and EWs of both components. This finding was particularly interesting in that we would not expect such correlations to exist if the two components traced material from entirely different winds as previously predicted. Furthermore, Banzatti et al. (2019) reintroduced the HVC (which was omitted from our analysis) and found additional correlations between LVC kinematics and the HVC EW for the LVC components that also had a HVC, as well as with accretion luminosity (L_{acc}). These correlations suggested that the LVC was kinematically linked to both the HVC and accretion, and that the LVC and HVC likely arose in the same outflow. Since the HVC is likely magnetic in origin, and MHD winds are thought to drive accretion through the removal of mass and angular momentum from the disk, the most probable scenario is that *both components* of the LVC (the BC and NC) are *also* part of the same MHD wind (Ferreira et al. 2006; Königl and Salmeron 2011; Banzatti et al. 2019).

Banzatti et al. (2019) found additional evidence in favor of a magnetic origin for the [O I] 6300 Å LVC when investigating the relationship between the LVC kinematic properties and disk inclination. They observed a linear relation between centroid velocity and disk inclination for the HVC with maximum blueshifts at 90°, corresponding to jets launched perpendicular to their disks. No such relation was found for either the BC or the NC of the LVC. The centroid velocities for the BC (and to a lesser extent the NC) were instead most blueshifted at a disk opening angle of $\approx 35°$. This finding suggests that the disk wind traced by the LVC is

likely launched toward the observer at an angle of 35° from the disk. The opening angle of 35° calculated by Banzatti et al. (2019) was consistent with the minimum angle between the disk rotation axis and magnetic field lines required to power an MHD wind (Blandford and Payne, 1982). This result, paired with the correlations described above served as direct evidence in favor of the entire LVC tracing an MHD wind.

In a parallel work, Fang et al. (2018) analyzed a sample of 48 T Tauri stars from Taurus, Lupus I, Lupus III, ρ Oph, and Corona Australis to determine whether the [O I] emission we observe is thermal or non-thermal. If the [O I] lines are thermally excited, their line ratios can provide insight into the temperature and electron density of the emitting gas (see e.g. Chapter 4 Section 4.5.7. A limitation of the work presented in Chapter 4 was that we did not obtain high spectral resolution observations of the [S II] line at 4068.6 Å. Since the [S II] line has nearly the same critical density as the [O I] line at 6300 Å and is likely thermally excited, an in depth analysis of the [S II] and [O I] line profiles, as well as their line ratios can be utilized to distinguish between thermal and non-thermal emission for the [O I] lines (Natta et al., 2014).

Fang et al. (2018) was able to expand on the work conducted in Chapter 4 by obtaining [S II] observations for 22 of the 48 sources in their sample. Following the gaussian fitting and classification technique described in Chapter 4, Fang et al. (2018) was able to decompose the line profiles into a HVC, and two components for the LVC (NC and BC). Ultimately, they found that the line profiles between the [S II] line and the [O I] lines were similar, indicating that they likely traced the same kinematic component, and their line ratios could be used to infer the temperature and density of the emitting gas. Most of the observed LVC ratios were consistent with a dense, thermally excited gas with temperatures between 5,000 and 10,000K (Fang et al., 2018).

An important question to consider for future work is, how efficiently do these MHD winds deplete the disk of material? Fang et al. (2018) used the temperatures approximated by the [S II] and [O I] line ratios, along with [O I] 6300 Å line lumi-

nosity, and constraints on the velocity and emitting radii to calculate preliminary wind mass-loss rates. They found that the mass-loss rate was a factor of 5 higher for the BC than the NC, meaning material was being depleted in the inner disk at a much quicker rate than in the outer disk. At some wind heights, Fang et al. (2018) found mass-loss rates consistent with or even higher than the values for the HVC tracing microjets. Their finding was consistent with *at least* the BC of LVC tracing the base of an MHD disk wind. This work was innovative in that it was the first to calculate mass loss-rates for the BC and NC of the LVC separately. It would be advantageous to explore this result in the future with additional wind diagnostics.

Currently, models including both photoevaporation and MHD disk winds are incomplete (Ercolano and Pascucci, 2017). To better constrain how efficiently different types of disk winds deplete the disk of protoplanetary material, it would be beneficial to build a model that involves EUV, X-Ray, and FUV heating in conjunction with hydrodynamics in order to reproduce the effects from different types of winds. Until such a model is constructed, it will continue to be difficult for observers to match their findings with models accurately portraying how disks evolve and disperse.

A.0 IRB Approval Form

In order to perform research involving human subjects, the researcher must receive approval from the university's institutional review board (IRB). The work conducted in Part I of this dissertation has been classified as *Exempt* by the IRB. This means that the project was not subject to continual review by the IRB, as it posed no threat to the participating human subjects. The students who participated in the research studies presented in Chapters 2 and 3 did so on a volunteer basis, and they remained completely anonymous throughout both the survey administration and data analysis processes.

Research
Office for Research & Discovery

Human Subjects
Protection Program

1618 E. Helen St.
P.O.Box 245137
Tucson, AZ 85724-5137
Tel: (520) 626-6721
http://rgw.arizona.edu/compliance/home

Date:	August 29, 2016
Principal Investigator:	Molly Nora Simon
Protocol Number:	1608796697
Protocol Title:	The Development and Validation of the Planet Formation Concept Inventory (PFCI)
Level of Review:	Exempt
Determination:	Approved

Documents Reviewed Concurrently:

HSPP Forms/Correspondence: *appendix_f.docx*
HSPP Forms/Correspondence: *IRB_signature_page.pdf*
HSPP Forms/Correspondence: *PFCI_IRB-Edited_2.docx*
HSPP Forms/Correspondence: *Verif_Training_Form.doc*
Informed Consent/PHI Forms: *SSR_disclosure.docx*
Informed Consent/PHI Forms: *SSR_disclosure.pdf*
Other Approvals and Authorizations: *Kuiper_Site_Auth.docx*
Other Approvals and Authorizations: *Steward_Site_Auth.pdf*

This submission meets the criteria for exemption under 45 CFR 46.101(b). This project has been reviewed and approved by an IRB Chair or designee.

- The University of Arizona maintains a Federalwide Assurance with the Office for Human Research Protections (FWA #00004218).
- All research procedures should be conducted according to the approved protocol and the policies and guidance of the IRB.
- Exempt projects do not have a continuing review requirement.
- Amendments to exempt projects that change the nature of the project should be submitted to the Human Subjects Protection Program (HSPP) for a new determination. See the Guidance on Exempt Research information on changes that affect the determination of exemption. Please contact the HSPP to consult on whether the proposed changes need further review.
- You should report any unanticipated problems involving risks to the participants or others to the IRB.
- All documents referenced in this submission have been reviewed and approved. Documents are filed with the HSPP Office. If subjects will be consented, the approved consent(s) are attached to the approval notification from the HSPP Office.

B.0 Chapter 2 Tables

Table B.1 General Themes for the Total Sample of Responses to Question 2

Code	**Total Responses** (N=192), n (%)
Prev. Astro	54 (28.1)
Not Codable	4 (2.1)
No Idea	9 (<1.0)

Table B.2 Most Common Themes Identified in Student Responses to the First Part of Question 2, "Describe the Characteristics of the Planets in our Solar System."

Code	**Codable Responses** (N=187), n (%)
Closer rocky, further gas	50 (26.7)
Further more ice	28 (15.0)
Closer gas, further rocky	7 (3.7)
Closer warm, further cold	40 (21.4)
Bigger planets further away	7 (3.7)

Note. — Responses could be coded for more than one theme, or students may have left this part of the question unanswered. Thus, total percentages do not necessarily add up to 100. Rows that are indented are subcategories. Responses deemed not codable or given the code "No Idea" were not included.

Table B.3 Most Common Themes Identified in Student Responses to the Second Part of Question 2, "What are They [Planets] Made of?"

Code	**Codable Responses** (N=187), n (%)
Mentioned Composition (generally)	176 (94.1)
Made of Solids	127 (67.9)
Made of Gas	114 (60.1)
Made of Small Particles	70 (37.4)
Made of Ice/Water	48 (25.7)
Made of Liquids	17 (9.1)
Made of Material from Star Formation	10 (5.3)

Note. — Responses could be coded for more than one theme, or students may have left this part of the question unanswered. Thus, total percentages do not necessarily add up to 100. Responses deemed not codable or given the code "No Idea" were not included.

Table B.4 Responses to the Third Part of Question 2, "Does Their [The Planets] Composition Change with Location (Distance from the Sun)?"

Code	**Total Responses** (N=187), n (%)
Yes	147 (78.6)
No	23 (12.3)
No Response	16 (8.6)
Both Yes and No	1 (<1.0)

Note. — Responses deemed not codable or given the code "No Idea" were not included.

Table B.5 Most Common Themes Identified in Student Responses to the Final Part of Question 2, Where Students Were Asked, "Why or Why Not" the Composition of the Planets in our Solar System Changed with Location

Code	**Codable Responses** (N=187), n (%)
Mentioned Why or Why Not (generally)	87 (46.5)
Sun's Heat	47 (25.1)
Elemental Abundance at Location	21 (11.2)
Sun's Gravity	13 (7.0)
Miscellaneous	13 (7.0)
Snow/Frost Line	3 (1.6)

Note. — Responses could be coded for more than one theme, or students may have left this part of the question unanswered. Thus, total percentages do not necessarily add up to 100. Responses deemed not codable or given the code "No Idea" were not included.

Table B.6 Numerical Results from the Classification of All Responses to Question 2

Classification	**Total Responses** (N=192), n (%)
Correct	4 (2.1)
Incomplete	36 (18.8)
Partial	98 (51.0)
True but Insufficient	11 (5.7)
Wrong	43 (22.4)

Note. — Responses that were deemed "Not Codable" were either classified as Wrong or True but Insufficient depending on the content of the response. Students who responded "No Idea" were classified as Wrong for this portion of the analysis.

Table B.7 General Themes for the Total Sample of Responses to Question 3

Code	**Total Responses** (N=168), n (%)
Prev. Astro	37 (22.0)
Not Codable	1 (<1.0)
No Idea	1 (<1.0)

Table B.8 Most Common Themes Identified in Student Responses to the First Part of Question 3, "Describe how Objects (Planets and Moons) Move in our Solar System. Do the Planets Orbit in the Same Direction or Different Directions?"

Code	**Codable Responses** (N=166), n (%)
SD	95 (57.2)
SD but Different Speeds	17 (10.2)
DD	69 (41.6)
DD but Different Speeds	4 (2.4)
Elliptical Orbits	6 (3.6)

Note. — Responses could be coded for more than one theme, or students may have left this part of the question unanswered. Thus, total percentages do not necessarily add up to 100. Rows that are indented are subcategories. Responses deemed not codable or given the code "No Idea" were not included. SD = same direction, DD = different directions

Table B.9 Responses to the Second Part of Question 3, "Did All Of The Planets Likely Form In The Same Locations They Are In Now?"

Code	**Total Responses** (N=166), n (%)
Yes	15 (9.0)
No	140 (84.3)
No Response	7 (4.2)
Both Yes and No	4 (2.4)

Note. — Responses deemed not codable or given the code "No Idea" were not included.

Table B.10 Most Common Themes Identified in Student Responses to the Final Part of Question 3, Where Students Were Asked to "Explain" Whether Or Not The [Solar System's] Planets Formed in the Same Locations They are in Now

Code	**Codable Responses** (N=166), n (%)
Provided an Explanation (generally)	121 (72.9)
Gravity/Pulled Into Orbit	46 (27.7)
Things in Space are Moving/Expanding	36 (21.7)
Alluded to Migration	14 (8.4)
Collisions	12 (7.2)
Collection of Surrounding Debris	10 (6.0)
Miscellaneous	10 (6.0)
Planets Stay Where They are Formed	3 (1.8)

Note. — Responses could be coded for more than one theme, or students may have left this part of the question unanswered. Thus, total percentages do not necessarily add up to 100. Responses deemed not codable or given the code "No Idea" were not included.

Table B.11 Numerical Results from the Classification of All Responses to Question 3

Classification	**Total Responses** (N=168), n (%)
Correct	3 (1.8)
Incomplete	43 (25.6)
Partial	108 (61.3)
True but Insufficient	0 (0)
Wrong	19 (11.3)

Note. — Responses that were deemed "Not Codable" were either classified as Wrong or True but Insufficient depending on the content of the response. Students who responded "No Idea" were classified as Wrong for this portion of the analysis.

Table B.12 General Themes for the Total Sample of Responses to Question 4

Code	**Total Responses** (N=167), n (%)
Prev. Astro	21 (12.6)
Not Codable	7 (4.2)
No Idea	5 (3.0)

Table B.13 Most Common Themes Identified in Student Responses to Question 4, "What is the Definition of a Planet? What Makes a Planet Different Than Other Objects in the Solar System (Like the Sun, Asteroids, Comets, etc.)?

Code	**Codable Responses** (N=155), n (%)
Orbit a Star/Sun	89 (57.4)
Small Bodies Orbit Other Objects	11 (7.1)
Clump of Mass/Matter	37 (23.9)
Made of Rock or Gas	35 (22.6)
Must be a Certain Size	34 (21.9)
Bigger than Asteroid/Comet/Moon	16 (10.3)
Smaller than a Star	8 (5.2)
Distinct Orbital Path	30 (19.4)
Not Free Floating	13 (8.4)
Own Gravity	26 (16.8)
Spherical	22 (14.2)
Has an Atmosphere	19 (12.3)
Has Moons	19 (12.3)
Can Support Life	18 (11.6)
Must Have Life	4 (2.6)
Has a Unique Composition	17 (11.0)
Has a Unique Formation Process	7 (4.5)
Clears its Orbit	6 (3.9)
Has Layers (Core, Mantle, Crust)	6 (3.9)
Is a Star	5 (3.2)

Note. — Responses (especially lengthy responses) could be coded for more than one theme, so percentages do not necessarily add up to 100. Rows that are indented are subcategories. Responses deemed not codable or given the code "No Idea" were not included in the codable responses.

Table B.14 Numerical Results from the Classification of All Responses to Question 4

Classification	**Total Responses** (N=167), n (%)
Correct	3 (1.8)
Incomplete	37 (22.2)
Partial	55 (32.9)
True but Insufficient	5 (3.0)
Wrong	67 (40.1)

Note. — Responses that were deemed "Not Codable" were either classified as Wrong or True but Insufficient depending on the content of the response. Students who responded "No Idea" were classified as Wrong for this portion of the analysis.

Table B.15 General Themes for the Total Sample of Responses to Question 5a

Code	**Total Responses** (N=175), n (%)
Prev. Astro	32 (18.3)
Not Codable	3 (1.7)
No Idea	0 (0)
Answered 5b	105 (60.0)

Table B.16 Most Common Themes Identified in Student Responses to the First Part of Question 5a, "What is a Solar System?"

Code	**Codable Responses** (N=172), n (%)
Planets (bodies) Orbiting a Star	94 (54.7)
Objects Close to Each Other in Space	37 (21.5)
An Area Including The Milky Way	7 (4.1)

Note. — Responses could be coded for more than one theme, or students may have left this part of the question unanswered. Thus, total percentages do not necessarily add up to 100. Responses deemed not codable or given the code "No Idea" were not included.

Table B.17 Most Common Themes Identified in Student Responses to the Final Part of Question 5a, "What Kinds of Objects Would You Expect to Find in a Solar System?"

Code	**Codable Responses** (N=172), n (%)
Planets	121 (70.3)
Multiple (many) Stars	58 (33.7)
Moons	55 (32.0)
Asteroids	52 (30.2)
Central Star/Sun	39 (22.7)
Comets	28 (16.3)
Galaxies/Nebulae	13 (7.6)
Meteors	10 (5.8)
Dust/Gas/Debris	10 (5.8)
Dwarf Planets	6 (3.5)
Aliens/Life	3 (1.7)
Constellations	3 (1.7)
Black Holes	2 (1.2)

Note. — Responses (especially lengthy responses) could be coded for more than one theme, so percentages do not necessarily add up to 100. Responses deemed not codable or given the code "No Idea" were not included.

Table B.18 Numerical Results from the Classification of All Responses to Question 5a

Classification	**Total Responses** (N=175), n (%)
Correct	24 (13.7)
Incomplete	50 (28.6)
Partial	72 (41.1)
True but Insufficient	0 (0)
Wrong	29 (16.6)

Note. — Responses that were deemed "Not Codable" were either classified as Wrong or True but Insufficient depending on the content of the response.

Table B.19 General Themes for the Total Sample of Responses to Question 5b

Code	**Total Responses** (N=105), n (%)
Prev. Astro	26 (24.8)
Not Codable	0 (0)
No Idea	0 (0)

Table B.20 Most Common Themes Identified in Student Responses to the First Part of Question 5b, "What is an Exoplanet?"

Code	**Codable Responses** (N=105), n (%)
Planet Outside of our Solar System	35 (33.3)
Planet at the Edge of the Solar System	16 (15.2)
Dwarf Planet	13 (12.4)
Pluto	10 (9.5)
Dead Planet/Not Habitable	7 (6.7)
Planet with an Irregular Orbit	7 (6.7)
Planet with Life	6 (5.7)
Rocky/Earth-like Planet	4 (3.8)
A Large Planet/Gas Planet	2 (1.9)
Rogue Planet	2 (1.9)
A Moon	2 (1.9)

Note. — Responses (especially lengthy responses) could be coded for more than one theme, so percentages do not necessarily add up to 100. Responses deemed not codable or given the code "No Idea" were not included.

Table B.21 Responses to the Second Part of Question 5b, "Would You Expect to Find Exoplanets in our Solar System?"

Code	**Total Responses** (N=105), n (%)
Yes	34 (32.4)
No	38 (26.2)
No Response	30 (28.6)
Both Yes and No	2 (2.8)

Table B.22 Numerical Results from the Classification of All Responses to Question 5b

Classification	**Total Responses** (N=105), n (%)
Correct	24 (22.9)
Incomplete	1 (<1.0)
Partial	9 (8.6)
True but Insufficient	0 (0)
Wrong	71 (67.6)

Table B.23 General Themes for the Total Sample of Responses to Question 6

Code	**Total Responses** (N=178), n (%)
Prev. Astro	36 (20.2)
Not Codable	4 (2.8)
No Idea	2 (1.1)

Table B.24 Most Common Themes Identified in Student Responses to the First Part of Question 6, "What Does the Layout of our Solar System tell us About how it Formed?"

Code	**Total Responses** (N=172), n (%)
Gravity Helped the Solar System Form	45 (26.2)
Dense Objects Closer, Have More Gravity	33 (19.2)
Sun's Gravity	14 (8.1)
Sun's Temperature Affects Layout	30 (17.4)
Giant Planets Unstable Close to Sun	14 (8.1)
Rocky Planets Formed First	10 (5.8)
Formed From Big Bang	9 (5.2)
Rocky Debris Exists Close In, Gas Further Out	9 (5.2)
Non-science Response	9 (5.2)
Snow Line/Frost Line	4 (2.3)
Gaseous Planets Formed First	2 (1.2)

Note. — Responses (especially lengthy responses) could be coded for more than one theme, so percentages do not necessarily add up to 100. Rows that are indented are subcategories. Responses deemed not codable or given the code "No Idea?" were not included.

Table B.25 Responses to the Second Part of Question 6, "Do you Think all Solar Systems Have to Follow the Same Layout?"

Code	**Total Responses** (N=172), n (%)
Yes	58 (33.7)
No	94 (54.7)
No Response	16 (9.3)
Both Yes and No	4 (2.3)

Note. — Responses deemed not codable or given the code "No Idea" were not included.

Table B.26 Numerical Results from the Classification of All Responses to Question 6

Classification	**Total Responses** (N=178), n (%)
Correct	2 (1.1)
Incomplete	1 (<1.0)
Partial	24 (13.5)
True but Insufficient	0 (0)
Wrong	151 (84.8)

Note. — Responses that were deemed "Not Codable" were either classified as Wrong or True but Insufficient depending on the content of the response. Students who responded "No Idea" were classified as Wrong for this portion of the analysis.

C.0 Final Version of the PFCI

The final version of the PFCI is presented here. This version is the same as Version 3 with the exception of item #9, which was revised so as to include distractors more aligned with known student reasoning difficulties (see Chapter 3, Section 3.4.1).

Final Version of the PFCI

Directions:

Read the entire question and ALL of the answer choices carefully before selecting an answer. Fill in the bubbles completely! Each question has *one* correct answer unless otherwise specified.

Instead of writing your name on this form, fill in the numerical bubbles with the ***last four digits of your phone number*** (we will not be able to look you up with this information, and your identity will remain anonymous).

Enter last four digits below:

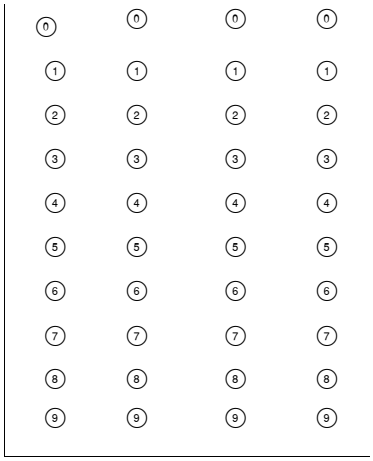

1. How did the planets in our Solar System form?

- O They formed from a collision between our Sun and a nearby star
- O They formed from the energy and matter released at the same time as the Big Bang
- O They formed from the collapse of a cloud composed of gas and dust
- O They formed from the remains of a massive stellar (star) explosion
- O They formed from material that was pulled in from a nearby solar system by our Sun

2. Which of the following statements is *FALSE?*

- O A planet must orbit around a star (sun)
- O A planet must have an atmosphere
- O A planet must clear its orbit of surrounding debris
- O A planet must be roughly spherical in shape

3. In our Solar System, what best describes the physical characteristics of Mercury, Venus, Earth, and Mars?

- O These planets are dense, small, and are made primarily of hydrogen and helium gas
- O These planets are dense, small, and are made primarily of rocks and metals
- O These planets are dense, large, and are made primarily of rocks and metals
- O These planets have low densities, are large, and are made primarily of hydrogen and helium gas
- O These planets have low densities, are large, and are made primarily of icy material

4. Which describes how the locations (relative to the Sun) of the planets in our Solar System may have changed over time?

O They changed because space is constantly moving and expanding

O They changed because the planets are constantly colliding with each other

O The larger planets may have changed locations early in the Solar System's history because of the gravitational interactions between them

O The locations of the planets have not changed over time; they formed in the same locations they are in now

5. Which of these objects would you expect to find in our Solar System? (*CIRCLE ALL THAT APPLY*)

O Comets

O Asteroids

O Dwarf Planets

O Exoplanets

O The Milky Way Galaxy

6. Which of these scenarios best describes the general planet formation (accretion) process?

O Dust grains continuously collide, accumulate more mass, and develop into planets

O Material is ejected into the Solar System from an explosion, and this material forms the planets

O Once the planets grow large enough, the Sun's gravity causes the growing planets to accumulate all of the matter around them

O A pressure build up in the solar nebula due to the birth of our Sun leads to the formation of the planets

O At the time of the Big Bang, material collides, grows in size, and forms planets

7. For our Solar System, which statement is *TRUE* regarding which planet[s] completed their formation process first?

O Mercury formed first because it is the closest to the Sun, and Neptune formed last because it is the farthest away

O The rocky planets all formed together first, and then the gas giant planets started their formation millions of years later

O The gas giant planets all formed together first, and then the rocky planets started their formation millions of years later

O Neptune formed first because it is the farthest from the Sun, Mercury formed last because it is the closest to the Sun

O All of the planets in our Solar System formed at approximately the same time

8. What is the definition of an exoplanet?

O A planet at the edge of the Solar System

O A planet outside of our Solar System

O A planet no longer bound by gravity to its star

O A planet that is habitable

O A planet that does not clear its orbit of surrounding debris

9. Jupiter, Saturn, Uranus, and Neptune (the outer planets) were able to grow much larger than Mercury, Venus, Earth, and Mars because:

- O In the locations where the giant planets formed metals, rocky minerals, and icy minerals were all able to solidify. As a result, all of these materials could be used to form the outer planets
- O The gravitational force far from the Sun was much weaker, allowing the outer planets to grow to much larger sizes
- O In the outer Solar System there was much more rocky material than icy material. This made it possible for the outer planets to attract their large gaseous envelopes
- O During the Solar System's formation, the Sun ejected additional solids into the outer Solar System. These solids were eventually used to form the outer planets

10. During the planet formation process, what is the primary role of the force of gravity?

- O Gravity helps bodies with enough mass attract surrounding dust and gas so they can continue to grow into planets
- O Gravity is the force that causes denser, more massive planets to form closer to the Sun
- O Gravity determines which material (e.g. metals and gas) will be prevalent at certain distances from the Sun
- O Gravity keeps the growing planets from collapsing on themselves if they get too massive during the formation process

11. In our Solar System, what best describes the physical characteristics of Jupiter, Saturn, Uranus, and Neptune?

- O These planets are dense, small, and are made primarily of hydrogen and helium gas
- O These planets are dense, small, and are made primarily of rocks and metals
- O These planets are dense, large, and are made primarily of rocks and metals
- O These planets have low densities, are large, and are made primarily of gases and icy material
- O These planets have low densities, are large, and are made of strictly hydrogen and helium gas

12. Which of these most accurately describes a planet?

- O A planet orbits around another larger, rocky body
- O A planet orbits around a star
- O A planet is an object that is massive enough to fuse hydrogen into helium
- O A planet must be able to sustain life

13. Why do the planets in our Solar System orbit the Sun in the same plane?

- O The planets were ejected into this configuration at the time of the Solar System's formation
- O The planets formed from a flattened disk-like structure, which caused the planets to orbit in this configuration
- O The planets orbit around the Sun on retrograde orbits, and these orbits require the planets to be in the same plane
- O The planets were pulled into this configuration by the gravity of nearby asteroids and comets

14. In our Solar System, why did rocky planets form close to the Sun while the gaseous planets formed further away?

O Close to the Sun, gravity was only strong enough to pull the rockier planets close in

O Close to the Sun, planets composed of mainly gas were incapable of remaining stable

O Close to the Sun, only heavy elements (like rocks and metals) could solidify at such high temperatures and eventually form a planet

O Close to the Sun, all of the gaseous material was used to create the young Sun, so there was no material left to form the gas planets close in

15. The planets in our Solar System orbit the Sun in ____ direction[s], at ____ speed[s], and on ____ orbits.

O The same, different, elliptical

O The same, the same, elliptical

O Different, the same, circular

O Different, different, elliptical

O The same, different, circular

16. Which of these best describes how the composition of the planets in our Solar System changes with *increasing* distance from the Sun?

O Rocky Planets → Gas Planets → Icy Planets

O Gas Planets → Rocky Planets → Icy Planets

O Icy Planets → Rocky Planets → Gas Planets

O Rocky Planets → Icy Planets → Gas Planets

O Gas Planets → Icy Planets → Rocky Planets

17. When did our Solar System form relative to the Big Bang?

- O Our Solar System formed before the Big Bang
- O Our Solar System formed at the same time as the Big Bang
- O Our Solar System formed immediately after the Big Bang
- O Our Solar System formed a long time after the Big Bang

18. The discovery of exoplanetary systems has supported the idea that:

- O Exoplanetary systems look exactly like our Solar System, with a combination of rocky and gaseous planets
- O Exoplanetary systems look entirely different than our Solar System, with planets made of materials not found in our Solar System
- O Exoplanetary systems must have Jupiter-sized planets orbiting close to their host stars
- O Exoplanetary systems are different from our Solar System in that every planet discovered in these systems has the potential for life
- O Exoplanetary systems are likely similar to our Solar System in terms of the general formation process, but the locations and compositions of the planets may be different

19. What is the definition of a dwarf planet?

- O A planet at the edge of a solar system
- O A planet outside of our Solar System
- O A planet with an irregular orbit around a star
- O A planet that is habitable
- O A planet that does not clear its orbit of surrounding debris

20. Below is a depiction of a hypothetical solar system. Based on the image below, which of the following answers correctly describes why the planets are in the locations shown?

NOTE: The sizes of the planets are not to scale relative to the distances between them.

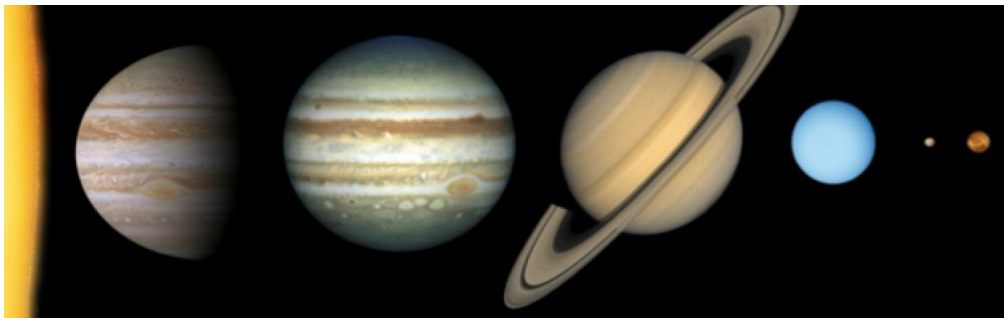

O All of the planets in this solar system formed exactly where they are shown

O The largest planets in this solar system moved inward during the formation process due to planetary migration

O The largest planets in this solar system moved inward during the formation process because the Universe is constantly moving and expanding

O The strong gravitational pull of the star caused the large and small planets to switch positions

21. Which of the following best characterizes your academic major(s)?

- O Science major (e.g. physics, chemistry, biology)
- O Non-science major (e.g. history, business, dance, etc…)
- O Double major
- O Undecided
- O Other

22. What gender do you identify with?

- O Male
- O Female
- O Non-binary
- O Non-conforming
- O Other

23. Have you ever taken a course <u>besides this course</u> that covered the topic of planet formation?

- O Yes, in high school
- O Yes, at a 4-year college
- O Yes, at a community college
- O Yes, other
- O No

D.0 Sky Subtraction and Slit Position Angle

As mentioned in Section 4.2.2 the MAKEE pipeline performs an automatic sky subtraction. We show in Figure D.1 the spectrum of FM Tau before (black) and after sky subtraction (red) to highlight that even the strong terrestrial [O I] emission line at 6300 Å is well removed by the pipeline.

The Keck spectra presented here were acquired in the standard mode which places the slit along the parallactic angle in order to minimize potential slit losses. This approach was taken because our main interest was to study the LVC, which was known to be compact, rather than the jet emission, which, most likely, extends beyond the slit width. For completeness, we provide in Table D.1 slit position angles and disk position angles (which should be close to 90° of the jet position angles). GO Tau, UX Tau A, and DS Tau have the slit most closely aligned of a possible jet, within $\sim 10°$, yet none of them show a jet signature in the [O I] spectra.

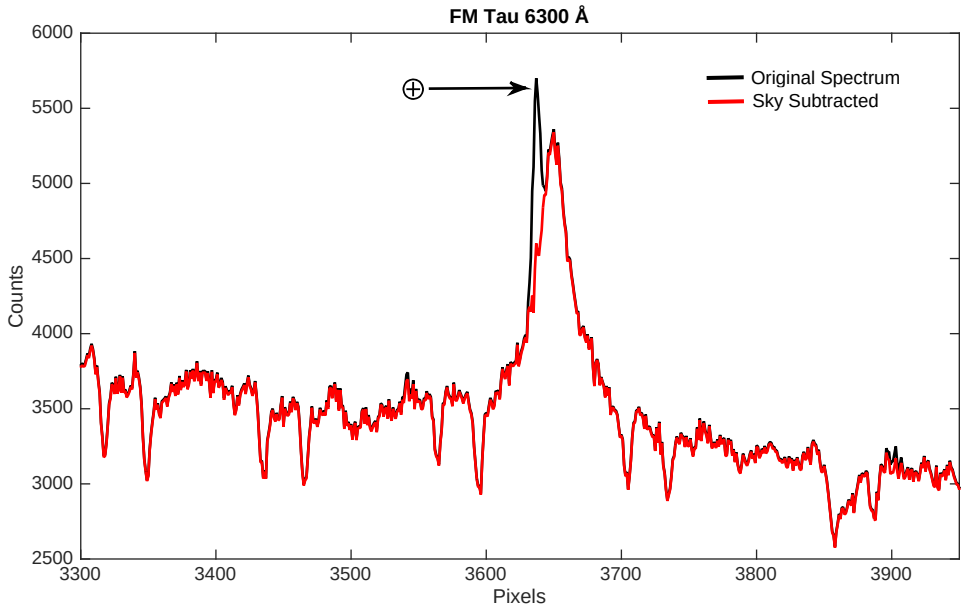

Figure D.1 FM Tau spectrum around the [O I] 6300 Å before (black) and after (red) sky subtraction. Note that the strong [O I] terrestrial line is well removed by the MAKEE pipeline.

Table D.1 Slit and disk position angles.

Source	Slit PA [°]	Disk PA [°]	REF (Disk PA)
AA Tau	105	97	C13
BP Tau	246	107	G11
CI Tau	84.8	285	G11
CoKu Tau 4	223	—	—
CW Tau	260	332	P14
CY Tau	251	63	G11
DF Tau	102	—	—
DG Tau	102	43	G11
DK Tau	190	15	AJ14
DL Tau	84.1	141	G11
DM Tau	95.6	155	AN11
DN Tau	236	86	I09
DO Tau	270	—	—
DR Tau	78.8	108	I09
DS Tau	252	165	AJ14
FM Tau	260	83	P14
FZ Tau	256	—	—
GH Tau	91.7	—	—
GI Tau	260	—	—
GK Tau	263	93	AJ14
GM Aur	92.1	144	G11
GO Tau	99.2	0	AW07
HN Tau	79.5	65	AJ14
HQ Tau	273	—	—
IP Tau	112	—	—
IT Tau	254	106	AJ14
TW Hya	337	332	PD08
UX Tau A	278	176	AN11
VY Tau	274	—	—
V710 Tau	96.4	82	AJ14
V773 Tau	270	—	—
V836 Tau	92.5	-122	P14

References. — Akeson and Jensen 2014 (AJ14); Andrews et al. 2011 (AN11); Andrews and Williams 2007 (AW07); Cox et al. 2013 (C13); Guilloteau et al. 2011 (G11); Isella et al. 2009 (I09); Piétu et al. 2014 (P14); Pontoppidan et al. 2008 (PD08)

E.0 Collisional Excitation Model

The collisional excitation model described here is used to gain physical insight in the temperature and electron density of the region traced by oxygen forbidden lines. We assume a homogeneous and isothermal slab of gas, where the excitation is due solely to electron collisions. We considered a ground state and four additional excited states (5-level atom) both for the neutral and ionized oxygen. We computed the relative populations of the levels as a function of gas temperature and density by including the processes of collisional excitation, collisional de-excitation, and spontaneous radiative decay. Einstein coefficients for radiative decay were taken from the NIST database[1] and electron collision strengths from Draine (2011). We have not included collisions with neutral hydrogen because the de-excitation cross section of the level $^1S_0$ is not known (see e.g. discussion in Ercolano and Owen 2010). However, neutral collisions should be negligible when the electron abundance is larger than $\sim 10^{-3}$, as suggested by the same disk models, because the electron rate coefficients ($\sim 10^{-9}\,\mathrm{cm}^3/\mathrm{s}$) are much larger than those for H ($\sim 10^{-12}\,\mathrm{cm}^3/\mathrm{s}$). Because of the very similar ionization potential of H and O we have taken the ratio of H^+/H to be equal to O^+/O, equal to 0.5 for an ionization fraction of 0.33, close to the value expected in the [O I] emitting region in some photoevaporative wind models (see Figure 2 in Owen et al. 2011).

[1] $http://physics.nist.gov/PhysRefData/ASD/lines\_form.html$

Bibliography

Akeson, R. L. and E. L. N. Jensen (2014). Circumstellar Disks around Binary Stars in Taurus. *ApJ*, **784**, 62. doi:10.1088/0004-637X/784/1/62.

Albanese, A., M. C. Danhoni Neves, and M. Vicentini (1997). Models in Science and in Education: A Critical Review of Research on Students' Ideas About the Earth and its Place in the Universe. *Science & Education*, **6**, pp. 573–590. doi:10.1023/A:1008697908361.

Alcalá, J. M., A. Natta, C. F. Manara, L. Spezzi, B. Stelzer, A. Frasca, K. Biazzo, E. Covino, S. Randich, E. Rigliaco, L. Testi, F. Comerón, G. Cupani, and V. D'Elia (2014). X-shooter spectroscopy of young stellar objects. IV. Accretion in low-mass stars and substellar objects in Lupus. *A&A*, **561**, A2. doi:10.1051/0004-6361/201322254.

Alexander, R., I. Pascucci, S. Andrews, P. Armitage, and L. Cieza (2014). The Dispersal of Protoplanetary Disks. *Protostars and Planets VI*, pp. 475–496. doi:10.2458/azu_uapress_9780816531240-ch021.

Alexander, R. D. (2008). [NeII] emission-line profiles from photoevaporative disc winds. *MNRAS*, **391**, pp. L64–L68. doi:10.1111/j.1745-3933.2008.00556.x.

Allen, M. J. and W. M. Yen (1979). *Introduction to Measurement Theory*. Waveland Press.

American Association for the Advancement of Science (1993). *Project 2061: Benchmarks for Science Literacy*. Oxford University Press. ISBN 0195089863.

Andrews, S. M. and J. P. Williams (2007). High-Resolution Submillimeter Constraints on Circumstellar Disk Structure. *ApJ*, **659**, pp. 705–728. doi:10.1086/511741.

Andrews, S. M., D. J. Wilner, C. Espaillat, A. M. Hughes, C. P. Dullemond, M. K. McClure, C. Qi, and J. M. Brown (2011). Resolved Images of Large Cavities in Protoplanetary Transition Disks. *ApJ*, **732**, 42. doi:10.1088/0004-637X/732/1/42.

Appenzeller, I. and C. Bertout (2013). Inclination effects in T Tauri star spectra. *A&A*, **558**, A83. doi:10.1051/0004-6361/201322160.

Appenzeller, I., R. Oestreicher, and I. Jankovics (1984). Forbidden-line profiles of T Tauri stars. *A&A*, **141**, pp. 108–115.

Armitage, P. J. (2010). *Astrophysics of Planet Formation*. Cambridge University Press.

Azuah, R. T., L. R. Kneller, Y. Qiu, P. L. Tregenna-Piggot, C. M. Brown, J. R. Copley, and R. M. Dimeo (2009). DAVE: A Comprehensive Software Suite for the Reduction, Visualization, and Analysis of Low Energy Neutron Spectroscopic Data. *J Res Natl Stand Technol*, **114**, pp. 341–358.

Bai, X.-N. and J. M. Stone (2013). Wind-driven Accretion in Protoplanetary Disks. I. Suppression of the Magnetorotational Instability and Launching of the Magnetocentrifugal Wind. *ApJ*, **769**, 76. doi:10.1088/0004-637X/769/1/76.

Bai, X.-N., J. Ye, J. Goodman, and F. Yuan (2016). Magneto-thermal Disk Winds from Protoplanetary Disks. *ApJ*, **818**, 152. doi:10.3847/0004-637X/818/2/152.

Bailey, J. M. (2009). Concept Inventories for ASTRO 101. *The Physics Teacher*, **47**, pp. 439–441. doi:10.1119/1.3225503.

Bailey, J. M., K. Coble, G. Cochran, D. Larrieu, R. Sanchez, and L. R. Cominsky (2012). A Multi-Institutional Investigation of Students' Preinstructional Ideas About Cosmology. *Astronomy Education Review*, **11**(1), p. 010302. doi:10.3847/AER2012029.

Bailey, J. M., B. Johnson, E. E. Prather, and T. F. Slater (2011). Development and Validation of the Star Properties Concept Inventory. *International Journal of Science Education*, **34**, pp. 2257–2286. doi:10.1080/09500693.2011.589869.

Bailey, J. M., E. E. Prather, B. Johnson, and T. F. Slater (2009). College Students' Preinstructional Ideas About Stars and Star Formation. *Astronomy Education Review*, **8**(1), p. 010110. doi:10.3847/AER2009038.

Bailey, J. M. and T. F. Slater (2003). A Review of Astronomy Education Research. *Astronomy Education Review*, **2**(2), pp. 20–45. doi:10.3847/AER2003015.

Banzatti, A., I. Pascucci, S. Edwards, M. Fang, U. Gorti, and M. Flock (2019). Kinematic Links and the Coevolution of MHD Winds, Jets, and Inner Disks from a High-resolution Optical [O I] Survey. *ApJ*, **870**, 76. doi:10.3847/1538-4357/aaf1aa.

Banzatti, A. and K. M. Pontoppidan (2015). An Empirical Sequence of Disk Gap Opening Revealed by Rovibrational CO. *ApJ*, **809**, 167. doi:10.1088/0004-637X/809/2/167.

Bardar, E. M., E. E. Prather, K. Brecher, and T. F. Slater (2006). Development and Validation of the Light and Spectroscopy Concept Inventory. *Astronomy Education Review*, **5**(2), pp. 103–113.

Bast, J. E., J. M. Brown, G. J. Herczeg, E. F. van Dishoeck, and K. M. Pontoppidan (2011). Single peaked CO emission line profiles from the inner regions of protoplanetary disks. *A&A*, **527**, A119. doi:10.1051/0004-6361/201015225.

Beristain, G., S. Edwards, and J. Kwan (2001). Helium Emission from Classical T Tauri Stars: Dual Origin in Magnetospheric Infall and Hot Wind. *ApJ*, **551**, pp. 1037–1064. doi:10.1086/320233.

Blandford, R. D. and D. G. Payne (1982). Hydromagnetic flows from accretion discs and the production of radio jets. *MNRAS*, **199**, pp. 883–903. doi:10.1093/mnras/199.4.883.

Bransford, J. D., A. L. Brown, and R. R. Cocking (1999). *How People Learn: Brain, Mind, Experience, and School*. National Academies Press.

Brown, J. M., K. M. Pontoppidan, E. F. van Dishoeck, G. J. Herczeg, G. A. Blake, and A. Smette (2013). VLT-CRIRES Survey of Rovibrational CO Emission from Protoplanetary Disks. *ApJ*, **770**, 94. doi:10.1088/0004-637X/770/2/94.

Cabrit, S. (2007). The accretion-ejection connexion in T Tauri stars: jet models vs. observations. In Bouvier, J. and I. Appenzeller (eds.) *Star-Disk Interaction in Young Stars*, volume 243 of *IAU Symposium*, pp. 203–214. doi:10.1017/S1743921307009568.

Cabrit, S., S. Edwards, S. E. Strom, and K. M. Strom (1990). Forbidden-line emission and infrared excesses in T Tauri stars - Evidence for accretion-driven mass loss? *ApJ*, **354**, pp. 687–700. doi:10.1086/168725.

Calvet, N. and E. Gullbring (1998). The Structure and Emission of the Accretion Shock in T Tauri Stars. *ApJ*, **509**, pp. 802–818. doi:10.1086/306527.

Cox, A. W., C. A. Grady, H. B. Hammel, J. Hornbeck, R. W. Russell, M. L. Sitko, and B. E. Woodgate (2013). Imaging the Disk and Jet of the Classical T Tauri Star AA Tau. *ApJ*, **762**, 40. doi:10.1088/0004-637X/762/1/40.

Crocker, L. and J. Algina (1986). *Introduction to Classical and Modern Test Theory*. New York: Holt.

DeLaughter, J. E., S. Stein, C. A. Stein, and K. R. Bain (1998b). *Rocks for Jocks: Preconceptions About the Earth*.

Ding, L. and R. Beichner (2009). Approaches to data analysis of multiple-choice questions. *Physical Review Physics Education Research*, **5**(2), 020103. doi:10.1103/PhysRevSTPER.5.020103.

Draine, B. T. (2011). *Physics of the Interstellar and Intergalactic Medium*.

Edwards, S., S. Cabrit, S. E. Strom, I. Heyer, K. M. Strom, and E. Anderson (1987). Forbidden line and H-alpha profiles in T Tauri star spectra - A probe of anisotropic mass outflows and circumstellar disks. *ApJ*, **321**, pp. 473–495. doi:10.1086/165646.

Edwards, S., W. Fischer, J. Kwan, L. Hillenbrand, and A. K. Dupree (2003). He I λ10830 as a Probe of Winds in Accreting Young Stars. *ApJ*, **599**, pp. L41–L44. doi:10.1086/381077.

Ercolano, B. and J. E. Owen (2010). Theoretical spectra of photoevaporating protoplanetary discs: an atlas of atomic and low-ionization emission lines. *MNRAS*, **406**, pp. 1553–1569. doi:10.1111/j.1365-2966.2010.16798.x.

Ercolano, B. and J. E. Owen (2016). Blueshifted [O I] lines from protoplanetary discs: the smoking gun of X-ray photoevaporation. *MNRAS*, **460**, pp. 3472–3478. doi:10.1093/mnras/stw1179.

Ercolano, B. and I. Pascucci (2017). The dispersal of planet-forming discs: theory confronts observations. *Royal Society Open Science*, **4**, 170114. doi:10.1098/rsos.170114.

Espaillat, C., J. Muzerolle, J. Najita, S. Andrews, Z. Zhu, N. Calvet, S. Kraus, J. Hashimoto, A. Kraus, and P. D'Alessio (2014). An Observational Perspective of Transitional Disks. *Protostars and Planets VI*, pp. 497–520. doi:10.2458/azu_uapress_9780816531240-ch022.

Fang, M., I. Pascucci, S. Edwards, U. Gorti, A. Banzatti, M. Flock, P. Hartigan, G. J. Herczeg, and A. K. Dupree (2018). A New Look at T Tauri Star Forbidden Lines: MHD-driven Winds from the Inner Disk. *ApJ*, **868**, 28. doi:10.3847/1538-4357/aae780.

Fedele, D., I. Pascucci, S. Brittain, I. Kamp, P. Woitke, J. P. Williams, W. R. F. Dent, and W.-F. Thi (2011). Water Depletion in the Disk Atmosphere of Herbig AeBe Stars. *ApJ*, **732**, 106. doi:10.1088/0004-637X/732/2/106.

Ferreira, J., C. Dougados, and S. Cabrit (2006). Which jet launching mechanism(s) in T Tauri stars? *A&A*, **453**, pp. 785–796. doi:10.1051/0004-6361:20054231.

Font, A. S., I. G. McCarthy, D. Johnstone, and D. R. Ballantyne (2004). Photoevaporation of Circumstellar Disks around Young Stars. *ApJ*, **607**, pp. 890–903. doi:10.1086/383518.

Furlan, E., K. L. Luhman, C. Espaillat, P. D'Alessio, L. Adame, P. Manoj, K. H. Kim, D. M. Watson, W. J. Forrest, M. K. McClure, N. Calvet, B. A. Sargent, J. D. Green, and W. J. Fischer (2011). The Spitzer Infrared Spectrograph Survey of T Tauri Stars in Taurus. *ApJS*, **195**, 3. doi:10.1088/0067-0049/195/1/3.

Gahm, G. F., F. M. Walter, H. C. Stempels, P. P. Petrov, and G. J. Herczeg (2008). Unveiling extremely veiled T Tauri stars. *A&A*, **482**, pp. L35–L38. doi:10.1051/0004-6361:200809488.

George, D. and P. Mallery (2010). *SPSS for Windows Step by Step: A Simple Guide and Reference, 17.0 update, 10th Edition.* Pearson Education: Boston.

Gillon, M., A. H. M. J. Triaud, B.-O. Demory, E. Jehin, E. Agol, K. M. Deck, S. M. Lederer, J. de Wit, A. Burdanov, J. G. Ingalls, E. Bolmont, J. Leconte, S. N. Raymond, F. Selsis, M. Turbet, K. Barkaoui, A. Burgasser, M. R. Burleigh, S. J. Carey, A. Chaushev, C. M. Copperwheat, L. Delrez, C. S. Fernandes, D. L. Holdsworth, E. J. Kotze, V. Van Grootel, Y. Almleaky, Z. Benkhaldoun, P. Magain, and D. Queloz (2017). Seven temperate terrestrial planets around the nearby ultracool dwarf star TRAPPIST-1. *Nature*, **542**, pp. 456–460. doi:10.1038/nature21360.

Glaser, B. G. and A. L. Strauss (1967). *The Discovery of Grounded Theory: Strategies for Qualitative Research.* Aldine Transaction. ISBN 202302601.

Gorti, U., D. Hollenbach, and C. P. Dullemond (2015). The Impact of Dust Evolution and Photoevaporation on Disk Dispersal. *ApJ*, **804**, 29. doi:10.1088/0004-637X/804/1/29.

Gorti, U., D. Hollenbach, J. Najita, and I. Pascucci (2011). Emission Lines from the Gas Disk around TW Hydra and the Origin of the Inner Hole. *ApJ*, **735**, 90. doi:10.1088/0004-637X/735/2/90.

Gressel, O., N. J. Turner, R. P. Nelson, and C. P. McNally (2015). Global Simulations of Protoplanetary Disks With Ohmic Resistivity and Ambipolar Diffusion. *ApJ*, **801**, 84. doi:10.1088/0004-637X/801/2/84.

Güdel, M., K. R. Briggs, K. Arzner, M. Audard, J. Bouvier, E. D. Feigelson, E. Franciosini, A. Glauser, N. Grosso, G. Micela, J.-L. Monin, T. Montmerle, D. L. Padgett, F. Palla, I. Pillitteri, L. Rebull, L. Scelsi, B. Silva, S. L. Skinner, B. Stelzer, and A. Telleschi (2007). The XMM-Newton extended survey of the Taurus molecular cloud (XEST). *A&A*, **468**, pp. 353–377. doi:10.1051/0004-6361:20065724.

Guilloteau, S., A. Dutrey, V. Piétu, and Y. Boehler (2011). A dual-frequency sub-arcsecond study of proto-planetary disks at mm wavelengths: first evidence for radial variations of the dust properties. *A&A*, **529**, A105. doi:10.1051/0004-6361/201015209.

Gullbring, E., L. Hartmann, C. Briceño, and N. Calvet (1998). Disk Accretion Rates for T Tauri Stars. *ApJ*, **492**, pp. 323–341. doi:10.1086/305032.

Hake, R. R. (1998). Interactive-engagement versus traditional methods: A six-thousand-student survey of mechanics test data for introductory physics courses. *American Journal of Physics*, **66**, pp. 64–74. doi:10.1119/1.18809.

Haladyna, T. M., S. M. Downing, and M. C. Rodriguez (2002). A Review of Multiple-Choice Item-Writing Guidelines for Classroom Assessment. *Applied Measurement in Education*, **15**.

Hamann, F. (1994). Emission-line studies of young stars. 4: The optical forbidden lines. *ApJS*, **93**, pp. 485–518. doi:10.1086/192064.

Hartigan, P., S. Edwards, and L. Ghandour (1995). Disk Accretion and Mass Loss from Young Stars. *ApJ*, **452**, p. 736. doi:10.1086/176344.

Hartigan, P., L. Hartmann, S. Kenyon, R. Hewett, and J. Stauffer (1989). How to unveil a T Tauri star. *ApJS*, **70**, pp. 899–914. doi:10.1086/191361.

Hartigan, P., J. A. Morse, and J. Raymond (1994). Mass-loss rates, ionization fractions, shock velocities, and magnetic fields of stellar jets. *ApJ*, **436**, pp. 125–143. doi:10.1086/174887.

Hartmann, L., N. Calvet, E. Gullbring, and P. D'Alessio (1998). Accretion and the Evolution of T Tauri Disks. *ApJ*, **495**, pp. 385–400. doi:10.1086/305277.

Herbig, G. H. (1962). The properties and problems of T Tauri stars and related objects. *Advances in Astronomy and Astrophysics*, **1**, pp. 47–103.

Herbst, W., D. K. Herbst, E. J. Grossman, and D. Weinstein (1994). Catalogue of UBVRI photometry of T Tauri stars and analysis of the causes of their variability. *Astronomical Journal*, **108**, pp. 1906–1923. doi:10.1086/117204.

Herczeg, G. J. and L. A. Hillenbrand (2008). UV Excess Measures of Accretion onto Young Very Low Mass Stars and Brown Dwarfs. *ApJ*, **681**, pp. 594–625. doi:10.1086/586728.

Herczeg, G. J. and L. A. Hillenbrand (2014). An Optical Spectroscopic Study of T Tauri Stars. I. Photospheric Properties. *ApJ*, **786**, 97. doi:10.1088/0004-637X/786/2/97.

Hirth, G. A., R. Mundt, and J. Solf (1997). Spatial and kinematic properties of the forbidden emission line region of T Tauri stars. *A&AS*, **126**, pp. 437–469. doi:10.1051/aas:1997275.

Hollenbach, D. and U. Gorti (2009). Diagnostic Line Emission from Extreme Ultraviolet and X-ray-illuminated Disks and Shocks Around Low-mass Stars. *ApJ*, **703**, pp. 1203–1223. doi:10.1088/0004-637X/703/2/1203.

Ingleby, L., N. Calvet, G. Herczeg, A. Blaty, F. Walter, D. Ardila, R. Alexander, S. Edwards, C. Espaillat, S. G. Gregory, L. Hillenbrand, and A. Brown (2013). Accretion Rates for T Tauri Stars Using Nearly Simultaneous Ultraviolet and Optical Spectra. *ApJ*, **767**, 112. doi:10.1088/0004-637X/767/2/112.

International Astronomical Union (2006). IAU 2006 General Assembly: Result of the IAU Resolution votes.

Isella, A., J. M. Carpenter, and A. I. Sargent (2009). Structure and Evolution of Pre-main-sequence Circumstellar Disks. *ApJ*, **701**, pp. 260–282. doi:10.1088/0004-637X/701/1/260.

Keane, J. T., I. Pascucci, C. Espaillat, P. Woitke, S. Andrews, I. Kamp, W.-F. Thi, G. Meeus, and W. R. F. Dent (2014). Herschel Evidence for Disk Flattening or Gas Depletion in Transitional Disks. *ApJ*, **787**, 153. doi:10.1088/0004-637X/787/2/153.

Keller, J. M. (2006). *Part I. Development of a concept inventory addressing students' beliefs and reasoning difficulties regarding the greenhouse effect, Part II. Distribution of chlorine measured by the Mars Odyssey Gamma Ray Spectrometer*. PhD Dissertation, University of Arizona.

Kennedy, G. M. and S. J. Kenyon (2008). Planet Formation around Stars of Various Masses: The Snow Line and the Frequency of Giant Planets. *ApJ*, **673**, pp. 502–512. doi:10.1086/524130.

Kenyon, S. J., M. Gómez, and B. A. Whitney (2008). *Low Mass Star Formation in the Taurus-Auriga Clouds*, p. 405.

Königl, A. and R. Salmeron (2011). *The Effects of Large-Scale Magnetic Fields on Disk Formation and Evolution*, pp. 283–352.

Kraus, A. L., M. J. Ireland, F. Martinache, and L. A. Hillenbrand (2011). Mapping the Shores of the Brown Dwarf Desert. II. Multiple Star Formation in Taurus-Auriga. *ApJ*, **731**, 8. doi:10.1088/0004-637X/731/1/8.

Kwan, J. and E. Tademaru (1995). Disk Winds from T Tauri Stars. *ApJ*, **454**, p. 382. doi:10.1086/176489.

Lada, C. J. and B. A. Wilking (1984). The nature of the embedded population in the Rho Ophiuchi dark cloud - Mid-infrared observations. *ApJ*, **287**, pp. 610–621. doi:10.1086/162719.

Lavalley, M., T. Isobe, and E. Feigelson (1992). ASURV: Astronomy Survival Analysis Package. In Worrall, D. M., C. Biemesderfer, and J. Barnes (eds.) *Astronomical Data Analysis Software and Systems I*, volume 25 of *Astronomical Society of the Pacific Conference Series*, p. 245.

Lawrenz, F., D. Huffman, and K. Appeldoorn (2005). Enhancing the Instructional Environment: Optimal Learning in Introductory Science Classes. *Journal of College Science Teaching*, **34**.

Lindell, R. S. and J. P. Olsen (2002). Developing the Lunar Phases Concept Inventory. In *The 125th National Meeting of the American Association of Physics Teachers*, Physics Education Research Conference.

Lissauer, J. J. (1993). Planet formation. *Annual Review of Astronomy and Astrophysics*, **31**, pp. 129–174. doi:10.1146/annurev.aa.31.090193.001021.

Lodders, K. (2003). Solar System Abundances and Condensation Temperatures of the Elements. *ApJ*, **591**, pp. 1220–1247. doi:10.1086/375492.

Lopresto, M. C. and S. R. Murrell (2009). Using the Star Properties Concept Inventory to Compare Instruction with Lecture Tutorials to Traditional Lectures. *Astronomy Education Review*, **8**(1), p. 010105. doi:10.3847/AER2009014.

Manara, C. F., L. Testi, E. Rigliaco, J. M. Alcalá, A. Natta, B. Stelzer, K. Biazzo, E. Covino, S. Covino, G. Cupani, V. D'Elia, and S. Randich (2013). X-shooter spectroscopy of young stellar objects. II. Impact of chromospheric emission on accretion rate estimates. *A&A*, **551**, A107. doi:10.1051/0004-6361/201220921.

Markus, K. A. and K. M. Smith (2012). *Encyclopedia of Research Design*. SAGE Publications, Inc.

McDermott, L. C. (1991). Millikan Lecture 1990: What we teach and what is learned-Closing the gap. *American Journal of Physics*, **59**, pp. 301–315. doi:10.1119/1.16539.

Mendigutía, I., R. D. Oudmaijer, E. Rigliaco, J. R. Fairlamb, N. Calvet, J. Muzerolle, N. Cunningham, and S. L. Lumsden (2015). On the origin of the correlations between the accretion luminosity and emission line luminosities in pre-main-sequence stars. *MNRAS*, **452**, pp. 2837–2844. doi:10.1093/mnras/stv1540.

Mordasini, C., H. Klahr, Y. Alibert, W. Benz, and K.-M. Dittkrist (2010). Theory of planet formation. *arXiv e-prints*.

Muzerolle, J., L. Hartmann, and N. Calvet (1998). A Brgamma Probe of Disk Accretion in T Tauri Stars and Embedded Young Stellar Objects. *Astronomical Journal*, **116**, pp. 2965–2974. doi:10.1086/300636.

NASA Exoplanet Science Institute (2018). NASA Exoplanet Archive.

National Academies of Sciences, Engineering, and Medicine (2018). *How People Learn II: Learners, Contexts, and Cultures*. The National Academies Press.

National Research Council (1996). *National Science Education Standards*. National Academies Press.

Natta, A., L. Testi, J. M. Alcalá, E. Rigliaco, E. Covino, B. Stelzer, and V. D'Elia (2014). X-shooter spectroscopy of young stellar objects. V. Slow winds in T Tauri stars. *A&A*, **569**, A5. doi:10.1051/0004-6361/201424136.

Nunnally, J. C. (1978). *Psychometric Theory. 2nd Edition.* McGraw Hill, New York.

Owen, J. E., C. J. Clarke, and B. Ercolano (2012). On the theory of disc photoevaporation. *MNRAS*, **422**, pp. 1880–1901. doi:10.1111/j.1365-2966.2011.20337.x.

Owen, J. E., B. Ercolano, and C. J. Clarke (2011). Protoplanetary disc evolution and dispersal: the implications of X-ray photoevaporation. *MNRAS*, **412**, pp. 13–25. doi:10.1111/j.1365-2966.2010.17818.x.

Owen, J. E., B. Ercolano, C. J. Clarke, and R. D. Alexander (2010). Radiation-hydrodynamic models of X-ray and EUV photoevaporating protoplanetary discs. *MNRAS*, **401**, pp. 1415–1428. doi:10.1111/j.1365-2966.2009.15771.x.

Owen, T., P. Mahaffy, H. B. Niemann, S. Atreya, T. Donahue, A. Bar-Nun, and I. de Pater (1999). A low-temperature origin for the planetesimals that formed Jupiter. *Nature*, **402**, pp. 269–270. doi:10.1038/46232.

Panoglou, D., S. Cabrit, G. Pineau Des Forêts, P. J. V. Garcia, J. Ferreira, and F. Casse (2012). Molecule survival in magnetized protostellar disk winds. I. Chemical model and first results. *A&A*, **538**, A2. doi:10.1051/0004-6361/200912861.

Partridge, B. and G. Greenstein (2003). Goals for "Astro 101": Report on Workshops for Department Leaders. *Astronomy Education Review*, **2**(2). doi:10.3847/AER2003016.

Pasachoff, J. M. (2002). What Should College Students Learn? *Astronomy Education Review*, **1**(1), pp. 124–130.

Pascucci, I., D. Apai, E. E. Hardegree-Ullman, J. S. Kim, M. R. Meyer, and J. Bouwman (2008). Medium-Separation Binaries Do Not Affect the First Steps of Planet Formation. *ApJ*, **673**, pp. 477–486. doi:10.1086/524100.

Pascucci, I., S. Edwards, M. Heyer, E. Rigliaco, L. Hillenbrand, U. Gorti, D. Hollenbach, and M. N. Simon (2015). Narrow Na and K Absorption Lines Toward T Tauri Stars: Tracing the Atomic Envelope of Molecular Clouds. *ApJ*, **814**, 14. doi:10.1088/0004-637X/814/1/14.

Pascucci, I., L. Ricci, U. Gorti, D. Hollenbach, N. P. Hendler, K. J. Brooks, and Y. Contreras (2014). Low Extreme-ultraviolet Luminosities Impinging on Protoplanetary Disks. *ApJ*, **795**, 1. doi:10.1088/0004-637X/795/1/1.

Pascucci, I., M. Sterzik, R. D. Alexander, S. H. P. Alencar, U. Gorti, D. Hollenbach, J. Owen, B. Ercolano, and S. Edwards (2011). The Photoevaporative Wind from the Disk of TW Hya. *ApJ*, **736**, 13. doi:10.1088/0004-637X/736/1/13.

Philips, W. C. (1991). Earth science misconceptions. *The Science Teacher*, **58**, pp. 21–23.

Pickles, A. J. (1998). A Stellar Spectral Flux Library: 1150-25000 Å. *PASP*, **110**, pp. 863–878. doi:10.1086/316197.

Piétu, V., S. Guilloteau, E. Di Folco, A. Dutrey, and Y. Boehler (2014). Faint disks around classical T Tauri stars: Small but dense enough to form planets. *A&A*, **564**, A95. doi:10.1051/0004-6361/201322388.

Plummer, J. D., C. Palma, A. Flarend, K. Rubin, Y. Shiou Ong, B. Botzer, S. McDonald, and T. Furman (2015). Development of a Learning Progression for the Formation of the Solar System. *International Journal of Science Education*, **37**, pp. 1381–1401. doi:10.1080/09500693.2015.1036386.

Pontoppidan, K. M., G. A. Blake, and A. Smette (2011). The Structure and Dynamics of Molecular Gas in Planet-forming Zones: A CRIRES Spectro-astrometric Survey. *ApJ*, **733**, 84. doi:10.1088/0004-637X/733/2/84.

Pontoppidan, K. M., G. A. Blake, E. F. van Dishoeck, A. Smette, M. J. Ireland, and J. Brown (2008). Spectroastrometric Imaging of Molecular Gas within Protoplanetary Disk Gaps. *ApJ*, **684**, pp. 1323–1329. doi:10.1086/590400.

Prather, E. E., A. L. Rudolph, and G. Brissenden (2009). Teaching and Learning Astronomy in the 21st Century. *Physics Today*, **62**(10), pp. 41–47.

Prather, E. E., T. F. Slater, J. P. Adams, J. M. Bailey, L. V. Jones, and J. A. Dostal (2004). Research on a Lecture-Tutorial Approach to Teaching Introductory

Astronomy for Non Science Majors. *Astronomy Education Review*, **3**(2), pp. 122–136.

Prather, E. E., T. F. Slater, and E. G. Offerdahl (2002). Hints of a Fundamental Misconception in Cosmology. *Astronomy Education Review*, **1**(2), pp. 28–34.

Ray, T., C. Dougados, F. Bacciotti, J. Eislöffel, and A. Chrysostomou (2007). Toward Resolving the Outflow Engine: An Observational Perspective. *Protostars and Planets V*, pp. 231–244.

Rigliaco, E., I. Pascucci, U. Gorti, S. Edwards, and D. Hollenbach (2013). Understanding the Origin of the [O I] Low-velocity Component from T Tauri Stars. *ApJ*, **772**, 60. doi:10.1088/0004-637X/772/1/60.

Rogers, L. A., P. Bodenheimer, J. J. Lissauer, and S. Seager (2011). Formation and Structure of Low-density exo-Neptunes. *ApJ*, **738**, 59. doi:10.1088/0004-637X/738/1/59.

Rosenfeld, K. A., C. Qi, S. M. Andrews, D. J. Wilner, S. A. Corder, C. P. Dullemond, S.-Y. Lin, A. M. Hughes, P. D'Alessio, and P. T. P. Ho (2012). Kinematics of the CO Gas in the Inner Regions of the TW Hya Disk. *ApJ*, **757**, 129. doi:10.1088/0004-637X/757/2/129.

Schegerer, A. A., S. Wolf, C. A. Hummel, S. P. Quanz, and A. Richichi (2009). Tracing the potential planet-forming regions around seven pre-main-sequence stars. *A&A*, **502**, pp. 367–383. doi:10.1051/0004-6361/200810782.

Schlingman, W. M., E. E. Prather, C. S. Wallace, A. L. Rudolph, and G. Brissenden (2012). A Classical Test Theory Analysis of the Light and Spectroscopy Concept Inventory National Study Data Set. *Astronomy Education Review*, **11**(1), p. 010107. doi:10.3847/AER2012010.

Schneps, M. P. (1989). A Private Universe, Video.

Sharp, J. (1996). Children's astronomical beliefs: a preliminary study of Year 6 children in south-west England. *International Journal of Science Education*, **18**, pp. 685–712. doi:10.1080/0950069960180604.

Shu, F., J. Najita, E. Ostriker, F. Wilkin, S. Ruden, and S. Lizano (1994). Magnetocentrifugally driven flows from young stars and disks. 1: A generalized model. *ApJ*, **429**, pp. 781–796. doi:10.1086/174363.

Simon, M. N., S. Buxner, and C. Impey (2018). A Survey and Analysis of College Students' Understanding of Planet Formation Before Instruction. *Astrobiology*, **18**, pp. 1594–1610. doi:10.1089/ast.2017.1815.

Simon, M. N., I. Pascucci, S. Edwards, W. Feng, U. Gorti, D. Hollenbach, E. Rigliaco, and J. T. Keane (2016). Tracing Slow Winds from T Tauri Stars via Low-velocity Forbidden Line Emission. *ApJ*, **831**, 169. doi:10.3847/0004-637X/831/2/169.

Simonelli, G. and C. A. Pilachowski (2003). First-Year College Students' Ideas About Astronomy: A Pilot Study. *Astronomy Education Review*, **2**(2), pp. 166–171. doi:10.3847/AER2003024.

Skrutskie, M. F., D. Dutkevitch, S. E. Strom, S. Edwards, K. M. Strom, and M. A. Shure (1990). A sensitive 10-micron search for emission arising from circumstellar dust associated with solar-type pre-main-sequence stars. *Astronomical Journal*, **99**, pp. 1187–1195. doi:10.1086/115407.

Slater, S. J. (2014). The Development and Validation of the Test of Astronomy Standards (TOAST). *Journal of Astronomy and Earth Sciences Education*, **1**, pp. 166–171.

Slater, T., J. P. Adams, G. Brissenden, and D. Duncan (2001). What topics are taught in introductory astronomy courses? *The Physics Teacher*, **39**, pp. 52–55. doi:10.1119/1.1343435.

Slater, T. F. and J. P. Adams (2003). *Learner-Centered Astronomy Teaching: Strategies for ASTRO 101*.

Sokoloff, D. R. and R. K. Thornton (1997). Using interactive lecture demonstrations to create an active learning environment. *The Physics Teacher*, **35**, pp. 340–347. doi:10.1119/1.2344715.

Stassun, K. G., A. Scholz, T. J. Dupuy, and K. M. Kratter (2014). The Impact of Chromospheric Activity on Observed Initial Mass Functions. *ApJ*, **796**, 119. doi:10.1088/0004-637X/796/2/119.

Stelzer, B. and J. H. M. M. Schmitt (2004). X-ray emission from a metal depleted accretion shock onto the classical T Tauri star TW Hya. *A&A*, **418**, pp. 687–697. doi:10.1051/0004-6361:20040041.

Trochim, W. M. K. (2006). *The Research Methods Knowledge Base*.

Turner, N. J., S. Fromang, C. Gammie, H. Klahr, G. Lesur, M. Wardle, and X.-N. Bai (2014). Transport and Accretion in Planet-Forming Disks. *Protostars and Planets VI*, pp. 411–432. doi:10.2458/azu_uapress_9780816531240-ch018.

University of Arizona (2016). The University of Arizona Factbook.

Vogt, S. S., S. L. Allen, B. C. Bigelow, L. Bresee, B. Brown, T. Cantrall, A. Conrad, M. Couture, C. Delaney, H. W. Epps, D. Hilyard, D. F. Hilyard, E. Horn, N. Jern, D. Kanto, M. J. Keane, R. I. Kibrick, J. W. Lewis, J. Osborne, G. H. Pardeilhan, T. Pfister, T. Ricketts, L. B. Robinson, R. J. Stover, D. Tucker, J. Ward, and M. Z. Wei (1994). HIRES: the high-resolution echelle spectrometer on the Keck 10-m Telescope. In Crawford, D. L. and E. R. Craine (eds.) *Instrumentation in Astronomy VIII*, volume 2198 of *Proc. SPIE*, p. 362. doi:10.1117/12.176725.

Vosniadou, S. and W. F. Brewer (1994). Mental models of day-night cycle. *Cognitive Science, Vol. 18, No. 1, p. 123-183*, **18**, pp. 123–183.

Wallace, C. S., T. G. Chambers, and E. E. Prather (2018). Item response theory evaluation of the Light and Spectroscopy Concept Inventory national data set. *Physical Review Physics Education Research*, **14**(1), 010149. doi: 10.1103/PhysRevPhysEducRes.14.010149.

Wallace, C. S., E. E. Prather, and D. K. Duncan (2012). A Study of General Education Astronomy Students' Understandings of Cosmology. Part IV. Common Difficulties Students Experience with Cosmology. *Astronomy Education Review*, **11**(1), p. 010104. doi:10.3847/AER2011032.

Williamson, K. E. and S. Willoughby (2012). Student Understanding of Gravity in Introductory College Astronomy. *Astronomy Education Review*, **11**(1), p. 010105. doi:10.3847/AER2011025.

Williamson, K. E., S. Willoughby, and E. E. Prather (2013). Development of the Newtonian Gravity Concept Inventory. *Astronomy Education Review*, **12**(1).

Yu, K. C., K. Sahami, and G. Denn (2010). Student Ideas about Kepler's Laws and Planetary Orbital Motions. *Astronomy Education Review*, **9**(1), p. 010108. doi:10.3847/AER2009069.